Analysis on Inclined Cables Under Distributed And Concentrated Loads

by

Long Yao

Graduate Program
in
Applied Mathematics

Submitted in partial fulfillment
of the requirements for the degree of
Master of Science

Faculty of Graduate Studies
The University of Western Ontario
London, Ontario
August 1999

ABSTRACT

This thesis extends the method of the Non-homogeneous Transfer Matrix to study the dynamics of inclined cables under distributed and concentrated loads. The NTM method is different from the method of the traditional homogeneous transfer matrix in that it not only involves homogeneous transfer matrices but also involves non-homogeneous transfer vectors which are caused by non-homogeneous terms in differential equations. This feature makes it possible to consider the dynamic response of the cables with concentrated loads. This thesis combines the NTM method with an approach of transforming the original coordinate system to a rotated coordinate system in order to analyze the inclined cable models. The models presented in this thesis include both horizontal and inclined extensible sagged cables with and without concentrated loads. The effect of concentrated loads on mode shapes is investigated. It is found that both the sag and the inclination of the cables have some influences on the mode shapes of the cables. Moreover, the effect of the inclination on the frequencies of the cables is also investigated. Closed-form expressions are derived and numerical results are given to show the use of the analytical formulas.

Keywords: cable dynamics, coordinate rotation, non-homogeneous transfer matrix(NTM) method, static analysis, dynamic analysis, mode shapes.

To my family.

ACKNOWLEDGEMENTS

It is my great pleasure to express my gratitude to my supervisor, Dr. Pei Yu, for the guidance and support that he has patiently provided for the extent of my graduate studies here at the University of Western Ontario.

I would also like to thank the staff and the graduate students from the Department of Applied Mathematics, UWO for being such a great bunch of people to work beside. Thank Hope Wolly for her generous offer of the Western style file for this thesis. A special thank goes to Pat, the graduate secretary of the department, for her help.

I am also glad to thank Natural Sciences and Engineering Research Council of Canada for its generous and obviously important financial support.

The last but not the least thank goes to Prof. Yuan Yuan for her inspiring discussion when I ran into problems.

TABLE OF CONTENTS

NOMENCLATURE

SYMBOL	QUANTITY
A	cross-sectional area of the cable
$[D_0^i]$	homogeneous transfer matrix
δ	Dirac Delta function
E	Young's modulus
F_i	external concentrated force in the illustration figures
g	constant of gravity
H	horizontal tension when $\theta = 0$
H_x	horizontal component of T in original coordinate system
h_x	horizontal component of τ in original coordinate system
I	identity matrix
J_k	slope of the k-th segment of a large-sagged cable
L_x	cable span in original coordinate system
L	span length for $\theta = 0$
L_s	cable length
M	the number of subsegments in the i-th segment
m	mass of the cable per unit length
m_i	mass of the external concentrated force
N	the total number of concentrated loads on the cable
ω	natural frequency
P_i	external concentrated force
q_y	in-plane distributed force in original coordinate system
q_z	out-of-plane distributed force in original coordinate system
$\vec{r}_i$	non-homogeneous transfer vector
r_{N1}, s_{N1}	the first elements of $\vec{r}_N$, $\vec{s}_N$
r_{N2}, s_{N2}	the second elements of $\vec{r}_N$, $\vec{s}_N$
r_{i1}, s_{i1}	the first elements of $\vec{r}_i$, $\vec{s}_i$
r_{i2}, s_{i2}	the second elements of $\vec{r}_i$, $\vec{s}_i$
s	Lagrangian coordinate along the cable

$\vec{s}_i$	non-homogeneous transfer vector in the out-of-plane direction
θ	angle of inclination of the cable
T	cable tension
t	time
τ	static or dynamic tension increase
x	horizontal axis in original coordinate system
y	in-plane axis in original coordinate system
z	out-of-plane axis in original coordinate system
x'	horizontal axis in rotated coordinate system
y'	in-plane axis in rotated coordinate system

LIST OF TABLES

LIST OF FIGURES

Chapter 1

Introduction

Cables have been investigated by many researchers since the 17th century because of its wide usage in many applications such as ocean and electrical engineering. The study of cable dynamics is important for the design of practical cable structures like cable-stayed bridges and guyed towers. In these applications, cable vibration is a crucial factor in determining the reliability of the structures [1].

The flexibility of cables is advantageous because it makes them easy to be employed in various practical situations. However, this flexibility also makes cables difficult to theoretically analyze. Furthermore, the flexibility of cables renders them susceptible to oscillations which might impair their performances. The failures of many suspension bridges such as Shipshaw [3] further necessitated the study of cable dynamics. The same problem also exists in ocean and electrical engineering, for example, the aeolian vibration and galloping on overhead transmission lines [4,5] and strumming of marine cables under the sea [6,7].

A brief literature review is given below as the beginning of this chapter.

1.1 Literature review

In 1676, Noble and Pigott found that a string has different modes of vibration, which initiated the research on cable dynamics [2], and the research continued until the lat-

ter half of the 19th century. The rapid increase in the usage of cable-stayed bridges and high-voltage transmission lines as well as other cable-related structures in early 20th century further extended the research on cables. Especially, a number of disastrous crashes of cable-stayed bridges and suspension bridges, [2] further showed the importance of the research in this field.

In the early studies, it was assumed that cables were inextensible or had infinite stiffness. In other words, the elasticity of cables was ignored in order to make it possible for an asymptotic analysis. Later, H. M. Irvine and T. K. Caughey pointed out that such a model was inherently unsuitable for the study of practical cables because the elasticity of cables must be included in order to obtain correct results [8]. A compromise made between inextensible and elastic cables was to assume that the cables were flat, i.e. it had small sag/length ratio. Because of the simplicity of this model and the wide usage of shallow sagged cables, many researchers have focused on such models, especially on those with horizontal supports [8,9,10].

However, in reality, models for large sagged cables are needed because shallow models are approximations and usually do not give correct results. As it was pointed out in [11] that investigations should be made for these models and some preliminary results have been obtained in [6]. Furthermore, it has been noted that not much attention has been paid to the cables with pointed mass or *concentrated loads* [12]. But in the real world, such concentrated loads are common , for example, the optical or acoustical instruments on the cables under the sea or the detuning pendulums on the overhead transmission lines.

A model with only one concentrated load was developed [15,16] . Later, more complicated cases with more concentrated loads are considered in [9,12] by using the method of transfer matrix.

Some other researchers have also explored the problem by methods such as Finite Element Method (FEM) [17] and finite difference [18]. However, as it was pointed out in [6] that when there are many concentrated loads on the cables, for example, a marine cable under the sea having enormous number of acoustical instruments, FEM becomes awkward because of the enormous matrix manipulations. A detailed review

on the history of cable dynamics can be found in [8.19] .

By using the method of Non-homogeneous Transfer Matrix (NTM) [12], this thesis will investigate static and dynamic behavior for both flat and large sagged cables with inclined as well as horizontal supporters. In particular, it concentrates on the study of cables with concentrated loads. Closed-form expressions and numerical results are obtained.

1.2 Methodology

Both static and dynamic analyses are given in this thesis but the latter is more important and more attention is paid to it. However, in order to perform the dynamic analysis, the static profile must be obtained first. A brief review on these two topics is given below.

1.2.1 Coordinate rotation

All the analyses given in this thesis are referred to a rotated coordinate system with respect to an inclined cable. Therefore, the rotation relationship is always needed when we transform the differential equations which describe the motion of the cable from original coordinate system to rotated coordinate system, as shown in Fig 1.1 with z-axis in the out-of-plane direction.

Suppose that point P see (Fig. 1.1) has the coordinates (x, y) in the original coordinate system and (x', y') in the rotated coordinates, then the following relationship holds for the transformation from original coordinate system to rotated coordinate system:

$$\begin{pmatrix} x \\ y \end{pmatrix} = \begin{bmatrix} \cos\theta & \sin\theta \\ -\sin\theta & \cos\theta \end{bmatrix} \begin{pmatrix} x' \\ y' \end{pmatrix}. \tag{1.1}$$

and the reverse transformation from the rotated coordinate system to the original coordinate system is given by as:

$$\begin{pmatrix} x' \\ y' \end{pmatrix} = \begin{bmatrix} \cos\theta & -\sin\theta \\ \sin\theta & \cos\theta \end{bmatrix} \begin{pmatrix} x \\ y \end{pmatrix}. \tag{1.2}$$

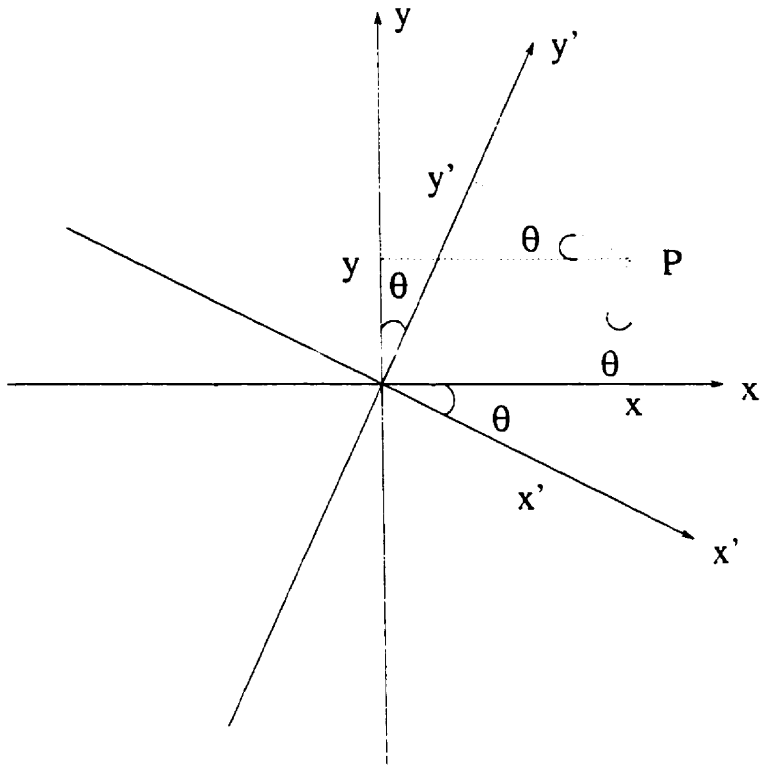

Figure 1.1: Coordinate systems

Because we frequently transform differential equations from the original coordinate system to the rotated coordinate system, Eq. (1.1) will be frequently used throughout the thesis.

1.2.2 Static analysis

A practical example for the cable models studied in this thesis is shown in Fig. 1.2 [15]. The theoretical abstraction is given in Fig. 1.2 (b) where z-axis is in out-of-plane direction, s denotes arc length coordinate measured along the planar equilibrium curve.

By using Fig. 1.2 (b), we can derive the following equations:

$$T_x = T\frac{dx}{ds}, \tag{1.3}$$

$$T_y = -T\frac{dy}{ds}, \tag{1.4}$$

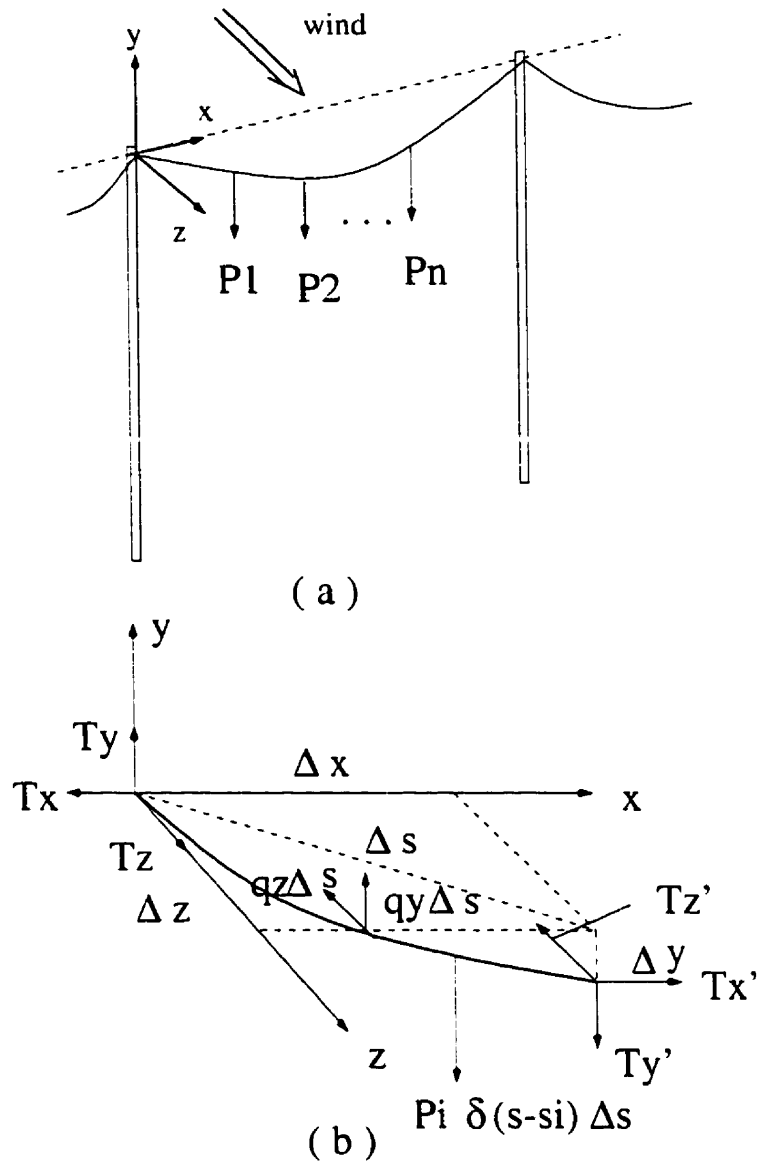

Figure 1.2: Cable analysis: (a) a span of a cable: and (b) cable dynamics

$$T_z = T\frac{dz}{ds}, \tag{1.5}$$

$$T'_x = T\frac{dx}{ds} + \frac{d}{ds}(T\frac{dx}{ds})\Delta s, \tag{1.6}$$

$$T'_y = -T\frac{dy}{ds} + \frac{d}{ds}(-T\frac{dy}{ds})\Delta s, \tag{1.7}$$

$$T'_z = T\frac{dz}{ds} + \frac{d}{ds}(T\frac{dz}{ds})\Delta s. \tag{1.8}$$

Next, balancing the forces in x direction yields equation $T'_x - T_x = 0$, and then using

Eq. (1.3) and (1.6) results in

$$\frac{d}{ds}(T\frac{dx}{ds}) = 0 \tag{1.9}$$

Similarly, balancing the forces in y direction gives $T_y - T_y' + q_y\Delta s - P_i\delta(s-s_i)\Delta s = 0$ which, with the aid of Eq. (1.4) and (1.7), in turn produces

$$\frac{d}{ds}(T\frac{dy}{ds}) = -q_y + P_i\delta(s-s_i) \tag{1.10}$$

A similar treatment in z direction yields $T_z - T_z' - q_z\Delta s = 0$, and substitute Eq. (1.5) and Eq. (1.8) into the equation to obtain

$$\frac{d}{ds}(T\frac{dz}{ds}) = -q_z. \tag{1.11}$$

Now, under the rotation equation given by Eq. (1.1), Eq. (1.9)- (1.11) can be written in the rotated coordinate system as

$$\frac{d}{ds}(H_x\frac{dx'}{dx}) = q_y\sin\theta - P_i\delta(s-s_i)\sin\theta, \tag{1.12}$$

$$\frac{d}{ds}(H_x\frac{dy'}{dx}) = -q_y\cos\theta + P_i\delta(s-s_i)\cos\theta, \tag{1.13}$$

$$\frac{d}{ds}(H_x\frac{dz}{dx}) = -q_z, \tag{1.14}$$

where the relation $T = H_x\frac{ds}{dx}$ has been used. If the cable doesn't have out-of-plane load q_z or concentrated loads P_i, then the problem becomes the special cases: $q_z = 0$ or $P_i = 0$. The equations Eq. (1.12)- (1.14) are key equations and will be frequently used in the following chapters.

We begin with a simple model which bears the simple mechanical characteristic of cables. This model has vertical distributed loads only due to the cable's weight. Then models with more complicated loads will be studied.

The differential equations describing the static profile of the simple model can be found in [20] where the detailed derivation is given. In particular, [20] introduced the equation $T = H\frac{ds}{dx}$ where T is the cable tension and H the horizontal component of the tension and s, x have the same meanings as shown in Fig. 1.2 (b). This equation simply indicates the mechanical characteristic of a cable provided it has no external

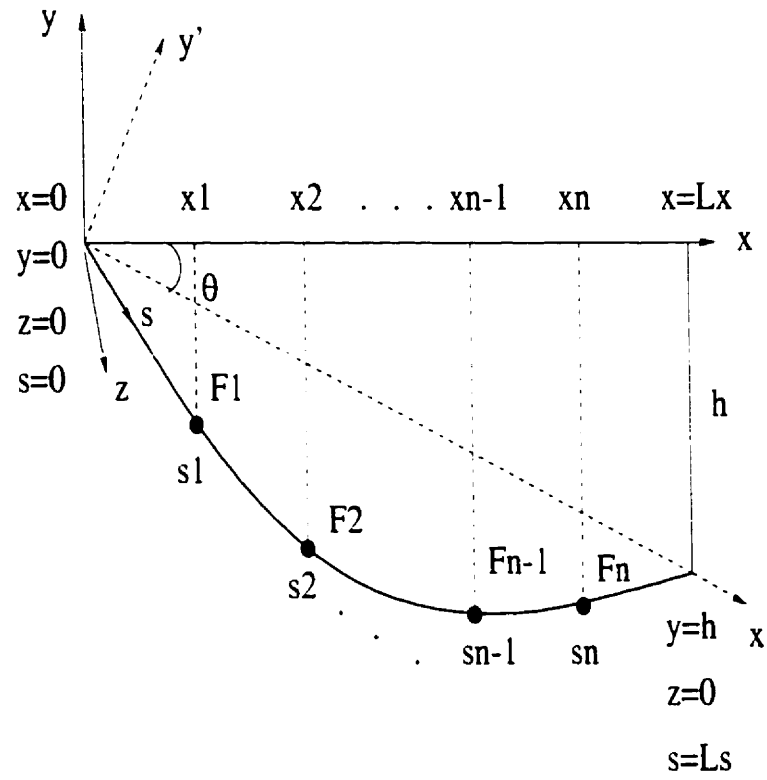

Figure 1.3: Static profile

horizontal force. Therefore, this equation is also valid for other situations such as inclined cables as long as external horizontal force is not presente. A generalization of this equation will be frequently used in this thesis. With the aid of the equation, the differential equations can be solved analytically and closed-form formulas can be obtained.

1.2.3 Static tension increase

Because the models to be discussed in the thesis are more complicated than the simple model, we need to generalize the results obtained from the simple model to allow more complicated loads. In the generalization, we should use the same kind of analysis in order for the general formulas obtained in the thesis still being valid for the simple case. However, for complicated loads, the static profile of the cable and the horizontal component of the cable tension differs from one case to another

due to different external forces. Once the cable tesion is determined, a similar set of differential equations can be solved in a similar way for the static profile associated with more complicated loads. Having found the static tension increase, we can then solve the static profile of the complicated models.

To find the static tension increase, we introduce another equation which is similar to equation $T = H\frac{ds}{dx}$. Supposed that τ is the static tension increase of the cable due to some additional loads and h_x the horizontal components of the tension, then $\tau = h_x\frac{ds}{dx}$. The procedure of solving τ is equivalent to that for h_x. The final equation obtained for h_x by using Hooke's Law is always a 3rd-degree polynomial which is similar to that found in [4,20]. Considering the cable segment shown in Fig. 1.2 (b), and Eq. (1.3)- (1.8) can still used here. However, the expression for the forces are different due to the static tension increase τ and the corresponding static displacement $\vec{\mathbf{V}}$ which has three components u, y_2 and z_2. Thus, we have

$$T_x = (T+\tau)(\frac{dx}{ds}+\frac{\partial u}{\partial s}). \tag{1.15}$$

$$T_y = -(T+\tau)(\frac{dy_1}{ds}+\frac{\partial y_2}{\partial s}). \tag{1.16}$$

$$T_z = (T+\tau)(\frac{dz_1}{ds}+\frac{\partial z_2}{\partial s}). \tag{1.17}$$

$$T'_x = (T+\tau)(\frac{dx}{ds}+\frac{\partial u}{\partial s})+\frac{d}{ds}[(T+\tau)(\frac{dx}{ds}+\frac{\partial u}{\partial s})]\Delta s. \tag{1.18}$$

$$T'_y = -(T+\tau)(\frac{dy_1}{ds}+\frac{\partial y_2}{\partial s})+\frac{d}{ds}[-(T+\tau)(\frac{dy_1}{ds}+\frac{\partial y_2}{\partial s})]\Delta s. \tag{1.19}$$

$$T'_z = (T+\tau)(\frac{dz_1}{ds}+\frac{\partial z_2}{\partial s})+\frac{d}{ds}[(T+\tau)(\frac{dz_1}{ds}+\frac{\partial z_2}{\partial s})]\Delta s. \tag{1.20}$$

Then balancing the forces in each direction (see Fig. 1.2) and transfroming the equations into the rotated coordinate system, we have

$$\frac{d}{ds}[\tau\frac{dx'}{ds}+(T+\tau)\frac{du'}{ds}] = -P_i\delta(s-s_i)\sin\theta \tag{1.21}$$

$$\frac{d}{ds}[\tau\frac{dy'_1}{ds}+(T+\tau)\frac{dy'_2}{ds}] = P_i\delta(s-s_i)\cos\theta \tag{1.22}$$

$$\frac{d}{ds}[\tau\frac{dz_1}{ds}+(T+\tau)\frac{dz_2}{ds}] = 0 \tag{1.23}$$

1.2.4 Dynamical analysis

For dynamical analysis, we assume that the movement is measured from the static profile. Thus referring to the cable segment (see Fig. 1.2 (b)), the expression for the forces are similar to that given by Eq. (1.15)- (1.20) except that the displacement $\vec{\mathbf{U}}$ which has three components u, y_2 and z_2 now represents dynamical displacement caused by the dynamic tension increase τ.

Suppose the mass of the cable per unit length is m and the mass of the i-th concentrated load is m_i, then there are two additional forces $m\frac{\partial^2\vec{\mathbf{U}}}{\partial t^2}$ and $m_i\delta(s-s_i)\frac{\partial^2\vec{\mathbf{U}}}{\partial t^2}$ which should be added at the right-hand-side of the forces balance equations Eq. (1.9)- (1.11). Therefore, the equations describing dynamic response of the cables are

$$\frac{\partial}{\partial s}[(T+\tau)(\frac{dx}{ds}+\frac{\partial u}{\partial s})] = m\frac{\partial^2 u}{\partial t^2}+m_i\delta(s-s_i)\frac{\partial^2 u}{\partial t^2}, \tag{1.24}$$

$$\frac{\partial}{\partial s}[(T+\tau)(\frac{dy_1}{ds}+\frac{\partial y_2}{\partial s})] = m\frac{\partial^2 y_2}{\partial t^2}+m_i\delta(s-s_i)\frac{\partial^2 y_2}{\partial t^2} - q_y + P_i\delta(s-s_i), \tag{1.25}$$

$$\frac{\partial}{\partial s}[(T+\tau)(\frac{dz_1}{ds}+\frac{\partial z_2}{\partial s})] = m\frac{\partial^2 z_2}{\partial t}+m_i\delta(s-s_i)\frac{\partial^2 z_2}{\partial t^2} - q_z. \tag{1.26}$$

The idea of the dynamical analysis is shown in Fig. 1.4, where similar notations as that given in Fig. 1.3 are used. Suppose that a point has a static profile represented by (x_1, y_1, z) in the original coordinate system, then its movement from the static curve can be decomposed into three components in the three orthogonal directions as u, y_2 and z_2. Therefore, its dynamical coordinates referring to the original coordinate system are expressed as $(x_1+u, y_1+y_2, z+z_2)$, see Fig. 1.4.

Eq. (1.24)- (1.26) can be transformed into rotated coordinate system by using Eq. (1.1) and can be simplified by using the differential equations Eq. (1.12)- (1.14) describing the static profile. The resulting equations are:

$$\frac{\partial}{\partial s}[(T+\tau)\frac{\partial u'}{\partial s}+\tau\frac{dx'}{ds}] = m\frac{\partial^2 u'}{\partial t^2}+m_i\delta(s-s_i)\frac{\partial^2 u'}{\partial t^2}, \tag{1.27}$$

$$\frac{\partial}{\partial s}[(T+\tau)\frac{\partial y_2'}{\partial s}+\tau\frac{dy_1'}{ds}] = m\frac{\partial^2 y_2'}{\partial t^2}+m_i\delta(s-s_i)\frac{\partial^2 y_2'}{\partial t^2}, \tag{1.28}$$

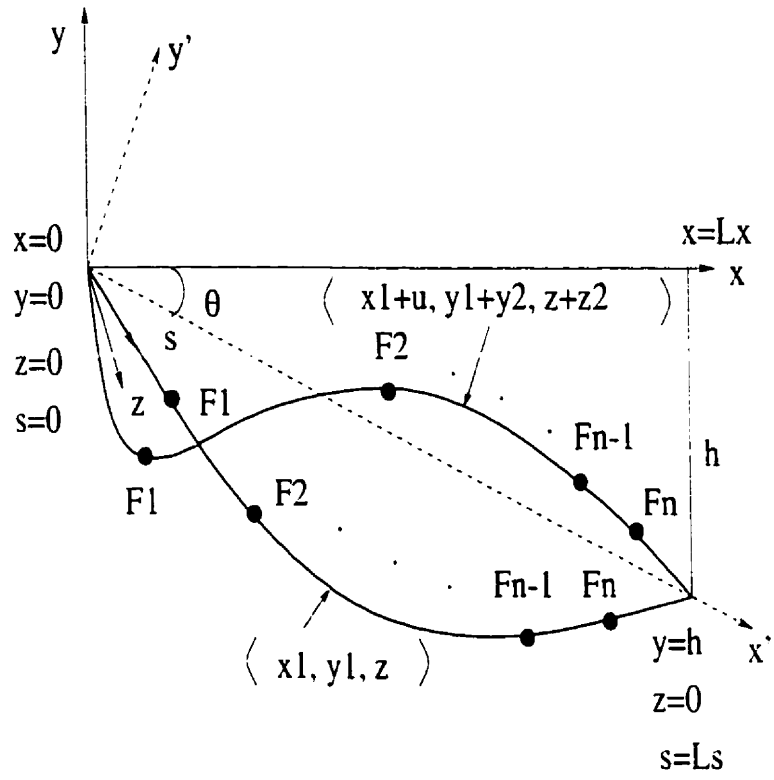

Figure 1.4: Dynamical displacement

$$\frac{\partial}{\partial s}[(T+\tau)\frac{\partial z_2}{\partial s}+\tau\frac{dz_1}{ds}] = m\frac{\partial^2 z_2}{\partial t^2}+m_i\delta(s-s_i)\frac{\partial^2 z_2}{\partial t^2}. \qquad (1.29)$$

The above equations are also key equations and will be frequently used in the following chapters. Useful discussions on this topic can be found, for exmple, in [20-24]. In order to find the frequencies of a cable, a numerical method is usually used. However, due to the convergence problem, it is difficult to obtain accurate high frequencies. The Non-homogeneous Transfer Matrix (NTM) [12] will be the method used in this thesis, and allows us to derive explicit formulas and thus overcome the convergence difficulty.

The *Holzer-van de Dungen* method in matrix form is called the method of transfer matrix. It makes use of the fact that in a large class of engineering problems, the vibrating system is arranged in a line and the behavior of every point in the system is influenced by the behavior at neighboring points only [25,26] . However, this transfer matrix method is only valid for homogenous differential equations. Since NTM

method introduced in [12] can deal with non-homogenous differential equations. The cable models to be discussed in the thesis involve the points at which the concentrated forces are imposed or some points whose introductions are due to the discontinuous of the cable slope, the NTM method can be employed easily to carry out the dynamic analysis. More detailed description about the NTM method can be found in [12].

1.3 Numerical computation

Although all the formulas given in the thesis are explicit expressions, numerical computation is still needed. In particular, the frequency equation needs to be solved numerically by an iterative approach. Once the frequencies are found, other formulas can be computed using the explicit formulas. Therefore, the numerical computation can be kept to a minimium.

The parameter values for the numerical computation adopted from a real transmission line are given in Table B.1 [12].

The numerical results are obtained by implementing the theoretical expressions in C programs. The subroutines for solving the equations and numerical integration of the C programs can be found in [27]. The bisection method is used to solve the frequency equations.

Numerical results are shown in several figures where each component of the figure consists of two independent mode shapes.

1.4 Contribution of the thesis

This thesis extends the NTM approach to study the dynamics of inclined cables. This approach is applied not only to flat cables but also to large-sagged cables and is very suitable for the usually complicated situation where cables are attached with many concentrated loads. A new method of discretization for the large-sagged cables with concentrated loads is also introduced. The method combined with NTM makes it easy to find the solutions of the large-sagged cables with concentrated loads.

1.5 Thesis outline

The purpose of this thesis is to use the Non-homogeneous Transfer Matrix (NTM) approach to extend the study given in [12] to inclined cables.

Chapter 1 is an introduction including two parts: one part gives a literature review, and the other part provides the necessary background for the analysis given in this thesis. The ideas to be used in this thesis are thoroughly discussed. Also, the outline and the contribution of this thesis are given in this chapter.

Chapter 2 begins with the discussion of flat cables. It focuses on the static and dynamic properties of a simple model, as well as inclined flat bare cables without concentrated loads.

Chapter 3 is again devoted to considering flat cables but with concentrated loads. After obtaining the static profile of this model, we extend the traditional Homogenous Transfer Matrix approach to NTM approach to obtain the dynamic response.

In Chapter 4, we discuss large-sagged cables and study the properties of inclined large-sagged cables without concentrated loads. From the complexity viewpoint, this model is a bridge between flat cables and large-sagged cables; while from the viewpoint of analysis, it is a bridge between the cables with and without concentrated loads.

Chapter 5 continues the discussion on large-sagged cables. But the cables now have concentrated loads. A new method of discretization the cable is introduced and the numerical results for this model are found.

Conclusions and future work are given in Chapter 6, and various constants which are used throughout this thesis are given in Appendix A. The parameter values for the numerical computation are given in Appendix B. Brief descriptions on the derivation of some important formulas are given in Appendix C.

Chapter 2

Flat bare cables

This chapter describes a relatively simple case, i.e. a flat cable without concentrated loads. We may use Fig. 1.3 and Fig. 1.4 as illustrations but assume that $F_i = 0$. The process of analyzing this case will follow that described in Chapter 1. That is, we will first transform the differential equations which describe the cable's motion in the original coordinate system to those in the rotated coordinate system.

Then, the static analysis is carried out. After finding the static tension due to q_z, we will finally perform the dynamic analysis. Analytical expressions and numerical results are also obtained for this case. For this simple model, some researchers used a parabolic function to approximate the static profile [28], some other researchers also tried to apply coordinate rotation to analyze inclined cables [29]. However, the method of rotating coordinates used in this thesis is more suitable for a consistent analysis.

2.1 Static analysis

We start with finding the static profile. First consider a flat bare cable with distributed self-weight only, and then extend the analysis to the model with a static horizontal q_z. Finally the dynamic analysis is carried out based on the static profile. The detailed discussion of the effect of out-of-plane loads on the cable can be found in [12].

2.1.1 Static analysis for the simple model

The differential equations describing this simple model are given by Eq. (1.9)- (1.11) in the original coordinate system, and by Eq. (1.12) and Eq. (1.13) in the rotated coordinate system. Because this model does not have concentrated loads, we can set $P_i = 0$ in these equations.

With the assumption $T\frac{dx}{ds} = H_x = const$ which is discussed in Section 1.2.2, Eq. (1.12) and Eq. (1.13) can be rewritten as:

$$H_x \frac{d^2x'}{dx^2} = q_y \sin\theta \frac{ds}{dx}. \tag{2.1}$$

$$H_x \frac{d^2y'}{dx^2} = -q_y \cos\theta \frac{ds}{dx}. \tag{2.2}$$

With the procedure detailed in Appendix C.1 we can obtain the solutions of the above differential equations as:

$$x' = \cos\theta x + \sin\theta \frac{H_x}{q_y} \cosh\left(\frac{q_y x}{H_x} - C_3\right) - C_4 \tan\theta, \tag{2.3}$$

$$y' = \sin\theta x - \cos\theta \frac{H_x}{q_y} \cosh\left(\frac{q_y}{H_x} x - C_3\right) + C_4. \tag{2.4}$$

where C_3 and C_4 are arbitrary integration constants, determined from the boundary conditions as

$$C_3 = -\frac{mgL_x}{2H_x} - \sinh^{-1}(\alpha_2). \tag{2.5}$$

$$C_4 = -\cos\theta \frac{H_x}{mg}\left[\cosh\left(\frac{mgL_x}{2H_x}\right)\sqrt{1+\alpha_2^2} + \sinh\left(\frac{mgL_x}{2H_x}\right)\alpha_2\right] \tag{2.6}$$

in which

$$\alpha_2 = \frac{\tan\theta L_x \frac{mg}{H_x}}{2\sinh\left(\frac{mgL_x}{2H_x}\right)}, \tag{2.7}$$

where $q_y = -mg$ have been used. Because the model under consideration is elastic, Hooke's Law must be satisfied and the geometric relationship,

$$\frac{ds}{dx} = \sqrt{\left(\frac{dx'}{dx}\right)^2 + \left(\frac{dy'}{dx}\right)^2} \tag{2.8}$$

should hold.

Substituting Eq. (2.3), Eq. (2.4) into Eq. (2.8) yields

$$s = \frac{H_x}{q_y}[\sinh(\frac{q_y}{H_x} - C_3) + \sinh(C_3)]. \tag{2.9}$$

For the special case $\theta = 0$, we have $\alpha_2 = 0$ and $H_x = H$, thus

$$C_3 = -\frac{mgL}{2H} \quad \text{and} \quad C_4 = -\frac{H}{mg}[\cosh(\frac{mgL}{2H})]$$

Therefore, when $\theta = 0$, Eq. (2.3) Eq. (2.4) and Eq. (2.9) become

$$x' = x. \tag{2.10}$$

$$y' = \frac{H}{mg}\{\cosh[\frac{mg}{H}(x - \frac{L}{2})] - \cosh(\frac{mgL}{2H})\}. \tag{2.11}$$

$$s = \frac{H}{mg}\{\sinh(\frac{mgL}{2H}) + \sinh[\frac{mg}{H}(x - \frac{L}{2})]\}. \tag{2.12}$$

It is noted from the above discussion that without the out-of-plane load q_z, the system is a planar system and can be easily dealt with. As it was pointed out in [12], the out-of-plane load greatly complicates the analysis because in this case the system is then no longer a planar system. In the case when the out-of-plane load $q_z \neq 0$ is present, we first need to find the static tension increase due to the load q_z and then do the static and dynamic solutions. By using the procedure described in Appendix C.1, we can obtain the equations for the static tension increase h_x:

$$\frac{d^2u'}{dx^2} = \frac{(q_y + mg)\sin\theta}{H_x + h_x}\frac{ds}{dx} - \frac{h_x}{H_x + h_x}\frac{d^2x'}{dx^2}. \tag{2.13}$$

$$\frac{d^2y_2'}{dx^2} = \frac{-(q_y + mg)\cos\theta}{H_x + h_x}\frac{ds}{dx} - \frac{h_x}{H_x + h_x}\frac{d^2y_1'}{dx^2}. \tag{2.14}$$

$$\frac{d^2z_2}{dx^2} = \frac{-q_z}{H_x + h_x}\frac{ds}{dx}. \tag{2.15}$$

The subscript 1 denotes the static profile without q_z (i.e $q_z = 0$), while the subscript 2 indicates the displacement due to $q_z \neq 0$.

Now, Hooke's Law is imposed together with Eq. (2.13) through Eq. (2.15) to find h_x. Hooke's Law is given by:

$$\frac{\tau}{AE} = \frac{ds' - ds}{ds} \approx \frac{(ds')^2 - (ds)^2}{2ds^2} \tag{2.16}$$

where $ds' << ds$ is assumed.

By using Eq. (2.13) to Eq. (2.16) (a detailed derivation can be found in Appendix C.1), the static tension increase due to $q_z \neq 0$ can be expressed by a 3rd-degree polynomial as:

$$(\frac{h_x}{H_x})^3 + a(\frac{h_x}{H_x})^2 + b(\frac{h_x}{H_x}) + c = 0 \tag{2.17}$$

where the coefficients a, b, and c are given below:

$$\begin{aligned} a &= 2 + \frac{1}{4}P_1P_3 + 2P_2P_4, \\ b &= 1 + \frac{1}{2}P_1P_3 + 4\frac{q_y}{(mg)^3}P_2P_4 + 4\frac{(mg+q_y)}{(mg)^3}P_2P_4, \\ c &= -\frac{1}{4}[\frac{(Q_2)}{(mg)^2} - 1]P_1P_3 + 4[\frac{(Q_2)}{(mg)^4} + \frac{q_y}{(mg)^3}]P_2P_4 \\ &\quad + 2[\frac{(Q_2)}{(mg)^4} + \frac{1}{(mg)^2} + \frac{2q_y}{(mg)^3}]P_2P_4. \end{aligned} \tag{2.18}$$

$P_i (i = 1, 2, 3, 4)$ here and Q_2 are given in Appendix A.

For the special case $\theta = 0$, Eq. (2.18) is reduced to

$$\begin{aligned} a &= 2 + \frac{1}{24}\lambda^2, \\ b &= 1 + \frac{1}{12}\lambda^2, \\ c &= -\frac{1}{24}\lambda^2[\frac{Q_2}{(mg)^2} - 1], \\ L_e &= \frac{H}{mg}[\sinh(\frac{mgL_x}{H} - \frac{mgL_x}{2h_x}) + \frac{1}{3}\sinh^3(\frac{mgL_x}{H} - \frac{mgL_x}{2H}) \\ &\quad + \sinh(\frac{mgL_x}{2h_x}) + \frac{1}{3}\sinh^3(\frac{mgL_x}{2h_x})]. \end{aligned}$$

where

$$\lambda^2 = 6(\frac{AE}{L_eH})[(\frac{H}{mg})\sinh(\frac{mgL_x}{H}) - L_x]$$

Note that the above expressions are identical to those given in [20].

In order to find h_x, we only need to solve for the root of polynomial Eq. (2.17). It is not difficult to solve Eq. (2.17), and in fact it has been shown that the polynomial has only one root [11].

2.1.2 Static analysis for the model with out-of-plane load

The procedure of finding the static profile of the cable with both static loads q_y and q_z is similar to that for the cable with q_y only. But now the horizontal component of the static tension, H_x, is the summation of that for the simple model and the horizontal static tension increase, h_x, which has been found in the previous subsection. Since the procedure is similar, we therefore omit the detail here for simplicity and only list the differential equations in rotated coordinate system and the final results here.

The differential equations for this case can be formulated in the rotated coordinate system as:

$$H_x \frac{d^2x'}{dx^2} = q_y \sin\theta \frac{ds}{dx}, \tag{2.19}$$

$$H_x \frac{d^2y'}{dx^2} = -q_y \cos\theta \frac{ds}{dx}, \tag{2.20}$$

$$H_x \frac{d^2z}{dx^2} = -q_z \frac{ds}{dx}. \tag{2.21}$$

The final static profile can be found by integrating Eq. (2.19) to Eq. (2.21) as

$$x' = -\tan\theta y' + \frac{x}{\cos\theta}, \tag{2.22}$$

$$y' = \sin\theta \frac{q_y^2}{q_y^2+q_z^2}x + \frac{q_y H_x}{q_y^2+q_z^2}\sqrt{\frac{\cos^2\theta q_y^2+q_z^2}{q_y^2+q_z^2}}\{\cosh(P_{31}) - \cosh[\frac{\sqrt{q_y^2+q_z^2}}{H_x}x - P_{31}]\}, \tag{2.23}$$

$$z = \frac{q_z}{q_y\cos\theta}y', \tag{2.24}$$

$$s = \frac{H_x\sqrt{\cos^2\theta q_y^2+q_z^2}}{\cos\theta(q_y^2+q_z^2)}\{\sinh[\frac{\sqrt{q_y^2+q_z^2}}{H_x}x - P_{31}] + \sinh(P_{31})\}, \tag{2.25}$$

where the constant P_{31} is given in Appendix A and $CONST_1$ is given by

$$CONST_1 = \sinh^{-1}[\frac{\sin\theta L_x}{2H_x\sqrt{\frac{\cos^2\theta q_y^2+q_z^2}{q_y^2+q_z^2}}\sinh(\frac{\sqrt{q_y^2+q_z^2}}{2H_x}L_x)}].$$

In the special case $\theta = 0$, we have $CONST_1 = 0$ and $H_x = H$, thus Eq. (2.22) to Eq. (2.25) become

$$x' = x,$$

$$y' = \frac{q_y H}{q_y^2+q_z^2}\{\cosh(\frac{\sqrt{q_y^2+q_z^2}}{2H}L_x) - \cosh[\frac{\sqrt{q_y^2+q_z^2}}{H}(x-\frac{L_x}{2})]\}.$$

$$z = \frac{q_z H}{q_y^2+q_z^2}\{\cosh(\frac{\sqrt{q_y^2+q_z^2}}{2H}L_x) - \cosh[\frac{\sqrt{q_y^2+q_z^2}}{H}(x-\frac{L_x}{2})]\}.$$

$$s = \frac{H}{\sqrt{q_y^2+q_z^2}}\{\sinh[\frac{\sqrt{q_y^2+q_z^2}}{H}(x-\frac{L_x}{2})] + \sinh(\frac{\sqrt{q_y^2+q_z^2}}{2H}L_x)\}.$$

which agree with those given in [11].

Note that the above static analysis applies not only to flat cables but also to large-sagged cables because the only assumption made here is that the horizontal component of the cable tension remains constant along the whole cable.

2.2 Dynamic analysis

The dynamic analysis given in this section is valid only for flat cables because of the particular assumptions which will be stated later. So, for the large sagged cables studied in the following chapter, we need to generalize the method used in this section.

For this case, the differential equations formulated in the original coordinate system can be obtained from Eq. (1.24)- (1.26) by setting $m_i = P_i = 0$. Thus we have

$$\frac{\partial}{\partial s}[(T+\tau)(\frac{dx}{ds}+\frac{\partial u}{\partial s})] = m\frac{\partial^2 u}{\partial t^2}, \tag{2.26}$$

$$\frac{\partial}{\partial s}[(T+\tau)(\frac{dy_1}{ds}+\frac{\partial y_2}{\partial s})] = m\frac{\partial^2 y_2}{\partial t^2} - q_y. \tag{2.27}$$

$$\frac{\partial}{\partial s}[(T+\tau)(\frac{dz_1}{ds}+\frac{\partial z_2}{\partial s})] = m\frac{\partial^2 z_2}{\partial t^2} - q_z. \tag{2.28}$$

Substituting the static profile obtained in the previous section into the above equations, with the aid of the transformation relationship, result in

$$\frac{\partial}{\partial s}[(T+\tau)\frac{\partial u'}{\partial s}+\tau\frac{dx'}{ds}] = m\frac{\partial^2 u'}{\partial t^2}, \tag{2.29}$$

$$\frac{\partial}{\partial s}[(T+\tau)\frac{\partial y_2'}{\partial s}+\tau\frac{dy_1'}{ds}] = m\frac{\partial^2 y_2'}{\partial t^2}, \tag{2.30}$$

$$\frac{\partial}{\partial s}[(T+\tau)\frac{\partial z_2}{\partial s}+\tau\frac{dz_1}{ds}] = m\frac{\partial^2 z_2}{\partial t^2}, \tag{2.31}$$

where the superscript denotes the differentiation with respect to rotated coordinate system and the subscript 1 represents the static profile and 2 indicates the dynamic

displacement. T is the static cable tension which is the same as that given in the last subsection and τ is the dynamic cable tension which is a function of time t and s.

For the two tensions T and τ, we can make a similar assumption as before, i.e.,

$$T = H_x \frac{ds}{dx}. \tag{2.32}$$

$$\tau(s,t) = h_x(t) \frac{ds}{dx}. \tag{2.33}$$

We will use h_x instead of $h_x(t)$ hereafter for simplicity. Substituting Eq. (2.32)-(2.33) into Eq. (2.29)- (2.31) yields

$$\frac{\partial^2 u'}{\partial x \partial s} = \frac{m}{H_x + h_x} \frac{\partial^2 u'}{\partial t^2} - \frac{h_x q_y \sin\theta}{H_x(H_x + h_x)}. \tag{2.34}$$

$$\frac{\partial^2 y_2'}{\partial x \partial s} = \frac{m}{H_x + h_x} \frac{\partial^2 y_2'}{\partial t^2} + \frac{h_x q_y \cos\theta}{H_x(H_x + h_x)}. \tag{2.35}$$

$$\frac{\partial^2 z_2}{\partial x \partial s} = \frac{m}{H_x + h_x} \frac{\partial^2 z_2}{\partial t^2} + \frac{h_x q_z}{H_x(H_x + h_x)}. \tag{2.36}$$

In order to perform linear analysis, we need another two assumptions: $H_x >> h_x$, which is usually satisfied in real applications and $dx = ds\cos\theta$ due to the assumption of a flat cable. The second assumption means that we can use the slope of the x'-axis to approximate the slope of the cable. Therefore, the results obtained in this chapter are only valid for flat cables. Large-sagged cables will be discussed in Chapters 4 and 5.

With the above two additional assumptions, Eq. (2.34)- (2.36) can be simplified to

$$\frac{\partial^2 u'}{\partial s^2} - \frac{m\cos\theta}{H_x} \frac{\partial^2 u'}{\partial t^2} = -\frac{q_y \sin\theta\cos\theta}{H_x^2} h_x, \tag{2.37}$$

$$\frac{\partial^2 y_2'}{\partial s^2} - \frac{m\cos\theta}{H_x} \frac{\partial^2 y_2'}{\partial t^2} = \frac{q_y \cos^2\theta}{H_x^2} h_x, \tag{2.38}$$

$$\frac{\partial^2 z_2}{\partial s^2} - \frac{m\cos\theta}{H_x} \frac{\partial^2 z_2}{\partial t^2} = \frac{q_z \cos\theta}{H_x^2} h_x. \tag{2.39}$$

By using the method of separation of variables [31,32] , we assume that

$$u'(s,t) = U(s)e^{j\omega t},$$

$$y_2'(s,t) = Y(s)e^{j\omega t},$$

$$z_2'(s,t) = Z(s)e^{j\omega t},$$
$$h_x(t) = he^{j\omega t}.$$

Then, Eq. (2.37)- (2.39) can be transformed to

$$\frac{d^2U(s)}{ds^2} + \beta^2 U(s) = -\frac{q_y \sin\theta\cos\theta}{H_x^2}h. \tag{2.40}$$
$$\frac{d^2Y(s)}{ds^2} + \beta^2 Y(s) = \frac{q_y \cos^2\theta}{H_x^2}h. \tag{2.41}$$
$$\frac{d^2Z(s)}{ds^2} + \beta^2 Z(s) = \frac{q_z \cos\theta}{H_x^2}h. \tag{2.42}$$

where

$$\beta^2 = \frac{m\omega^2\cos\theta}{H_x}. \tag{2.43}$$

The solutions of Eq. (2.40)- (2.42) can be easily obtained and the integral coefficients can be determined from the boundary conditions. They are given by

$$U(s) = f_1\cos(\beta s) + f_2\sin(\beta s) - \frac{q_y\sin\theta\cos\theta}{H_x^2\beta^2}h. \tag{2.44}$$
$$Y(s) = f_3\cos(\beta s) + f_4\sin(\beta s) + \frac{q_y\cos^2\theta}{H_x^2\beta^2}h. \tag{2.45}$$
$$Z(s) = f_5\cos(\beta s) + f_6\sin(\beta s) + \frac{q_z\cos\theta}{H_x^2\beta^2}h. \tag{2.46}$$

where

$$f_1 = \frac{q_y\sin\theta\cos\theta}{H_x^2\beta^2}h. \tag{2.47}$$
$$f_3 = -\frac{q_y\cos^2\theta}{H_x^2\beta^2}h. \tag{2.48}$$
$$f_5 = -\frac{q_z\cos\theta}{H_x^2\beta^2}h. \tag{2.49}$$
$$f_2\sin(\beta L_s) = \frac{q_y\sin\theta\cos\theta}{H_x^2\beta^2}h[1-\cos(\beta L_s)]. \tag{2.50}$$
$$f_4\sin(\beta L_s) = \frac{q_y\cos^2\theta}{H_x^2\beta^2}h[\cos(\beta L_s)-1]. \tag{2.51}$$
$$f_6\sin(\beta L_s) = \frac{q_z\cos\theta}{H_x^2\beta^2}h[\cos(\beta L_s)-1]. \tag{2.52}$$

To find the frequency equation, we need to find an equation derived from the Hooke's Law Eq. (2.16).Using the following relations

$$\begin{aligned}(ds')^2 &= (dx' + du')^2 + (dy_1' + dy_2')^2 + (dz_1 + dz_2)^2, \\ (ds)^2 &= (dx')^2 + (dy_1')^2 + (dz_1')^2,\end{aligned}$$

in Eq. (2.16) and keeping the resulting terms up to quadratic terms yields

$$\frac{h_x}{AE}(\frac{ds}{dx})^2 = (\frac{dx'}{dx})(\frac{du'}{ds}) + (\frac{dy_1'}{dx})(\frac{dy_2'}{ds}) + (\frac{dz_1}{dx})(\frac{dz_2}{ds}). \tag{2.53}$$

where the subscript 1 denotes the static profile obtained in Section 2.1.2 . The frequency equation can be now found by substituting the static profile into Eq. (2.53), then integrating the resulting equation from 0 to L_s. The final form of the frequency equation is found to be

$$\begin{aligned}&[\frac{(\beta L_s)^3}{\lambda^2} - \beta L_s]h + h\sin(\beta L_s) \\ - \;&(-q_y\sin\theta f_2 + q_y\cos\theta f_4 + q_z f_6)\frac{H_x^2\beta^2[1-\cos(\beta L_s)]}{\cos\theta(q_y^2+q_z^2)} = 0.\end{aligned} \tag{2.54}$$

where λ^2 is given in Appendix A.

The vibration solutions for this case are given by Eq. (2.44)- (2.47) and Eq. (2.52). Once the frequencies are solved from Eq. (2.54), then the mode shapes can be explicitly expressed by Eq. (2.44)- (2.46). There are two different cases needed to consider, according to the value of h: $h = 0$ or $h \neq 0$.

1. When $h = 0$, it is obvious to see from Eq. (2.47)- (2.49) that $f_1 = f_3 = f_5 = 0$. Then it follows from Eq. (2.44)- (2.46) that $\sin(\beta L_s)$ must be zero because otherwise there are only trivial solutions. Thus in this case, the frequency equation Eq. (2.54) is reduced to

$$(-q_y\sin\theta f_2 + q_y\cos\theta f_4 + q_z f_6)[1-\cos(\beta L_s)] = 0 \tag{2.55}$$

provided that the cable is not entirely in the vertical direction.

However, note that since Eq. (2.55) involves three constants f_2, f_4 and f_6, we need another equation to discuss the possibilities of dynamic solutions. This

additional equation can be obtained from Eq. (2.53) by using the right-end boundary conditions and the static profile as

$$f_2 = Af_4 + Bf_6. \tag{2.56}$$

where $f_1 = f_3 = f_5 = 0$ and the static profile have been used. The constants A and B are given in Appendix A. Now eliminating f_2 from Eq. (2.55) and Eq. (2.56) yields the equation

$$\tilde{C}f_4 + \tilde{D}f_6 = 0 \tag{2.57}$$

where the constants $\tilde{C}$ and $\tilde{D}$ are listed in Appendix A. According to the values of $\tilde{C}$ and $\tilde{D}$, Eq. (2.57) may have four different solutions

(a) If $\tilde{C} = \tilde{D} = 0$, f_4 and f_6 are independent while f_2 is determined by Eq. (2.56) in terms of f_4 and f_6. Thus, the mode shape functions are given by

$$f_u(s) = f_2 \sin(\beta s). \tag{2.58}$$

$$f_y(s) = f_4 \sin(\beta s). \tag{2.59}$$

$$f_z(s) = f_6 \sin(\beta s). \tag{2.60}$$

Hence, for this case, there are two independent mode shape functions with only one frequency, which is called *repeated frequency* [12].

(b) If $\tilde{C} \neq 0$, but $\tilde{D} = 0$, then Eq. (2.57) gives $f_4 = 0$ and f_6 can be chosen arbitrarily. Therefore, the mode shape functions are

$$f_u(s) = f_2 \sin(\beta s), \tag{2.61}$$

$$f_y(s) = 0, \tag{2.62}$$

$$f_z(s) = f_6 \sin(\beta s), \tag{2.63}$$

where f_2 can be obtained from Eq. (2.56) as $f_2 = Bf_6$.

(c) If $\tilde{C} = 0$, but $\tilde{D} \neq 0$, then similarly we can obtain from Eq. (2.57) that $f_6 = 0$ but f_4 can be chosen arbitrarily. Thus, Eq. (2.56) results in $f_2 = Af_4$. So the mode shape functions in this case are given by

$$f_u(s) = f_2 \sin(\beta s), \tag{2.64}$$

$$f_y(s) = f_4 \sin(\beta s), \tag{2.65}$$

$$f_z(s) = 0. \tag{2.66}$$

(d) Finally, if $\tilde{C} \neq 0$ and $\tilde{D} \neq 0$, then from Eq. (2.57), we have

$$f_6 = -\frac{\tilde{C}}{\tilde{D}} f_4$$

and then from Eq. (2.56) one can find

$$f_2 = (A - B\frac{\tilde{C}}{\tilde{D}}) f_4.$$

Therefore, the mode shape functions are given by

$$f_u(s) = f_2 \sin(\beta s), \tag{2.67}$$

$$f_y(s) = f_4 \sin(\beta s), \tag{2.68}$$

$$f_z(s) = f_6 \sin(\beta s). \tag{2.69}$$

It should be noted that for all the four cases, there exist only one frequency, determined from equation $\sin(\beta L_s) = 0$. However, there is a significant difference between case (a) and the remaining three cases: in case (a), there exist two independent mode shapes while in the remaining three cases there is only one mode shape. Therefore, for the cases (b), (c) and (d), we need to find another independent mode shape associated with $h \neq 0$.

2. When $h \neq 0$, the second mode shape is determined by Eq. (2.54). Due to $h \neq 0$, we can find from Eq. (2.50)- (2.52) that $\sin(\beta L_s) \neq 0$ and thus $\cos(\beta L_s) \neq 1$. Otherwise, a contradiction $h = 0$ will be deduced either from Eq. (2.50)- (2.52) or from Eq. (2.54). Thus, f_2, f_4 and f_6 can be uniquely be determined from

Eq. (2.50)- (2.52). Having found f_2, f_4 and f_6, we substitute them into Eq. (2.54) and simplify the resulting equation to obtain

$$\sin(\gamma)[\frac{4\gamma^3}{\lambda^2} - \gamma + \tan(\gamma)] = 0 \tag{2.70}$$

where $\gamma = \frac{\beta L_s}{2}$, and λ^2 is given in Appendix A.

The second frequency is then determined from Eq. (2.70) which actually generates an infinite series of frequencies, as expected. The mode shape functions associated with this frequency can then be found from Eq. (2.45)- (2.46) and from Eq. (2.50)- (2.52).

Finally, the mode shapes in y' and z' directions can be obtained as

$$Y(s) = -\frac{q_y \cos^2\theta}{H_x^2 \beta^2} h\{\frac{[1-\cos(\beta L_s)]}{\sin(\beta L_s)}\sin(\beta s) + [\cos(\beta s) - 1]\}. \tag{2.71}$$

$$Z(s) = -\frac{q_z \cos\theta}{H_x^2 \beta^2} h\{\frac{[1-\cos(\beta L_s)]}{\sin(\beta L_s)}\sin(\beta s) + [\cos(\beta s) - 1]\}. \tag{2.72}$$

To find the mode shape in x' direction, Eq. (2.53) is used again together with

$$(\frac{ds}{dx})^2 = (\frac{dx'}{dx})^2 + (\frac{dy'}{dx})^2 + (\frac{dz'}{dx})^2 \tag{2.73}$$

Substituting the static profile given by Eq. (2.23)- (2.25) into Eq. (2.53) with the aid of Eq. (2.71)- (2.73) yields the differential equation for the mode shape in x' direction

$$\begin{aligned}\frac{dU}{ds} &= \frac{\frac{h}{AE}[\frac{q_y^2+q_z^2}{q_y^2\cos^2\theta} TCS_1^2 - \frac{2\sin\theta}{\cos^2\theta} TCS_1 + \frac{1}{\cos^2\theta}]}{TCS_2} \\ &+ \frac{TCS_1 \frac{q_y \cos^2\theta}{H_x^2\beta^2} hTCC}{TCS_2} \\ &+ \frac{\frac{q_z}{q_y\cos\theta} TCS_1 \frac{q_z\cos\theta}{H_x^2\beta^2} hTCC}{TCS_2},\end{aligned} \tag{2.74}$$

where the constants TCS_1, TCS_2 and TCC are given in Appendix A.

Although the u'-mode defined by the differential expression Eq. (2.74) can be solved analytically, it may be easy to use some numerical method such as the one described in [27] to obtain a numerical solution. Therefore, the three mode shapes for this subcase $h \neq 0$ are given by Eq. (2.71) and Eq. (2.72), and the integration of Eq. (2.74).

2.3 Results and discussion

The results obtained in this chapter are based on a practical transmission line whose parameter values are listed in Appendix B [12] and Fig. 1.4 can serve as an illustration by assuming $F_i = 0$. The cable is studied in three situations, with horizontal, 30^o inclined, and 60^o inclined supports. For each situation, we show the mode shapes in each direction of u', y' and z.

There are two general situations according to the values of h based on the derivations in the last section. The results given in this chapter are obtained when both $\bar{C}$ and $\bar{D}$ are nonzero, see Eq. (2.57). Therefore, from the discussion given in the last section, there are two sets of mode shapes for each direction. Consequently, there are two curves shown in the figures. The solid lines correspond to the situation when $h \neq 0$ while the dash lines correspond to the situation when $h = 0$. This feature is also applicable to the results given in the following chapters. ω_1 and ω_2 in the figures are frequencies respectively correspond to the solid and dash mode shapes.

Because the Lagrangian coordinate along the cable differs from one case to another and it is different even when the angle of inclination is different, we use nondimesional Lagrangian coordinate to facilitate the comparison, as it was used in [6.9] . This nondimension characteristic will also be used in the following chapters.

The results are shown in Fig. 2.1 to Fig. 2.6. Each figure gives vibration components in u', y' and z directions, and each component has two independent mode shapes. It can be seen from these figures that, for different order of frequencies, there always exist both symmetric and asymmetric mode shapes, especially in the u' direction (see part (a) in each of the figures). For the same order of frequencies, the two sets of mode shapes in u' direction are totally different. The center for u'-mode at about the midpoint of the cable when $h \neq 0$ (solid lines) and the cable is horizontal (see Fig. 2.1 and 2.2) but no such region when $h = 0$ (dash lines). The y' and z modes are approximately sine waves for both $h = 0$ and $h \neq 0$. From part (a) of Fig. 2.3 to Fig. 2.6, it can be observed that the central region graduately moves from the midpoint to the left of the cable when the cable is inclined. This is reasonable

to be seen from Fig. 1.4. However, the u mode shapes associated with $h = 0$ (dash lines) do not have the same sensitivity to the inclination of the cable. Neither do the y' and z mode shapes.

An interesting result is observed when we compare the two mode shape curves in each graph on y' mode with z mode. The behavior of the two mode shapes associated respectively with $h = 0$ and $h \neq 0$ for the y' direction is just opposite to the behavior of the two mode shapes for the z direction. For example, in Fig. 2.3 (b), the two mode shapes in y' direction are almost superimposed while in (c), the two mode shapes in z direction have an almost 180^o phase difference. The same phenomenon can also be observed in Fig. 2.4 (b) and (c).

Furthermore, from the process of solving the frequency equation, we find that for the same order frequencies, the frequency is a little lower when the support is inclined than that when the support is horizontal.

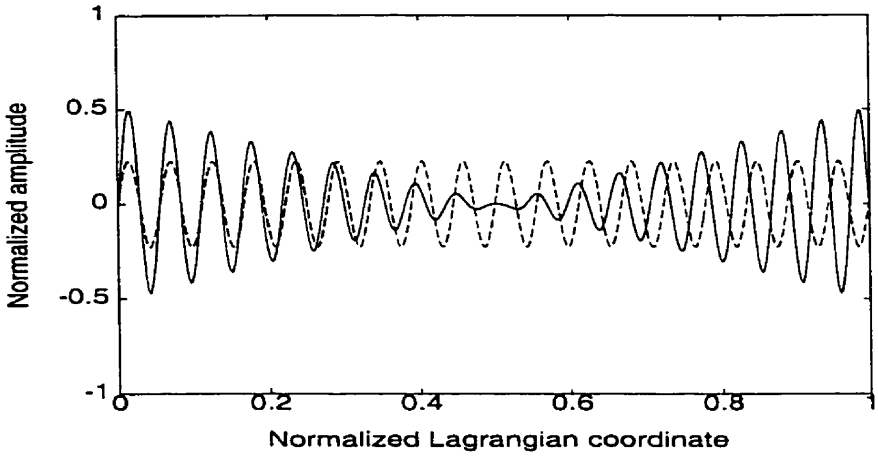

(a)

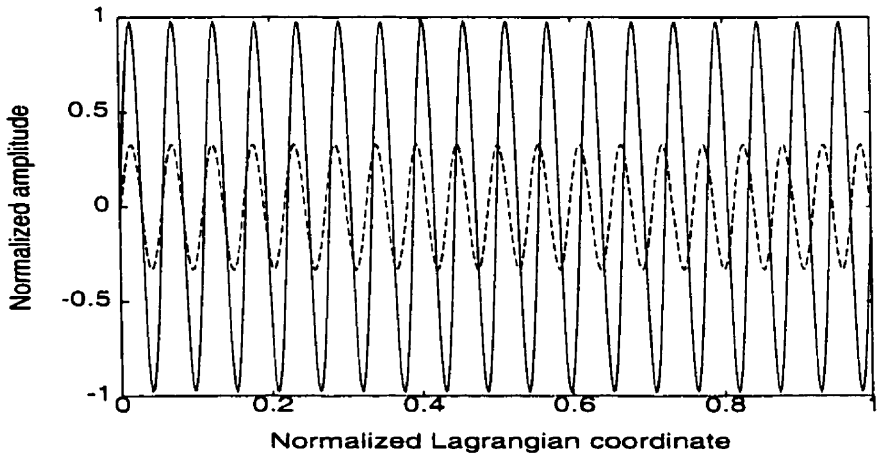

(b)

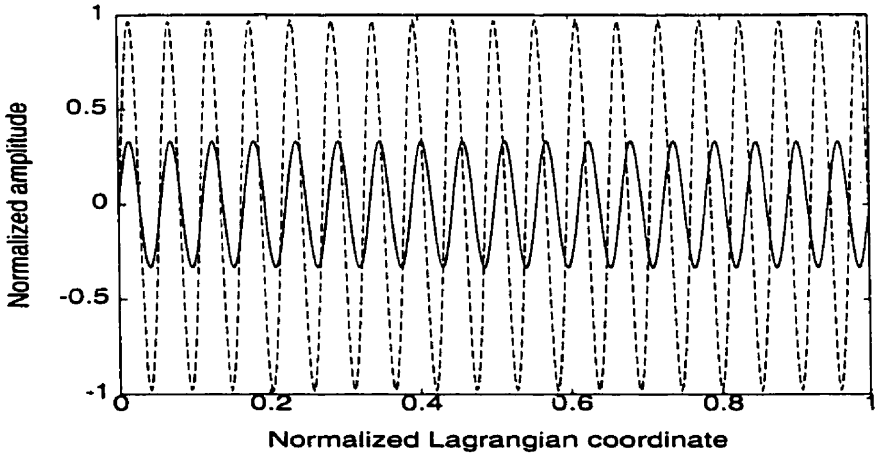

(c)

Figure 2.1: Symmetric mode shapes associated with frequencies $\omega_1 = 10.32Hz$, $\omega_2 = 11.2Hz$ for the horizontal support:

(a) u'-mode; (b) y'-mode; and (c) z-mode

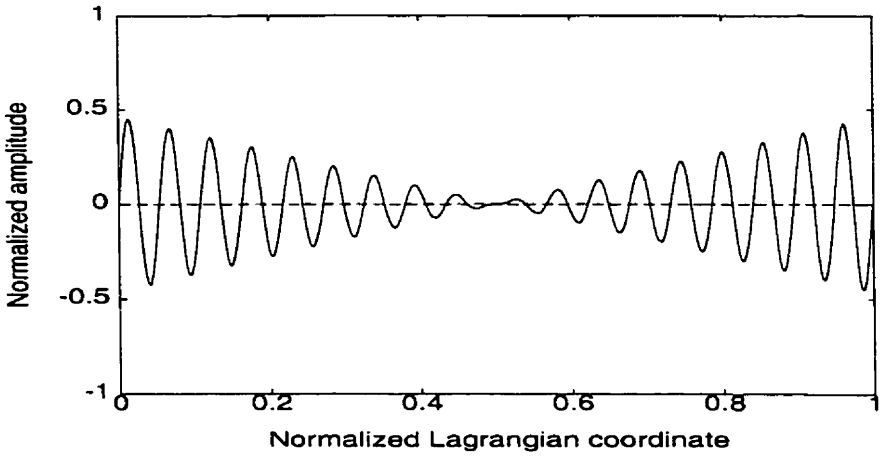

(a)

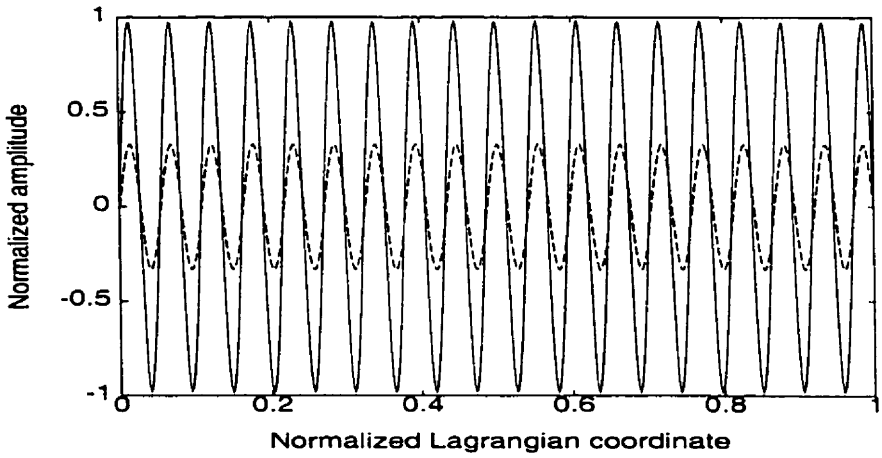

(b)

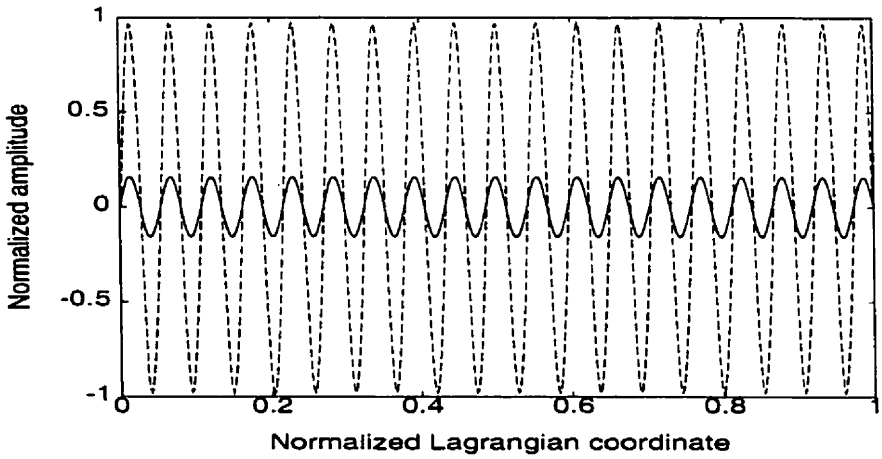

(c)

Figure 2.2: Asymmetric mode shapes associated with frequencies $\omega = 10.28Hz$, $\omega_2 = 12.3Hz$ for the horizontal support:

(a) u'-mode; (b) y'-mode; and (c) z-mode

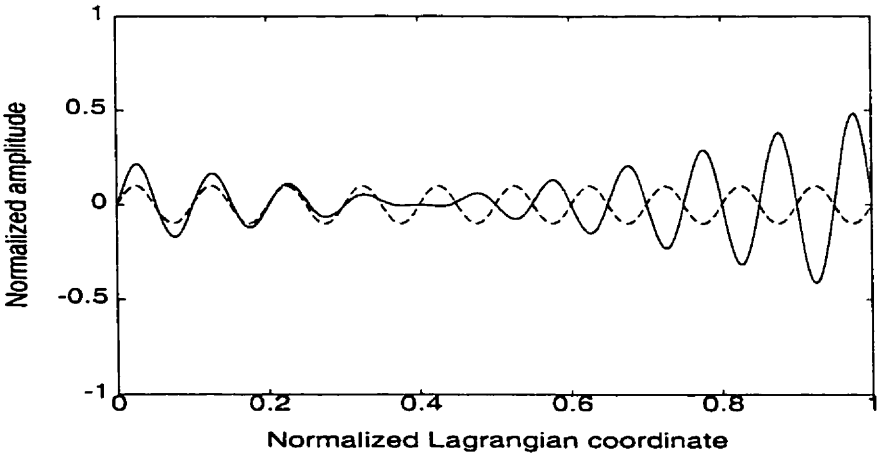

(a)

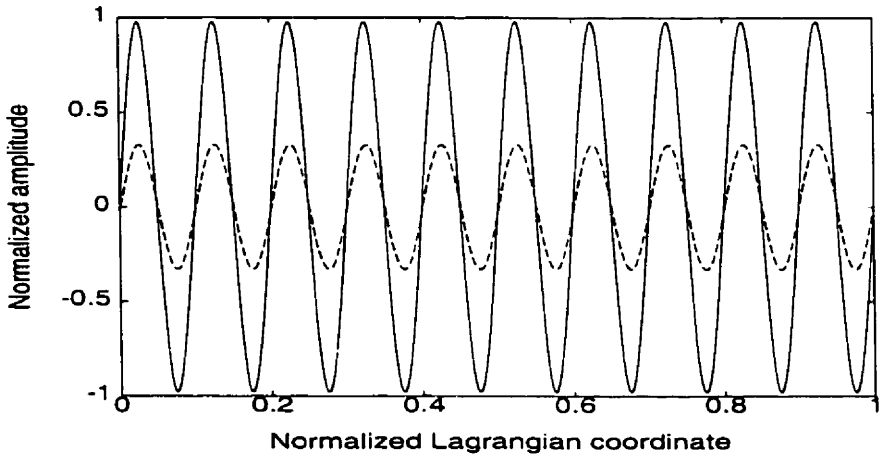

(b)

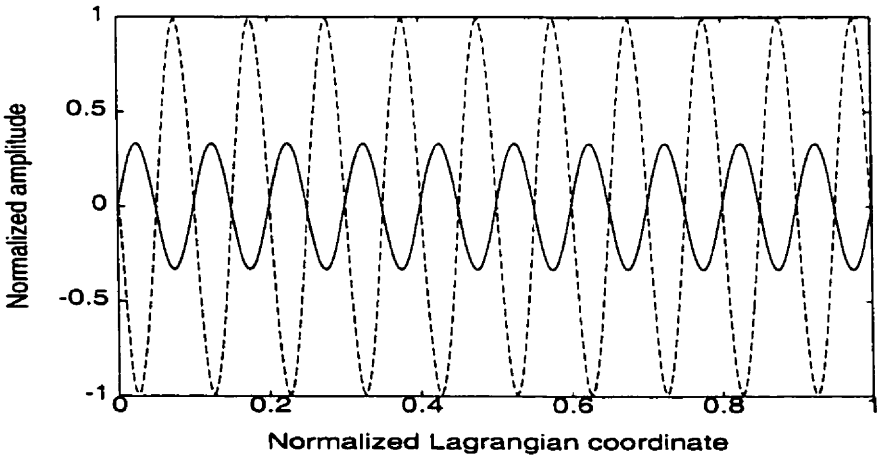

(c)

Figure 2.3: Symmetric mode shapes associated with frequencies $\omega = 5.15Hz$, $\omega_2 = 10.68Hz$ for the inclined support with 30°:

(a) u'-mode; (b) y'-mode; and (c) z-mode

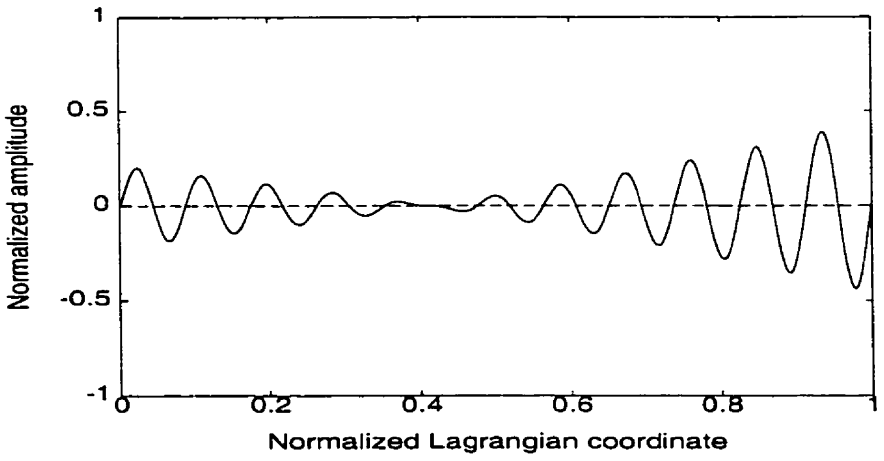

(a)

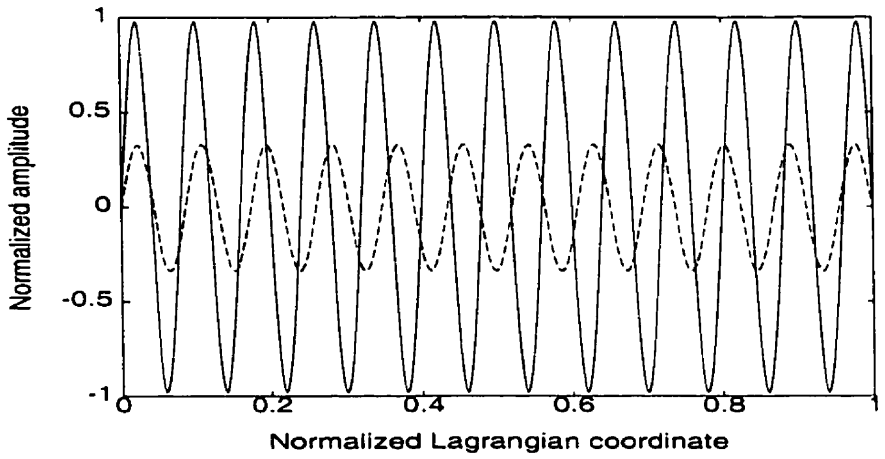

(b)

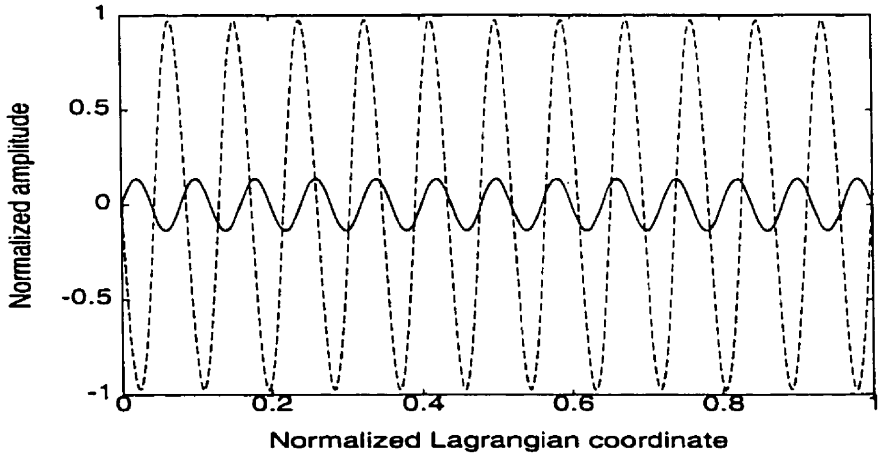

(c)

Figure 2.4: Asymmetric mode shapes assoicated with frequencies $\omega = 6.08Hz$, $\omega_2 = 11.6Hz$ for the inclined support with 30^o:

(a) u'-mode; (b) y'-mode: and (c) z-mode

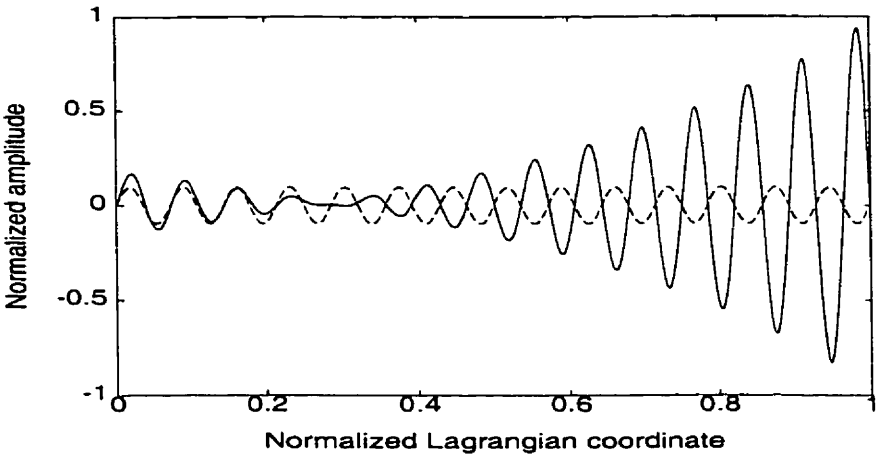

(a)

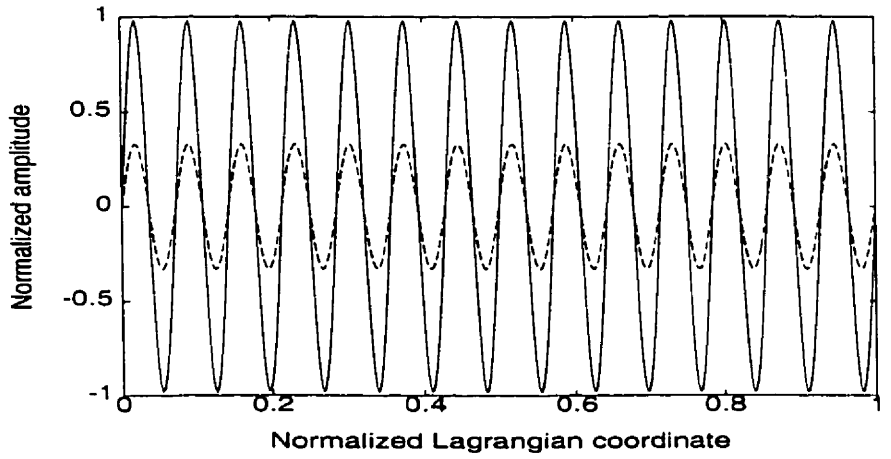

(b)

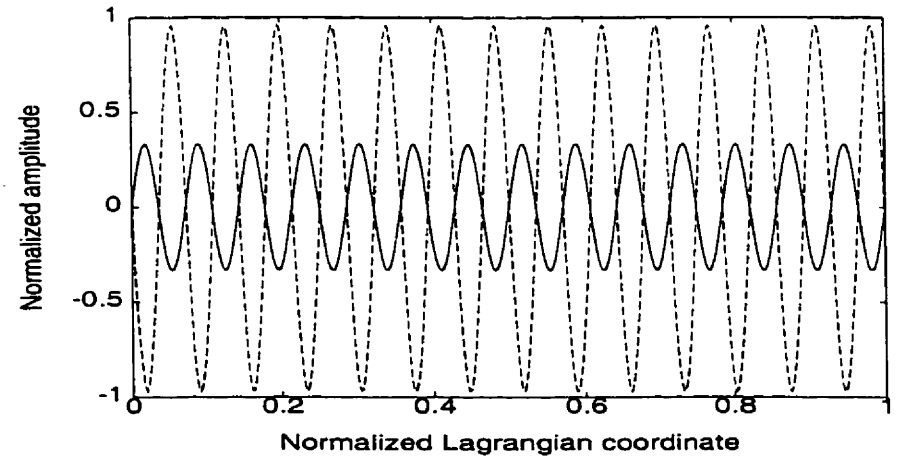

(c)

Figure 2.5: Symmetric mode shapes associated with frequencies $\omega = 4.12Hz$, $\omega_2 = 6.2Hz$ for the inclined support with 60^o:

(a) u'-mode; (b) y'-mode; and (c) z-mode

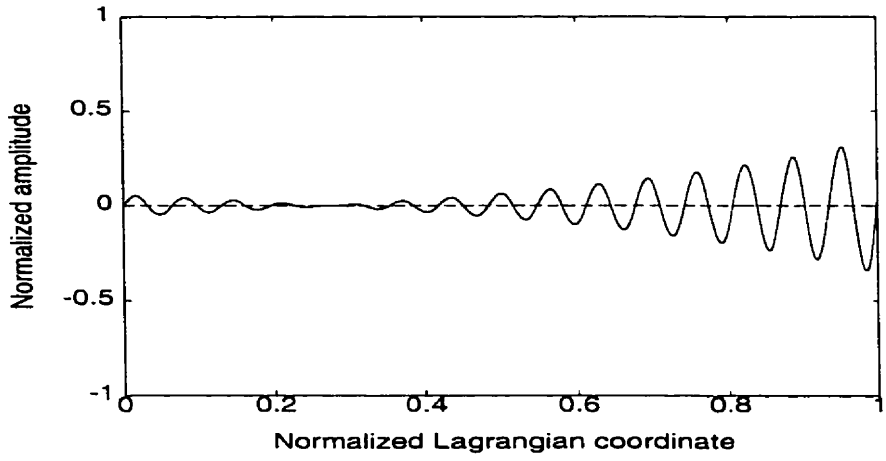

(a)

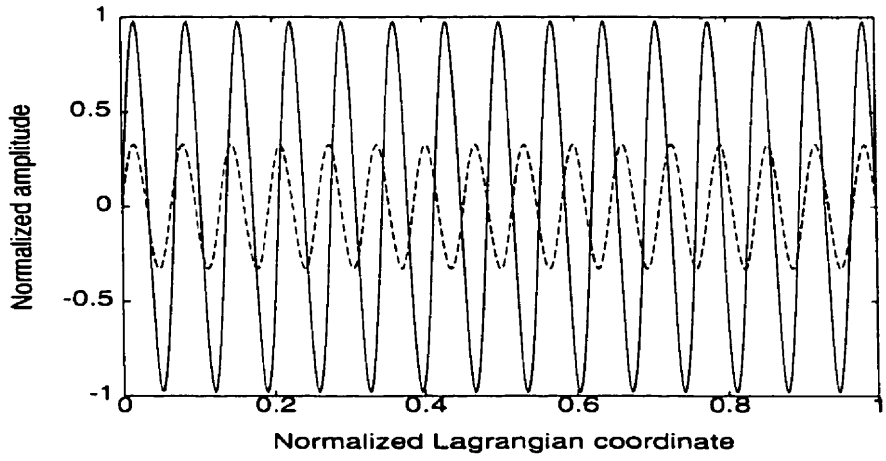

(b)

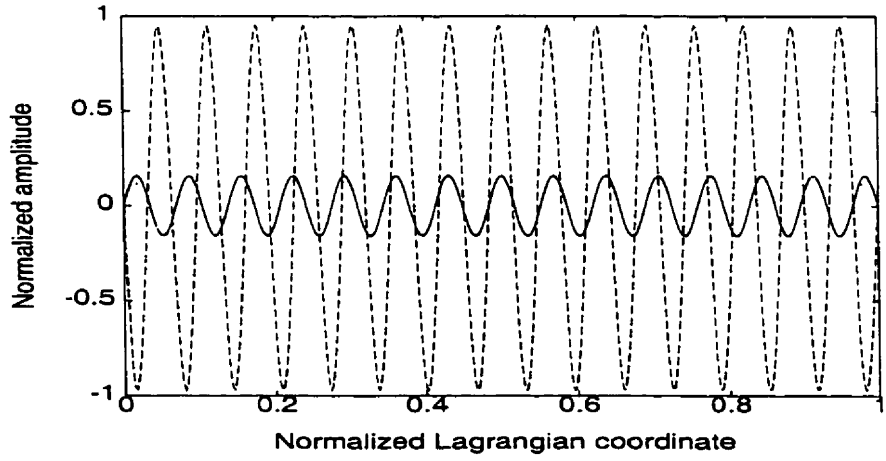

(c)

Figure 2.6: Asymmetric mode shapes associated with frequencies $\omega = 4.39Hz$, $\omega_2 = 6.8Hz$ for the inclined support with 60^o:

(a) u'-mode; (b) y'-mode; and (c) z-mode

Chapter 3

Flat cables with concentrated loads

In Chapter 2 we have discussed both static and dynamic analysis for flat cables without concentrated loads. In this chapter, we will extend the analysis to the cables with concentrated loads. As it will be seen later, the static analysis is similar to that in Chapter 2, while the dynamic analysis has significant difference.

Although we will follow the similar procedure described in the previous chapter, it should be noted that the differential equations discussed in this chapter are piece wisely smooth. Therefore, not only the boundary conditions but also the continuity conditions are needed for solving the equations. Moreover, the discontinuity at the points where concentrated loads are imposed must be taken into account. To do this, δ-function is introduced to make it easy to discuss the effect of the point forces. The illustrating figures used in this chapter can be still referred to Fig. 1.3 and Fig. 1.4.

3.1 Static analysis

In order to find the static profile of the cable with concentrated loads, the first step is to find the static tension increase due to concentrated loads. The differential equations to determine the static tension increase can be formulated as

$$\frac{d}{ds}[h_x\frac{dx'}{dx} + (H_x + h_x)\frac{du'}{dx}] = -P_i\delta(s - s_i)\sin\theta, \tag{3.1}$$

$$\frac{d}{ds}[h_x\frac{dy_1'}{dx} + (H_x + h_x)\frac{dy_2'}{dx}] = P_i\delta(s - s_i)\cos\theta, \tag{3.2}$$

$$\frac{d}{ds}[h_x\frac{dz_1}{dx} + (H_x + h_x)\frac{dz_2}{dx}] = 0, \tag{3.3}$$

where the rotation relationship given by Eq. (1.1) and the static profile described by Eq. (2.22)- (2.25) as well as the assumptions $T = H_x\frac{ds}{dx}$ and $\tau = h_x\frac{ds}{dx}$ have been used. The δ represents the Dirac Delta function with the property

$$\int_{-\infty}^{+\infty} \delta(0) \;=\; 1$$

In Eq. (3.1)- (3.3)), the subscript 1 denotes the static profile of the cable without concentrated loads, while 2 represents the displacement caused by the concentrated loads. The subscript i denotes the i-th point at which a concentrated loads is imposed.

With the properties of δ-function, we can rewrite Eq. (3.1) and Eq. (3.2) as

$$\frac{d}{ds}[h_x\frac{dx'}{dx} + (H_x + h_x)\frac{du_i'}{dx}] \;=\; 0. \tag{3.4}$$

$$\frac{d}{ds}[h_x\frac{dy_1'}{dx} + (H_x + h_x)\frac{dy_{2i}'}{dx}] \;=\; 0. \tag{3.5}$$

and integrate Eq. (3.1)- (3.3) to obtain the discontinuity conditions on the slope of the cable as follows:

$$\frac{du_{i+1}'(x_{i+1})}{dx} - \frac{du_i'(x_{i+1})}{dx} \;=\; \frac{-P_{i+1}\sin\theta}{H_x + h_x}. \tag{3.6}$$

$$\frac{dy_{2i+1}'(x_{i+1})}{dx} - \frac{dy_{2i}'(x_{i+1})}{dx} \;=\; \frac{P_{i+1}\cos\theta}{H_x + h_x}. \tag{3.7}$$

$$\frac{dz_{2i+1}(x_{i+1})}{dx} - \frac{dz_{2i}(x_{i+1})}{dx} \;=\; 0. \tag{3.8}$$

The subscript 2 in Eq. (3.4)- (3.8) denotes the cable displacement due to the concentrated loads. The continuity conditions of the cable at the points can be easily obtained as

$$u_{i+1}'(x_{i+1}) = u_i'(x_{i+1}), \tag{3.9}$$

$$y_{2i+1}'(x_{i+1}) = y_{2i}'(x_{i+1}), \tag{3.10}$$

$$z_{2i+1}(x_{i+1}) = z_{2i}(x_{i+1}). \tag{3.11}$$

The boundary conditions for the cable are assumed to be fixed as

$$x'(0) = 0 \qquad x'(L_x) = L, \tag{3.12}$$

$$y_1'(0) = 0 \qquad y_1'(L_x) = 0, \tag{3.13}$$

$$z_1(0) = 0 \qquad z_1(L_x) = 0, \tag{3.14}$$

for the original static profile, and

$$u_0'(0) = 0 \qquad u_N'(L_x) = 0. \tag{3.15}$$

$$y_{20}'(0) = 0 \qquad y_{2N}'(L_x) = 0. \tag{3.16}$$

$$z_{20}(0) = 0 \qquad z_{2N}(L_x) = 0. \tag{3.17}$$

for the static tension increase.

The solutions for Eq. (3.4), (3.5) and Eq. (3.3) can be obtained as

$$u_i' = \frac{C_i}{H_x + h_x}x - \frac{h_x}{h_x + H_x}x_i' + D_i. \tag{3.18}$$

$$y_{2i}' = \frac{E_i}{H_x + h_x}x - \frac{h_x}{H_x + h_x}y_{1i}' + F_i. \tag{3.19}$$

$$z_{2i} = -\frac{h_x}{H_x + h_x}z_1. \tag{3.20}$$

where C_i, D_i, E_i and F_i are the integral constants determined from the conditions Eq. (3.6)- (3.17) and the explicit expressions are given in Appendix A.

Following the procedure discussed in Chapter 2, we can similarly use the Hooke's Law to find the equation for the static tension increase due to concentrated loads, given by

$$\begin{aligned}\frac{h_x}{AE}(\frac{ds}{dx})^3 = {} & \frac{1}{2}(\frac{du_i'}{dx})^2 + \frac{1}{2}(\frac{dy_{2i}'}{dx})^2 + \frac{1}{2}(\frac{dz_{2i}'}{dx})^2 \\ & + (\frac{dx'}{dx})(\frac{du_i'}{dx}) + (\frac{dy_{1i}'}{dx})(\frac{dy_{2i}'}{dx}) + (\frac{dz_1}{dx})(\frac{dz_{2i}}{dx}).\end{aligned} \tag{3.21}$$

Substituting the static profile of the cable without concentrated loads which are given by Eq. (2.22)- (2.25) into Eq. (3.21) and integrating the resulting equation yields a similar 3rd-degree polynomial for $\frac{h_x}{H_x}$.

$$(\frac{h_x}{H_x})^3 + a(\frac{h_x}{H_x})^2 + b(\frac{h_x}{H_x}) + c = 0. \tag{3.22}$$

where the coefficients a, b, and c are given in Appendix A. In the special case $\theta = 0$, Eq. (3.22) becomes the one obtained in [11].

We can analytically solve $\frac{h_x}{H_x}$ from the polynomial Eq. (3.22) which has only one positive root. H_x has already been obtained in Chapter 2, so the static tension increase h_x is uniquely determined, and thus τ is found from $\tau = h_x\frac{ds}{dx}$.

Having found h_x, we can now formulate the equations to determine the static profile for the cable with concentrated loads

$$\frac{d}{ds}(H_x\frac{dx'}{dx}) = q_y\sin\theta - P_i\delta(s-s_i)\sin\theta. \quad (3.23)$$

$$\frac{d}{ds}(H_x\frac{dy'}{dx}) = -q_y\cos\theta + P_i\delta(s-s_i)\cos\theta. \quad (3.24)$$

$$\frac{d}{ds}(H_x\frac{dz}{dx}) = -q_z. \quad (3.25)$$

where the equation $T = H_x\frac{ds}{dx}$ has been used. Note that here H_x includes the static tension increase h_x due to the concentrated loads.

With the property of δ-function, Eq. (3.23)- (3.24) can be further simplified as

$$\frac{d^2x_i'}{dx^2} = (\frac{q_y\sin\theta}{H_x})\frac{ds_i}{dx}. \quad (3.26)$$

$$\frac{d^2y_i'}{dx^2} = (-\frac{q_y\cos\theta}{H_x})\frac{ds_i}{dx}. \quad (3.27)$$

$$\frac{d^2z_i'}{dx^2} = (-\frac{q_z}{H_x})\frac{ds_i}{dx}. \quad (3.28)$$

and integrating Eq. (3.23)- (3.25) yields the discontinuity conditions on the slope of the cable:

$$\frac{dx_{i+1}'(x_{i+1})}{dx} - \frac{dx_i'(x_{i+1})}{dx} = -\frac{P_{i+1}\sin\theta}{H_x}. \quad (3.29)$$

$$\frac{dy_{i+1}(x_{i+1})}{dx} - \frac{dy_i(x_{i+1})}{dx} = \frac{P_{i+1}\cos\theta}{H_x}. \quad (3.30)$$

$$\frac{dz_{i+1}(x_{i+1})}{dx} - \frac{dz_i(x_{i+1})}{dx} = 0. \quad (3.31)$$

where the subscript i again denotes the i-th point at which a concentrated load is located. The continuity conditions of the cable and the boundary conditions are given by

$$x_{i+1}'(x_{i+1}) = x_i'(x_{i+1}), \quad (3.32)$$

$$y_{i+1}'(x_{i+1}) = y_i'(x_{i+1}), \quad (3.33)$$

$$z_{i+1}'(x_{i+1}) = z_i'(x_{i+1}), \quad (3.34)$$

$$x_0'(0) = 0 \qquad x_N'(L_x) = L, \quad (3.35)$$

$$y_0'(0) = 0 \qquad y_N'(L_x) = 0, \quad (3.36)$$

$$z_0'(0) = 0 \qquad z_N'(L_x) = 0. \quad (3.37)$$

It is not difficult to solve the differential equations Eq. (3.26)- (3.28) with the boundary conditions as well as the discontinuity conditions and continuity conditions. The static profile given in the Lagrangian coordinate s can be obtained using the same method described in Section 2.1.2, given by

$$x_i'(x) = -\tan\theta y_i' + \frac{x}{\cos\theta}, \tag{3.38}$$

$$y_i'(x) = -\frac{(q_z\cos\theta D_{1i} - q_y\sin\theta)q_y}{q_y^2+q_z^2}x - \frac{q_y H_x\cos\theta}{q_y^2+q_z^2}TI_1\cosh(TI_2) + F_{1i}, \tag{3.39}$$

$$z_i(x) = \frac{q_z}{q_y\cos\theta}y_i' + D_{1i}x + D_{2i}, \tag{3.40}$$

$$s_i(x) = G_i + \frac{H_x}{\sqrt{q_y^2+q_z^2}}TI_1\sinh(TI_2). \tag{3.41}$$

where the constants D_{1i}, D_{2i}, F_{1i}, TI_1, TI_2 and G_i can be found in Appendix A.

There are two constants E_{1i} and F_{1i}, involved in the above expressions, which are given in coupled formulas:

$$F_{10} = \frac{q_y H_x\cos\theta}{q_y^2+q_z^2}TI_0\cosh(E_{10}).$$

$$F_{1N} = \frac{(q_z\cos\theta D_{1N} - q_y\sin\theta)q_y}{q_y^2+q_z^2}L_x + \frac{q_y H_x\cos\theta}{q_y^2+q_z^2}TI_N\cosh(TI_{3N}).$$

$$F_{1(i+1)} = F_{1i} + x_{i+1}TI_4 + \frac{q_y H_x\cos\theta}{q_y^2+q_z^2}[TI_{11}\cosh(TI_{31}) - TI_1\cosh(TI_3)].$$

$$E_{1(i+1)} = \frac{\sqrt{q_y^2+q_z^2}}{H_x}x_{i+1} - \sinh^{-1}\left\{\frac{\frac{\sqrt{q_y^2+q_z^2}}{q_y\cos\theta}\left[-\frac{P_{i+1}\cos\theta}{H_x} - TI_4\right]}{TI_{11}} + \frac{TI_1}{TI_{11}}\sinh(TI_3)\right\}.$$

These equations can be solved by finding E_0 first with a simple numerical method, and then all the other expressions can be explicitly obtained.

3.2 Dynamic analysis

The dynamic analysis on the cable with concentrated loads is more involved than the cable without concentrated loads. It requires to use NTM approach due to the

existence of the concentrated loads on the cable which give rise to non-homogeneous terms in the transfer matrix. The traditional method of transfer matrix [54] can not deal with the non-homogeneous terms. However, we can use the NTM approach to easily deal with the terms as seen next.

The differential equations describing the dynamic response of the cable are given in rotated coordinate system by

$$\frac{\partial^2 u'}{\partial x \partial s} - \frac{m}{H_x + h_x}\frac{\partial^2 u'}{\partial t^2} - \frac{m_i \delta(s - s_i)}{H_x + h_x}\frac{\partial^2 u'}{\partial t^2} = -\frac{h_x}{H_x + h_x}\frac{d^2 x'}{dxds}. \quad (3.42)$$

$$\frac{\partial^2 y'_2}{\partial x \partial s} - \frac{m}{H_x + h_x}\frac{\partial^2 y'_2}{\partial t^2} - \frac{m_i \delta(s - s_i)}{H_x + h_x}\frac{\partial^2 y'_2}{\partial t^2} = -\frac{h_x}{H_x + h_x}\frac{d^2 y'}{dxds}. \quad (3.43)$$

$$\frac{\partial^2 z_2}{\partial x \partial s} - \frac{m}{H_x + h_x}\frac{\partial^2 z_2}{\partial t^2} - \frac{m_i \delta(s - s_i)}{H_x + h_x}\frac{\partial^2 z_2}{\partial t^2} = -\frac{h_x}{H_x + h_x}\frac{d^2 z}{dxds}. \quad (3.44)$$

where the rotation relationship Eq. (1.1) and the assumptions $T = H_x\frac{ds}{dx}$ and $\tau = h_x(t)\frac{ds}{dx}$ have been used. The subscript 2 denotes the displacements with respect to the static profile.

Substituting the static profile described by Eq. (3.38)- (3.41) into Eq. (3.42)- (3.44) results in

$$\frac{\partial^2 u'}{\partial x \partial s} - \frac{m}{H_x}\frac{\partial^2 u'}{\partial t^2} - \frac{m_i \delta(s - s_i)}{H_x}\frac{\partial^2 u'}{\partial t^2} = -\frac{h_x q_y \sin\theta}{H_x^2} + \frac{h_x P_i \delta(s - s_i)\sin\theta}{H_x^2} \quad (3.45)$$

$$\frac{\partial^2 y'_2}{\partial x \partial s} - \frac{m}{H_x}\frac{\partial^2 y'_2}{\partial t^2} - \frac{m_i \delta(s - s_i)}{H_x}\frac{\partial^2 y'_2}{\partial t^2} = \frac{h_x q_y \cos\theta}{H_x^2} - \frac{h_x P_i \delta(s - s_i)\cos\theta}{H_x^2}. \quad (3.46)$$

$$\frac{\partial^2 z_2}{\partial x \partial s} - \frac{m}{H_x}\frac{\partial^2 z_2}{\partial t^2} - \frac{m_i \delta(s - s_i)}{H_x}\frac{\partial^2 z_2}{\partial t^2} = \frac{h_x q_z}{H_x^2}. \quad (3.47)$$

where it has been assumed that $H_x >> h_x$. Furthermore, with the aid of the property of δ-function, Eq. (3.45)- (3.47) can be transformed to

$$\frac{\partial^2 u'_i}{\partial s^2} - \frac{m\cos\theta}{H_x}\frac{\partial^2 u'_i}{\partial t^2} = -\frac{h_x q_y \sin\theta\cos\theta}{H_x^2}. \quad (3.48)$$

$$\frac{\partial^2 y'_{2i}}{\partial s^2} - \frac{m\cos\theta}{H_x}\frac{\partial^2 y'_{2i}}{\partial t^2} = \frac{h_x q_y \cos^2\theta}{H_x^2}. \quad (3.49)$$

$$\frac{\partial^2 z'_{2i}}{\partial s^2} - \frac{m\cos\theta}{H_x}\frac{\partial^2 z'_{2i}}{\partial t^2} = \frac{h_x q_z \cos\theta}{H_x^2}. \quad (3.50)$$

The discontinuity conditions can be found by integrating Eq. (3.45)- (3.47) as follows:

$$\frac{\partial u'_{i+1}(s_{i+1})}{\partial x} - \frac{\partial u'_i(s_{i+1})}{\partial x} = \frac{m_{i+1}}{H_x}\frac{\partial^2 u'_i}{\partial t^2} + \frac{h_x P_{i+1}\sin\theta}{H_x^2}. \quad (3.51)$$

$$\frac{\partial y'_{2(i+1)}(s_{i+1})}{\partial x} - \frac{\partial y'_{2i}(s_{i+1})}{\partial x} = \frac{m_{i+1}}{H_x}\frac{\partial^2 y'_{2i}}{\partial t^2} - \frac{h_x P_{i+1}\cos\theta}{H_x^2}. \tag{3.52}$$

$$\frac{\partial z_{2(i+1)}(s_{i+1})}{\partial x} - \frac{\partial z_{2i}(s_{i+1})}{\partial x} = \frac{m_{i+1}}{H_x}\frac{\partial^2 z_{2i}}{\partial t^2}. \tag{3.53}$$

The boundary conditions and the continuity conditions are the same as that given in Section 3.1 (Eq. (3.6)- (3.17)).

In order to derive the frequency equation, we again start from the Hooke's Law, which gives the equation

$$\frac{h_x}{AE}(\frac{ds}{dx})^2 = \frac{dx'_{1i}}{dx}\frac{du'_{2i}}{ds} + \frac{dy'_{1i}}{dx}\frac{dy'_{2i}}{ds} + \frac{dz_{1i}}{dx}\frac{dz_{2i}}{ds} \tag{3.54}$$

where only terms up to quadratic are used. The subscript 1 denotes the static profile while 2 the dynamic displacement measured from the static profile.

The mode shape functions can be found by using the method of separation of variables. It is similar to that discussed in Section 2.2. However, in this case the solutions are piece wisely smooth, and can be written as

$$U_i(s) = C_{1i}\cos\beta(s-s_i) + C_{2i}\sin\beta(s-s_i) - \frac{hq_y\sin\theta\cos\theta}{\beta^2 H_x^2}, \tag{3.55}$$

$$Y_i(s) = C_{3i}\cos\beta(s-s_i) + C_{4i}\sin\beta(s-s_i) + \frac{hq_y\cos^2\theta}{\beta^2 H_x^2}, \tag{3.56}$$

$$Z_i(s) = C_{5i}\cos\beta(s-s_i) + C_{6i}\sin\beta(s-s_i) + \frac{hq_z\cos\theta}{\beta^2 H_x^2}. \tag{3.57}$$

In order to solve the integration constants, the boundary conditions and continuity conditions given by Eq. (3.29)- (3.37) need to be modified according to the method of separation of variables. The discontinuity conditions are

$$\frac{dU_{i+1}(s_{i+1})}{ds} - \frac{dU_i(s_{i+1})}{ds} = -\frac{m_{i+1}\omega^2\cos\theta}{H_x}U_i + \frac{hP_{i+1}\sin\theta\cos\theta}{H_x^2}, \tag{3.58}$$

$$\frac{dY_{i+1}(s_{i+1})}{ds} - \frac{dY_i(s_{i+1})}{ds} = -\frac{m_{i+1}\omega^2\cos\theta}{H_x}Y_i - \frac{hP_{i+1}\cos^2\theta}{H_x^2}, \tag{3.59}$$

$$\frac{dZ_{i+1}(s_{i+1})}{ds} - \frac{dZ_i(s_{i+1})}{ds} = -\frac{m_{i+1}\omega^2\cos\theta}{H_x}Z_i. \tag{3.60}$$

The boundary conditions are

$$U_0(0) = 0 \qquad U_N(L_s) = 0, \tag{3.61}$$

$$Y_0(0) = 0 \qquad Y_N(L_s) = 0, \tag{3.62}$$

$$Z_0(0) = 0 \qquad Z_N(L_s) = 0. \tag{3.63}$$

and the continuity conditions are

$$U_{i+1}(s_{i+}) = U_i(s_{i+1}). \tag{3.64}$$

$$Y_{i+1}(s_{i+}) = Y_i(s_{i+1}). \tag{3.65}$$

$$Z_{i+1}(s_{i+}) = Z_i(s_{i+1}). \tag{3.66}$$

The integration constants in Eq. (3.55)- (3.57) can be obtained from these modified discontinuity conditions as well as boundary conditions and continuity conditions. They are given by:

$$\begin{pmatrix} C_{1i} \\ C_{2i} \end{pmatrix} = [D_0^i] \begin{pmatrix} C_{10} \\ C_{20} \end{pmatrix} + \vec{r}_i(\frac{h \sin\theta \cos\theta}{\beta^2 H_x^2}). \tag{3.67}$$

$$\begin{pmatrix} C_{3i} \\ C_{4i} \end{pmatrix} = [D_0^i] \begin{pmatrix} C_{30} \\ C_{40} \end{pmatrix} - \vec{r}_i(\frac{h \cos^2\theta}{\beta^2 H_x^2}). \tag{3.68}$$

$$\begin{pmatrix} C_{5i} \\ C_{6i} \end{pmatrix} = [D_0^i] \begin{pmatrix} C_{50} \\ C_{60} \end{pmatrix} - \vec{s}_i(\frac{h \cos\theta}{\beta^2 H_x^2}). \tag{3.69}$$

where $[D_0^i]$ is the transfer matrix, given by

$$[D_0^i] = [D_{i-1}^i][D_0^{i-1}].$$

$$[D_{i-1}^i] = \begin{bmatrix} D_{i-1}^i(1,1) & D_{i-1}^i(1,2) \\ D_{i-1}^i(2,1) & D_{i-1}^i(2,2) \end{bmatrix}.$$

with $[D_0^0] = I$, I is 2 identity matrix, and

$$\begin{aligned} D_{i-1}^i(1,1) &= \cos\beta(s_i - s_{i-1}). \\ D_{i-1}^i(1,2) &= \sin\beta(s_i - s_{i-1}). \\ D_{i-1}^i(2,1) &= -\sin\beta(s_i - s_{i-1}) - (\frac{m_i}{m})\beta\cos\beta(s_i - s_{i-1}). \\ D_{i-1}^i(2,2) &= \cos\beta(s_i - s_{i-1}) - (\frac{m_i}{m})\beta\sin\beta(s_i - s_{i-1}). \end{aligned}$$

The vectors $\vec{r}_i$ and $\vec{s}_i$ are given by:

$$\vec{r}_i = [D_{i-1}^i]\vec{r}_{i-1} + \begin{pmatrix} 0 \\ \beta[P_i + (\frac{m_i}{m})q_y] \end{pmatrix} \quad i = 2, 3, \ldots, n$$

$$\vec{s}_i = [D_{i-1}^i]\vec{s}_{i-1} + \begin{pmatrix} 0 \\ (\frac{m_i}{m})\beta q_z \end{pmatrix} \quad i = 2, 3, \ldots, n$$

with $\vec{r}_0 = \vec{s}_0 = \vec{0}$. The initial value for the above recursive relations are:

$$C_{10} = \frac{hq_y \sin\theta\cos\theta}{\beta^2 H_x^2}. \tag{3.70}$$

$$C_{30} = -\frac{hq_y \cos^2\theta}{\beta^2 H_x^2}, \tag{3.71}$$

$$C_{50} = -\frac{hq_z \cos\theta}{\beta^2 H_x^2}. \tag{3.72}$$

$$QDC_{20} = Q.N_x(\frac{h\sin\theta\cos\theta}{\beta^2 H_x^2}). \tag{3.73}$$

$$QDC_{10} = Q.N_y(-\frac{h\cos^2\theta}{\beta^2 H_x^2}). \tag{3.74}$$

$$QDC_{60} = Q.N_z(-\frac{h\cos\theta}{\beta^2 H_x^2}). \tag{3.75}$$

where

$$\begin{aligned}
QD &= D_0^N(1,2)\cos\beta(L_s - s_N) + D_0^N(2,2)\sin\beta(L_s - s_N).\\
Q.N_x &= q_y - [r_{N1} + q_y D_0^N(1,1)]\cos\beta(L_s - s_N)\\
&\quad - [r_{N2} + q_y D_0^N(2,1)]\sin\beta(L_s - s_N).\\
Q.N_y &= Q.N_x.\\
Q.N_z &= q_z - [D_0^N(1,1)q_z + s_{N1}]\cos\beta(L_s - s_N)\\
&\quad - [D_0^N(2,1)q_z + s_{N2}]\sin\beta(L_s - s_N).
\end{aligned}$$

Now, the procedure used in Chapter 2 can be applied here: substituting the static profile obtained in the previous section into Eq. (3.54).

And then using Eq. (3.55)- (3.57) with the boundary conditions and continuity conditions.and finally integrating the resulted equation yields the frequency equation

$$\begin{aligned}
&[\frac{\beta^3 L_s^3}{\lambda^2} - \beta\cos\theta L_s]h\\
&- \frac{\beta^3 H_x^2 \sin\theta}{q^2}\sum_{k=1}^{n}\{P_i[D_0^i(1,1)C_{10} + D_0^i(1,2)C_{20}\\
&\quad + r_{i1}(\frac{h\sin\theta\cos\theta}{\beta^2 H_x^2}) - \frac{hq_y\sin\theta\cos\theta}{\beta^2 H_x^2}]\}\\
&+ \frac{\beta^3 H_x^2\cos\theta}{q^2}\sum_{k=1}^{n}\{P_i[D_0^i(1,1)C_{30} + D_0^i(1,2)C_{40}\\
&\quad - r_{i1}(\frac{h\cos^2\theta}{\beta^2 H_x^2}) + \frac{hq_y\cos^2\theta}{\beta^2 H_x^2}]\}
\end{aligned}$$

$$
\begin{aligned}
&+ \frac{\mathcal{J}^2 H_x^2}{q^2} \sum_{k=0}^{n} \{(\sin \mathcal{J}(s_{i+1} - s_i), 1 - \cos \mathcal{J}(s_{i+1} - s_i))[D_0^i] \cdot \\
&\quad \left(q_y \sin\theta \begin{pmatrix} C_{10} \\ C_{20} \end{pmatrix} - q_y \cos\theta \begin{pmatrix} C_{30} \\ C_{40} \end{pmatrix} - q_z \begin{pmatrix} C_{50} \\ C_{60} \end{pmatrix} \right) \} \\
&+ \frac{\cos\theta h}{q^2} \sum_{k=0}^{n} \{(\sin \mathcal{J}(s_{i+1} - s_i), 1 - \cos \mathcal{J}(s_{i+1} - s_i)) \left(q_y \vec{r}_i + q_z \vec{s}_i \right) \} \\
&= 0
\end{aligned} \tag{3.76}
$$

where λ^2 is defined before and can be found in Appendix A.

Similarly, there are two cases we need to discuss: $h = 0$ and $h \neq 0$.

1. When $h = 0$, it follows from Eq. (3.70)- (3.72) that $C_{10} = C_{30} = C_{50} = 0$ and the right-hand side of Eq. (3.73)- (3.75) are also equal to zero. In order for Eq. (3.55)- (3.57) to have non-trivial solutions, it is easy to observe from Eq. (3.73)- (3.75) that QD must be zero. This yields an equation, $QD = 0$, which involves only one undetermined variable, frequency $\mathcal{J}$, and thus it can be used to solve for $\mathcal{J}$ with a simple iterative numerical method.

   Further substituting $h = 0$ into Eq. (3.76) results in

$$q_y C_{20} A + q_y C_{40} B - q_z C_{60} C = 0 \tag{3.77}$$

   where constants A, B, and C are listed in Appendix A. Because there are three undetermined coefficients C_{20}, C_{40} and C_{60} in Eq. (3.77), we need another equation to discuss mode shape functions. This additional equation can be obtained by imposing the right-end boundary conditions in Eq. (3.54), (i.e. at the point $N + 1$, see Fig. 1.3). The final expression of the equation is given by

$$C_{20} = DC_{40} + EC_{60}, \tag{3.78}$$

   where the static profile obtained in Section 3.1 has been used. The constants D and E are given in Appendix A.

   Now eliminating C_{20} from Eq. (3.78) and Eq. (3.77) produces the equation

$$\tilde{D}C_{40} + \tilde{E}C_{60} = 0, \tag{3.79}$$

where the expressions for $\tilde{D}$ and $\tilde{E}$ can be found in Appendix A.

Similarly, there are four subcases we need to discuss according to the values of $\tilde{D}$ and $\tilde{E}$.

(a) If $\tilde{D} = \tilde{E} = 0$, then Eq. (3.79) suggests that both C_{40} and C_{60} can be chosen arbitrarily while C_{20} can be determined from Eq. (3.78). The mode shape functions are then given by

$$U_i(s) = \begin{pmatrix} \cos\beta(s-s_i) & \sin\beta(s-s_i) \end{pmatrix} \begin{pmatrix} D_0^i(1,2) \\ D_0^i(2,2) \end{pmatrix} C_{20}, \tag{3.80}$$

$$Y_i(s) = \begin{pmatrix} \cos\beta(s-s_i) & \sin\beta(s-s_i) \end{pmatrix} \begin{pmatrix} D_0^i(1,2) \\ D_0^i(2,2) \end{pmatrix} C_{40}, \tag{3.81}$$

$$Z_i(s) = \begin{pmatrix} \cos\beta(s-s_i) & \sin\beta(s-s_i) \end{pmatrix} \begin{pmatrix} D_0^i(1,2) \\ D_0^i(2,2) \end{pmatrix} C_{60}. \tag{3.82}$$

In this subcase, there are two independent mode shapes $Y(s)$ and $Z(s)$ associated with one repeated frequency. This is similar to the cable without concentrated loads.

(b) If $\tilde{D} = 0$ but $\tilde{E} \neq 0$, then it follows from Eq. (3.79) that $C_{60} = 0$ while C_{40} can be chosen arbitrarily. Eq. (3.78) then gives $C_{20} = DC_{40}$. The mode shape functions in this subcases are given by

$$U_i(s) = \begin{pmatrix} \cos\beta(s-s_i) & \sin\beta(s-s_i) \end{pmatrix} \begin{pmatrix} D_0^i(1,2) \\ D_0^i(2,2) \end{pmatrix} C_{20}, \tag{3.83}$$

$$Y_i(s) = \begin{pmatrix} \cos\beta(s-s_i) & \sin\beta(s-s_i) \end{pmatrix} \begin{pmatrix} D_0^i(1,2) \\ D_0^i(2,2) \end{pmatrix} C_{40}, \tag{3.84}$$

$$Z_i(s) = 0. \tag{3.85}$$

(c) If $\tilde{D} \neq 0$ but $\tilde{E} = 0$, similarly, we have $C_{20} = EC_{60}$ whereas C_{60} is arbitrary, and C_{40} is zero. The mode shape functions are then given by:

$$U_i(s) = \begin{pmatrix} \cos\beta(s-s_i) & \sin\beta(s-s_i) \end{pmatrix} \begin{pmatrix} D_0^i(1,2) \\ D_0^i(2,2) \end{pmatrix} C_{20}, \tag{3.86}$$

$$Y_i(s) = 0, \tag{3.87}$$

$$Z_i(s) = \begin{pmatrix} \cos \beta(s - s_i) & \sin \beta(s - s_i) \end{pmatrix} \begin{pmatrix} D_0^i(1,2) \\ D_0^i(2,2) \end{pmatrix} C_{60}. \qquad (3.88)$$

(d) If $\tilde{D} \neq 0$ and $\tilde{E} \neq 0$, then solving Eq. (3.78) and Eq. (3.79) yields $C_{60} = -\frac{\tilde{D}}{\tilde{E}}$ and $C_{20} = (D - E\frac{\tilde{D}}{\tilde{E}})C_{40}$. The expressions of the mode shape functions in this subcase are in the same form as those given in case (a), but they are actually different because C_{20}, C_{40} and C_{60} take different values.

It is noted that the first case (a) gives two independent mode shapes with one repeated frequency determined by $QD = 0$, while the remaining three cases only give one mode shape function associated with the frequency obtained from the same equation. The second frequency together with the second set of mode shapes for the three cases (b), (c) and (d) can be found next for the case $h \neq 0$.

2. When $h \neq 0$, the mode shapes in y' and z' directions are given by Eq. (3.56) and Eq. (3.57) which can be rewritten in a more compact way as

$$Y_i(s) = C_{3i} \cos[\beta(s - s_i)] + C_{4i} \sin[\beta(s - s_i)] - C_{30}, \qquad (3.89)$$

$$Z_i(s) = C_{5i} \cos[\beta(s - s_i)] + C_{6i} \sin[\beta(s - s_i)] - C_{50} \qquad (3.90)$$

by using the recursive formulas given in Eq. (3.67) to Eq. (3.69) and the initial values for these recursions given by Eq. (3.70) to Eq. (3.72).

With the formulas described in Appendix C.2, the mode shape in x' direction can be obtained by using the Hooke's Law together with Eq. (3.89), Eq. (3.90) and the static profile given in Section 3.1 as well as the following relation

$$(\frac{ds_i}{dx})^2 = (\frac{dx_i'}{dx})^2 + (\frac{dy_i'}{dx})^2 + (\frac{dz_i'}{dx})^2.$$

The final differential equation is

$$\frac{dU_i(s)}{ds} = (SU_7 + SU_8 + SU_9)/SU_3 \qquad (3.91)$$

where SU_i $(i = 1 \ldots 8)$ can be found in Appendix A. Then, the mode shape in x' direction in this case can be found by integrating Eq. (3.91) with a simple numerical method such as that given in [27].

3.3 Results and discussion

The results given here are obtained from the cable considered in the previous chapter (the parameter values listed in Appendix B) with two additional concentrated loads. The positions of these two concentrated loads are at $\frac{1}{3}L_x$ and $\frac{2}{3}L_x$, respectively, where L_x is the horizontal span length. Because we are using nondimensionalized Lagrangian coordinate to present our results, the positions of the concentrated loads are given as the relative values of the cable length L_s. Note that for different inclinations the Lagrangian coordinates for the point with the same x or x' coordinates are different, so the relative positions of concentrated loads given in the figures are slightly different. The weights of the two concentrated loads are 0.902145 N and 0.423465 N, respectively. Simialrly, ω_1 and ω_2 in the figures are frequencies respectively correspond to the solid and dash mode shapes.

Similar to the figures given in previous chapter, there are two sets of mode shapes represented by dash and solid lines, respectively. The solid curves represent the mode shapes associate with $h = 0$ while the dash curves represent those associated with $h \neq 0$. Also similarly, the cable is considered in three situations, namely with horizontal, 30^o inclination, 60^o inclination.

It is obvious to see from the figures that the concentrated loads have dramatic effects on the mode shapes. Jumps can be observed in the mode shapes, occurred at the positions of the imposed concentrated loads. The concentrated loads can reduce either the left part or the right part of the amplitude of the mode shapes. This randomness causes difficulty in practice to optimally control cable vibrations.

For the same order frequencies, the mode shapes associated with $h = 0$ (solid curves) look similar, however, those associated with $h \neq 0$ (dash lines) in each of u', y' and z directions are significantly different. It can be seen from the dash lines for u mode shapes that the numerical integration does not always give fully satisfactory results.

For the different order frequencies, there are always three different types of mode shapes for each direction of u', y' and z. This tendency is more clear in the mode

shapes associated with the solid curves ($h = 0$). It is noted that both the results given in [9,12] can be obtained from one of these three different mode shapes. However, whether quantitative relationship may exist between these three types of mode shapes is still under investigation.

When the cable is inclined, it can be seen that increasing the inclination of cable diminishes the effect of concentrated loads, especially in Figs. 3.7- 3.9 which represent the mode shapes for 60^o inclination. This conclusion is also valid to both solid ($h = 0$) and dash ($h \neq 0$) mode shapes. Furthermore, unlike what found in the last chapter, there does not exist any movement in the central region for the u mode shapes with the inclination of the cable.

The three different types of mode shapes for different order frequencies under the same support conditions show the sensitivity of cables' mode shapes to the concentrated loads when the inclination is not very large, which has been noticed before [9]. Therefore, parametric study is necessary for practical designs to obtain optimal control of cable vibrations [5].

Similarly, for the same order frequency, the values of the frequency is a little lower when the support is inclined than when the support is horizontal.

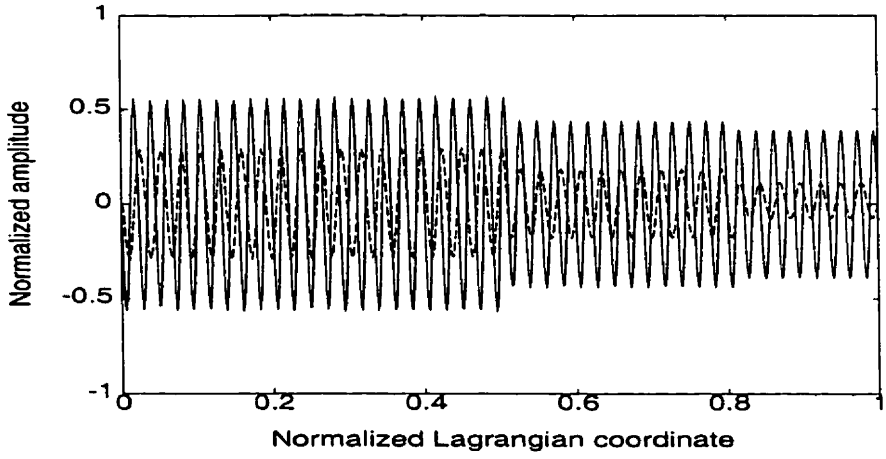

(a)

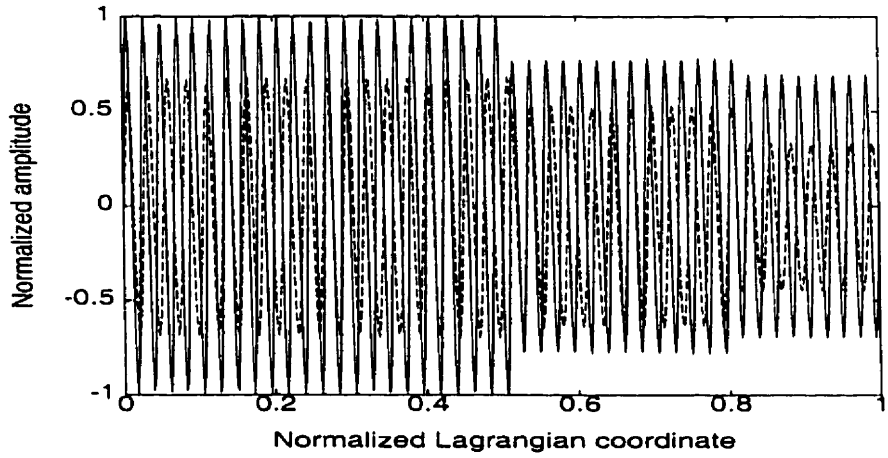

(b)

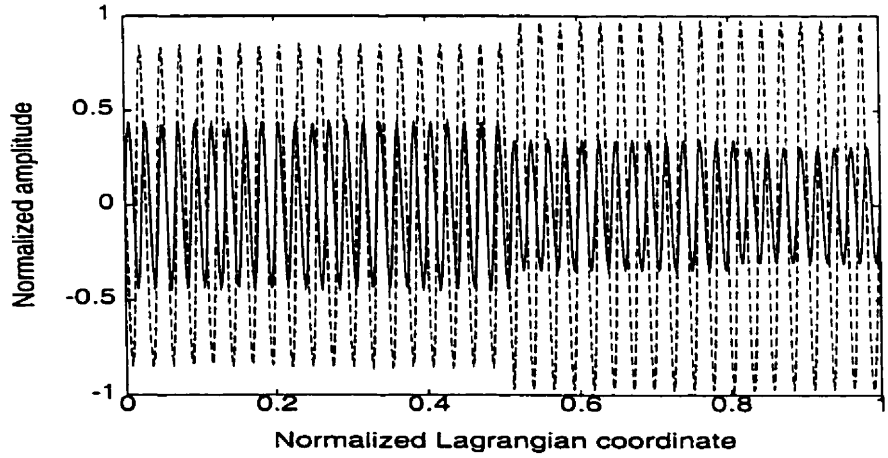

(c)

Figure 3.1: Mode shapes associated with frequencies $\omega_1 = 9.04Hz$, $\omega_2 = 7.6Hz$ for the horizontal support with concentrated loads. Two concentrated loads are in $0.514623L_s$ and $0.814665L_s$ respectively.

Type I: (a) u'-mode; (b) y'-mode; and (c) z-mode

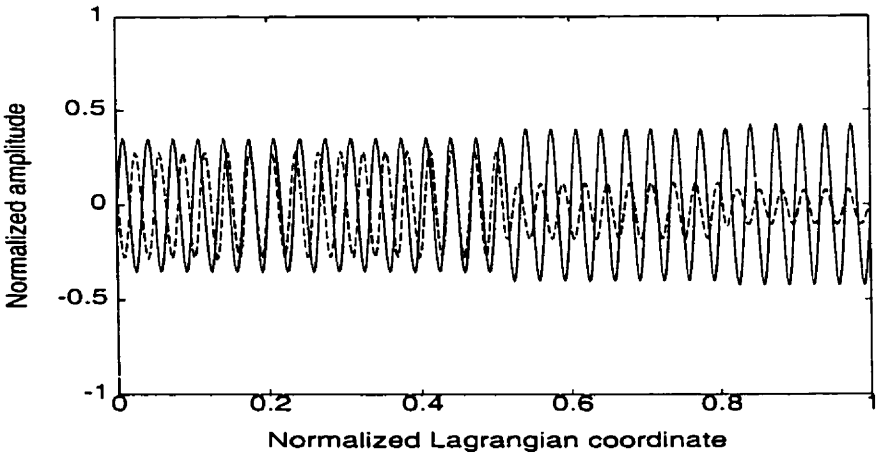

(a)

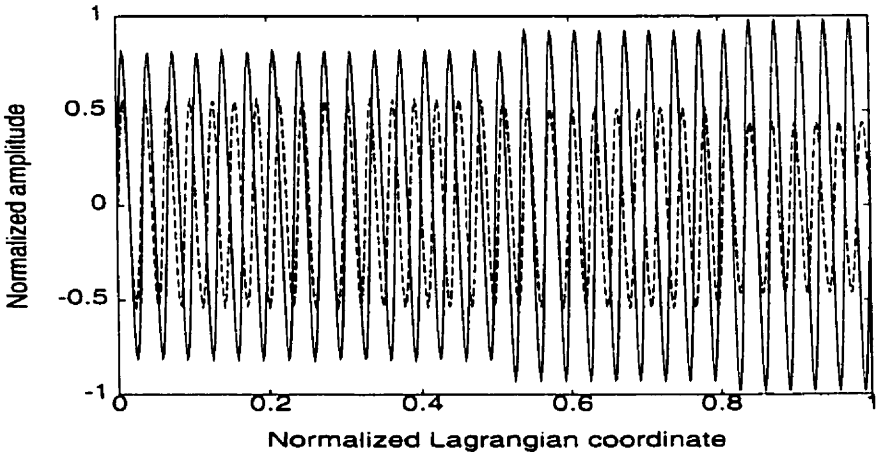

(b)

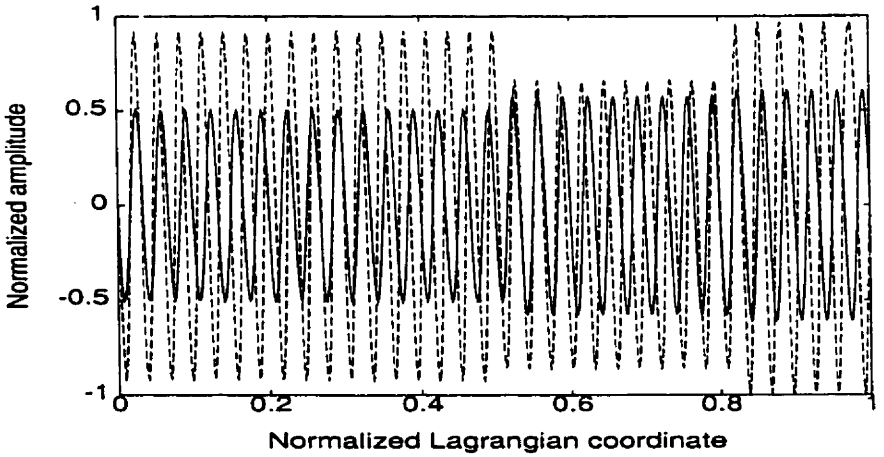

(c)

Figure 3.2: Mode shapes associated with frequencies $\omega_1 = 6.04Hz$, $\omega_2 = 6.8HZ$ for the horizontal support with concentrated loads. Two concentrated loads are in $0.514623L_s$ and $0.814665L_s$ respectively.

Type II: (a) u'-mode; (b) y'-mode; and (c) z-mode

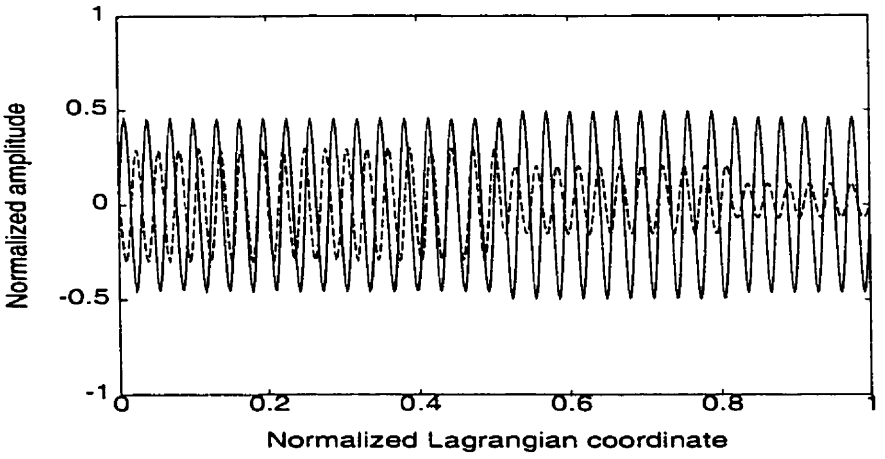

(a)

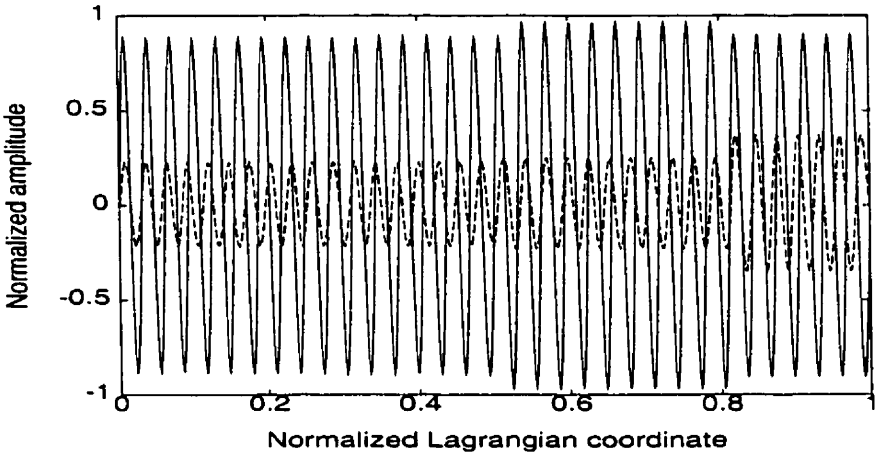

(b)

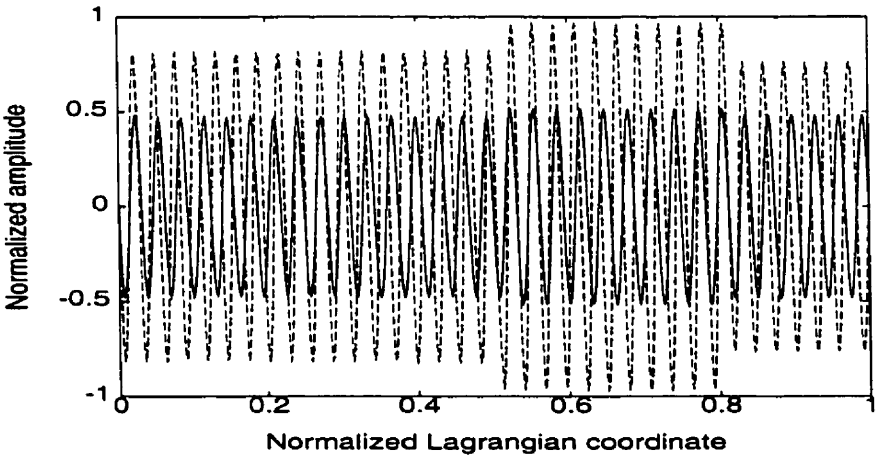

(c)

Figure 3.3: Mode shapes associate with frequencies $\omega_1 = 6.44Hz$, $\omega_2 = 7.2Hz$ for the horizontal support with concentrated loads. Two concentrated loads are in $0.514623L_s$ and $0.814665L_s$ respectively.

Type III: (a) u'-mode; (b) y'-mode; and (c) z-mode

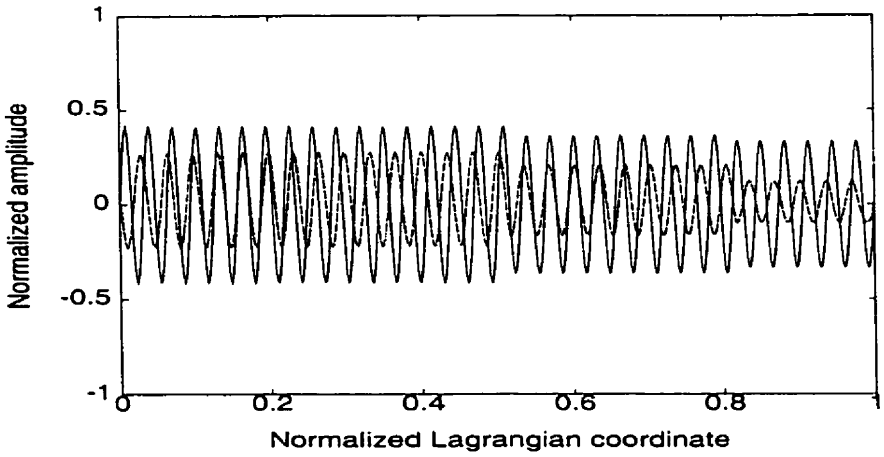

(a)

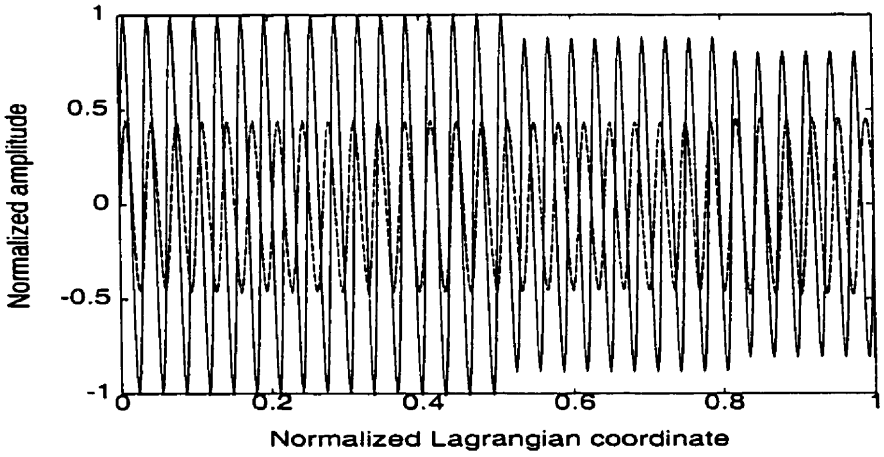

(b)

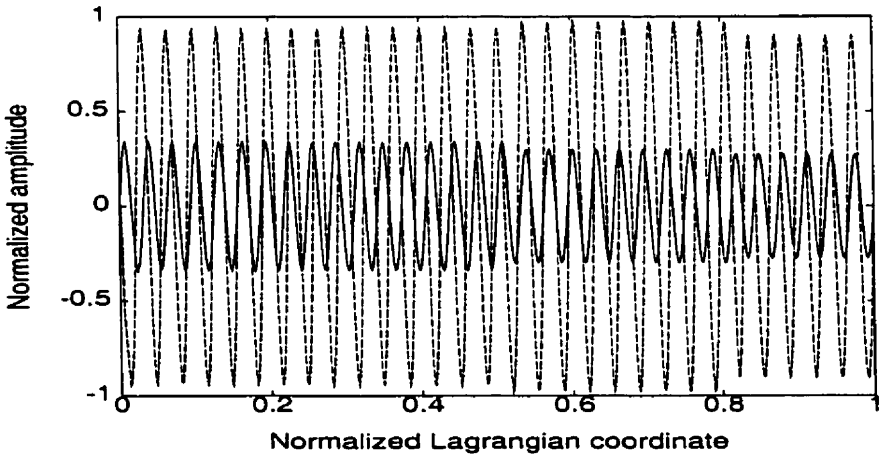

(c)

Figure 3.4: Mode shapes associated with frequencies $\omega_1 = 6.47Hz$. $\omega_2 = 6.0Hz$ for the support inclined 30^o with concentrated loads. Two concentrated loads are in $0.517705L_s$ and $0.817172L_s$ respectively.

Type I: (a) u'-mode; (b) y'-mode; and (c) z-mode

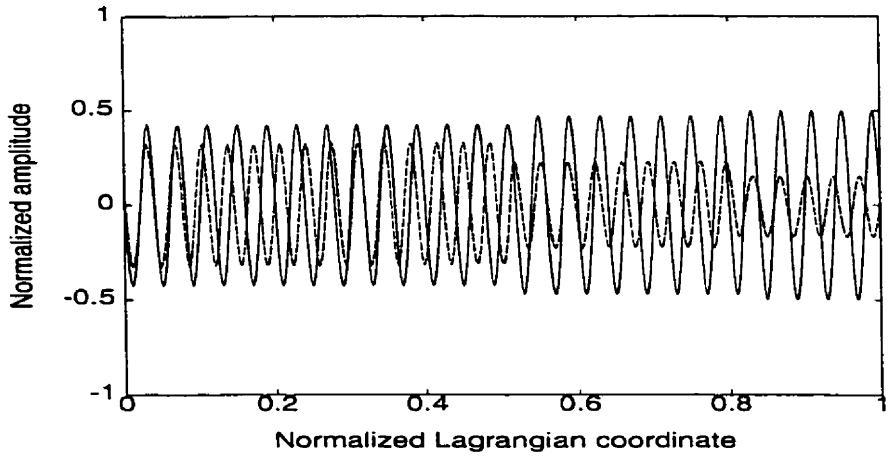

(a)

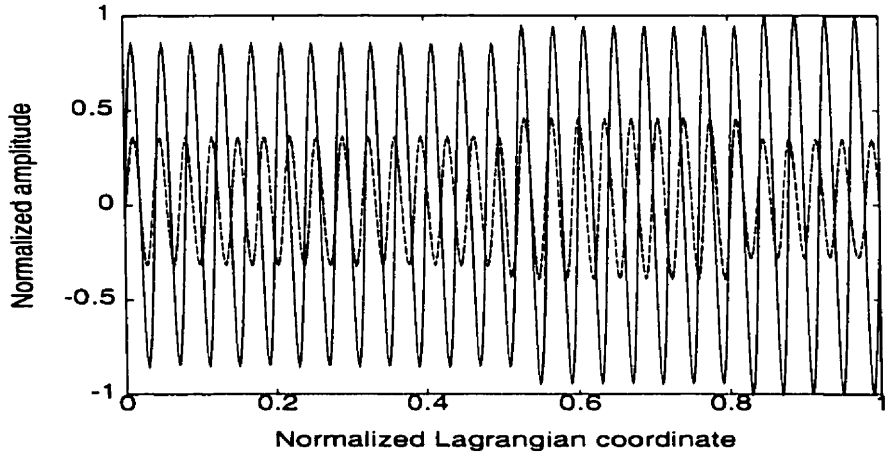

(b)

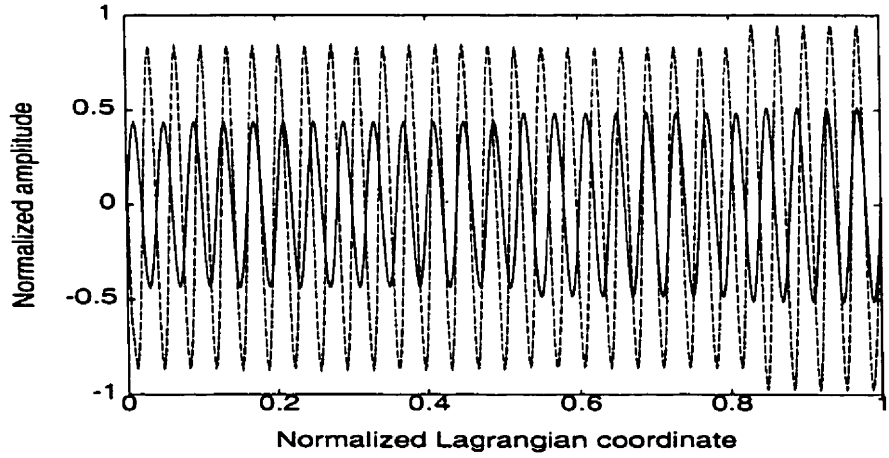

(c)

Figure 3.5: Mode shapes associated with frequencies $\omega_1 = 5.06Hz$, $\omega_2 = 5.8Hz$ for the support inclined 30^o with concentrated loads. Two concentrated loads are in $0.517705L_s$ and $0.817172L_s$ respectively.

Type II: (a) u'-mode; (b) y'-mode; and (c) z-mode

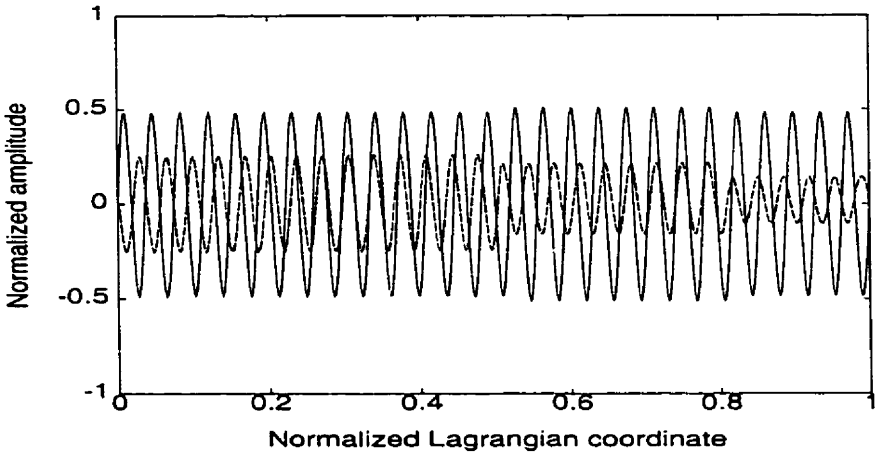

(a)

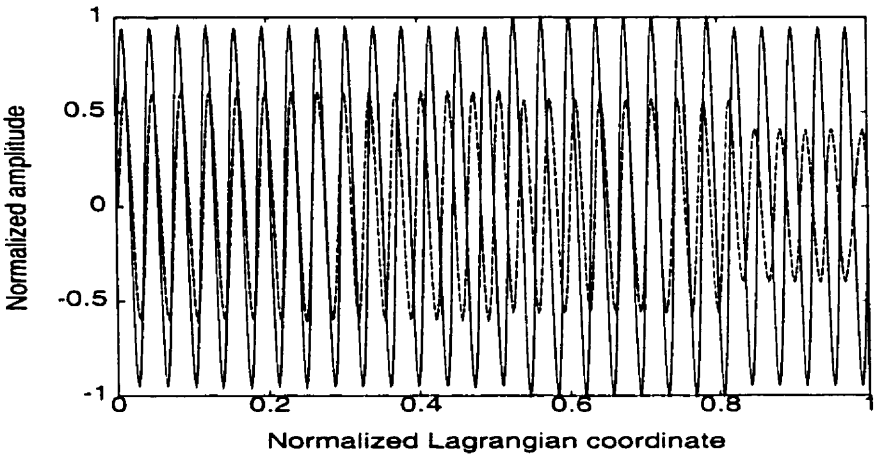

(b)

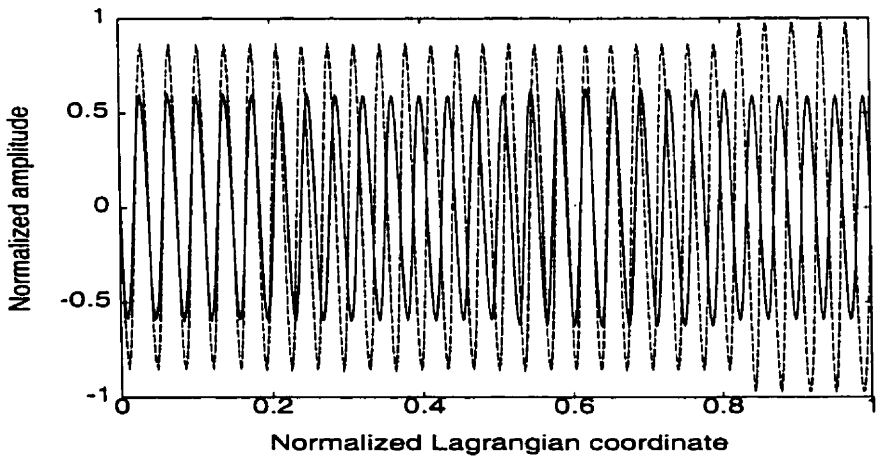

(c)

Figure 3.6: Mode shapes associated with $\omega_1 = 5.46Hz$, $\omega_2 = 5.9Hz$ for the support inclined 30° with concentrated loads. Two concentrated loads are in $0.517705L_s$ and $0.817172L_s$ respectively.

Type III: (a) u'-mode; (b) y'-mode; and (c) z-mode

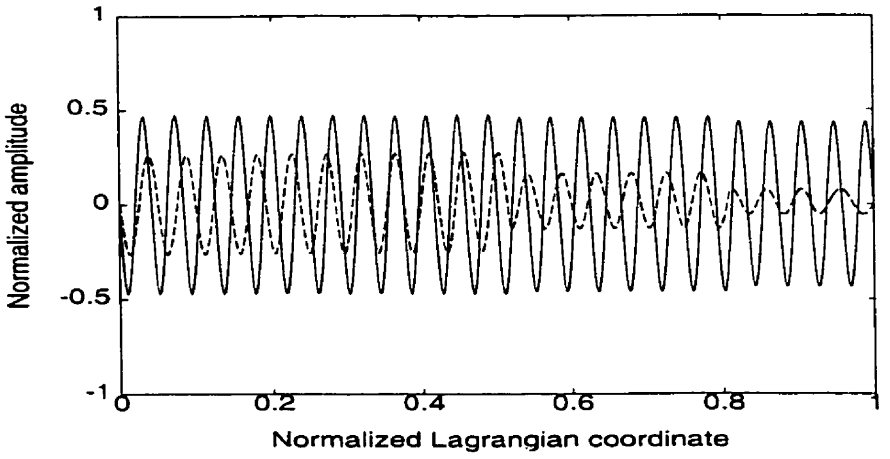

(a)

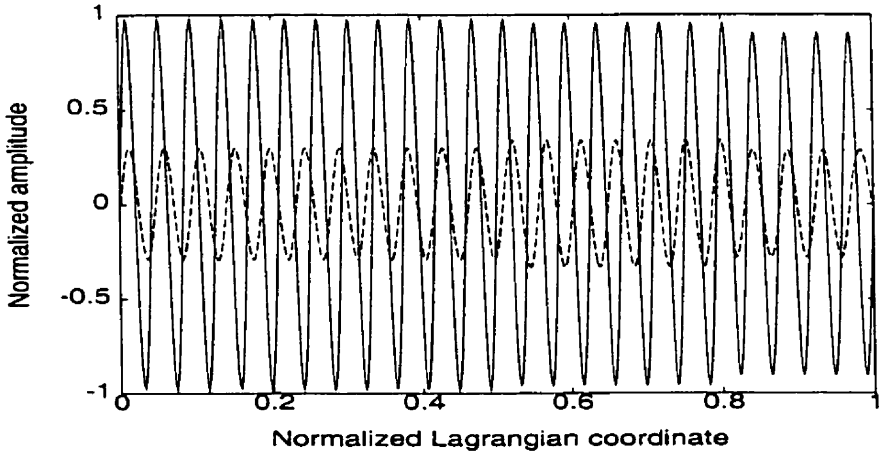

(b)

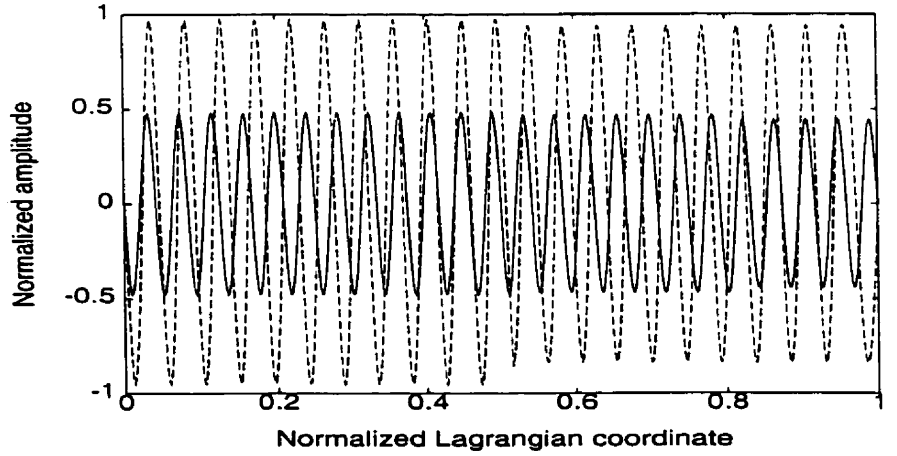

(c)

Figure 3.7: Mode shapes associated with $\omega_1 = 6.74Hz$, $\omega_2 = 6.1Hz$ for the support inclined 60^o with concentrated loads. Two concentrated loads are in $0.521817L_s$ and $0.821122L_s$ respectively.

Type I: (a) u'-mode; (b) y'-mode; and (c) z-mode

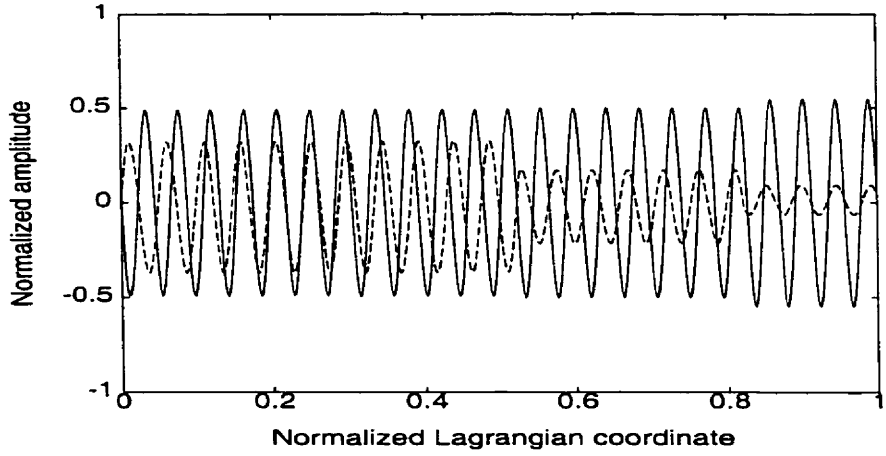

(a)

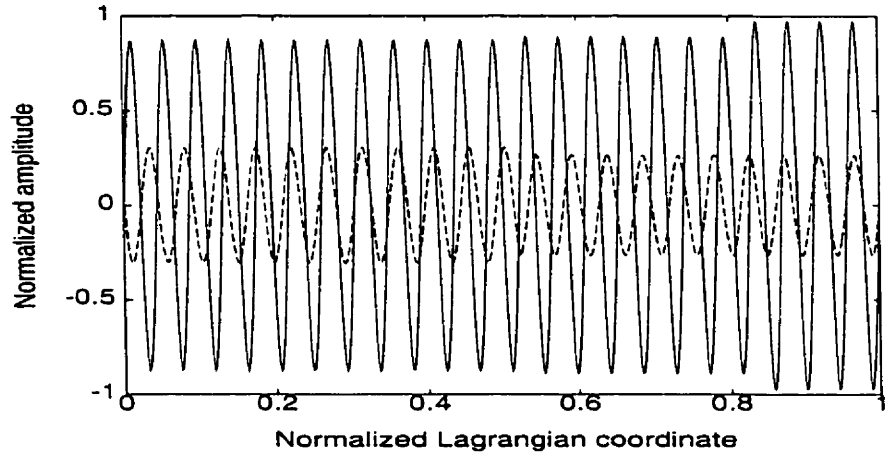

(b)

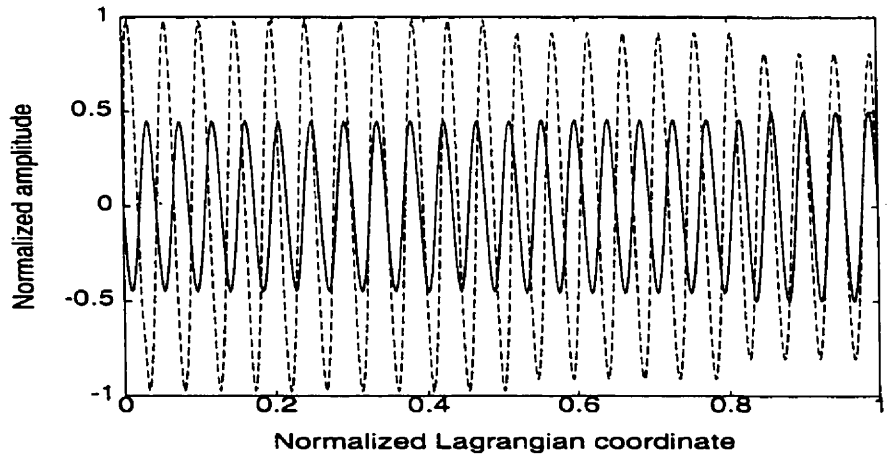

(c)

Figure 3.8: Mode shapes associated with $\omega_1 = 6,46Hz$, $\omega_2 = 6.0Hz$ for the support inclined 60^o with concentrated loads. Two concentrated loads are in $0.521817L_s$ and $0.821122L_s$ respectively.

Type II: (a) u'-mode; (b) y'-mode; and (c) z-mode

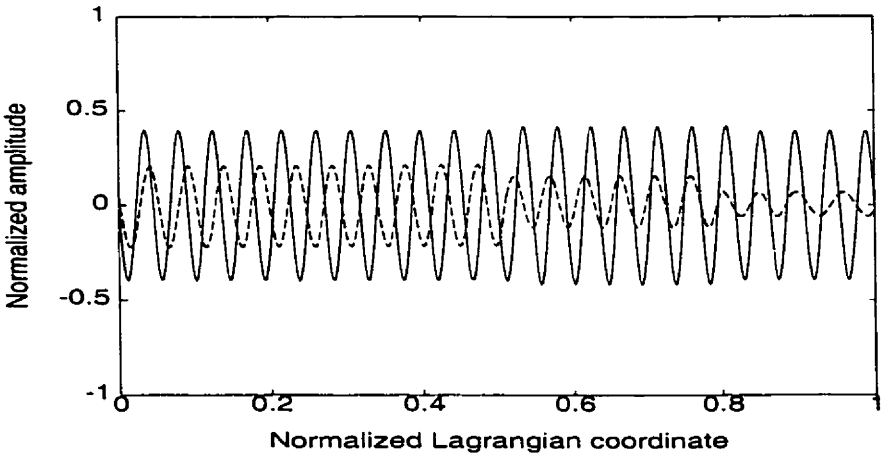

(a)

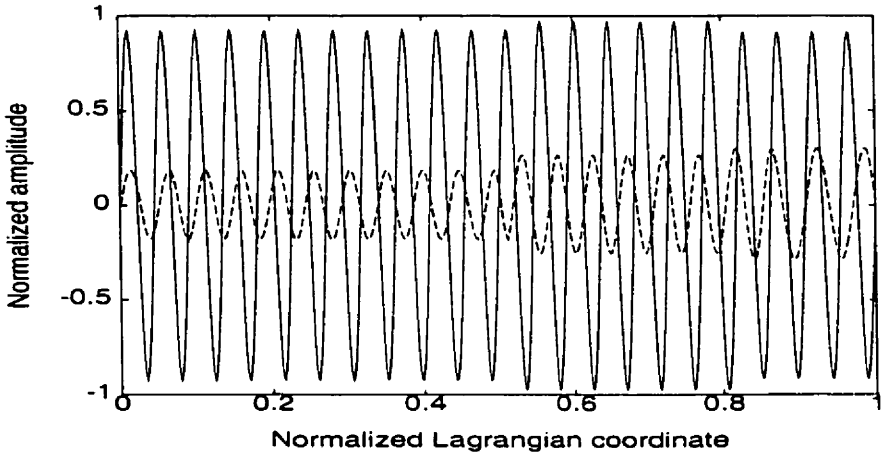

(b)

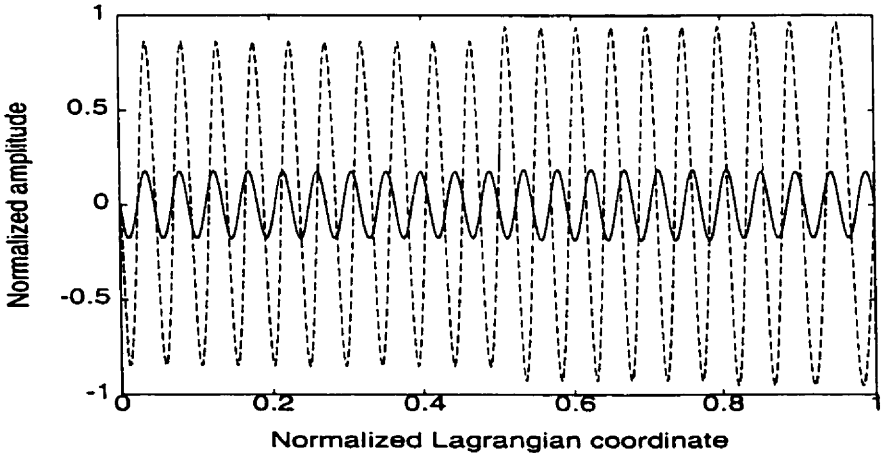

(c)

Figure 3.9: Mode shapes associated with $\omega_1 = 6.18Hz$, $\omega_2 = 5.9Hz$ for the support inclined 60^o with concentrated loads. Two concentrated loads are in $0.521817L_s$ and $0.821122L_s$ respectively.

Type III: (a) u'-mode; (b) y'-mode; and (c) z-mode

Chapter 4

Large sagged bare cables

In Chapters 2 and 3, we have obtained both static and dynamic solutions for a flat cable, i.e. the sag/length ratio of the cable is small. As we pointed out in the previous chapters that the static analysis for a flat cable is also valid for large sagged cables because no assumptions have been made there to limit the analysis. However, the dynamic analysis is only valid for flat cables because the assumption $dx = ds\cos\theta$ implies that the slope of the whole cable is a constant $\frac{1}{\cos\theta}$. For large sagged cables, the slope of the cable cannot be approximated by a constant for the whole cable. Therefore, we need to modify the approach given in previous chapter to allow for the large sag/length ratio.

Since the static analyses given in Chapters 2 and 3 are still valid for this case, thus only dynamic analysis will be presented.

4.1 Dynamic analysis

For the dynamic analysis, the relations $T = H_x\frac{ds}{dx}$ and $\tau = h_x(t)\frac{ds}{dx}$ are still valid because they were derived under the assumption that the cable has no horizontal external forces. Some new assumptions will be introduced to incorporate the special properties of the large sagged cable.

The differential equations describing the dynamic response of the cable in rotated coordinate system can be written as

$$\frac{\partial^2 u_k'}{\partial x \partial s} = \frac{m}{H_x + h_x}\frac{\partial^2 u_k'}{\partial t^2} - \frac{h_x}{H_x + h_x}\frac{d^2x'}{dxds}, \tag{4.1}$$

$$\frac{\partial^2 y'_{2k}}{\partial x \partial s} = \frac{m}{H_x + h_x}\frac{\partial^2 y'_{2k}}{\partial t^2} - \frac{h_x}{H_x + h_x}\frac{d^2 y_1}{dx ds}. \tag{4.2}$$

$$\frac{\partial^2 z_{2k}}{\partial x \partial s} = \frac{m}{H_x + h_x}\frac{\partial^2 z_{2k}}{\partial t^2} - \frac{h_x}{H_x + h_x}\frac{d^2 z_1}{dx ds}. \tag{4.3}$$

where the relations $T = H_x\frac{ds}{dx}$ and $\tau = h_x(t)\frac{ds}{dx}$ have been used. The meaning of the subscripts are the same as before defined in the previous chapters except that i is replaced by k.

Note that the assumption $H_x >> h_x$ is still valid since the cable under consideration is assumed to have small strain no matter whether the cable is flat or not. But for large sagged cables, we need to use $dx = J_k^2\, ds\cos\theta$ to replace $dx = ds\cos\theta$ where $\frac{1}{J_k^2\cos\theta}$ is the slope of consecutive segments of the cable.

Substituting the static profile obtained in Section 2.1.2 and the relation $dx = J_k^2\, ds\cos\theta$ into Eq. (4.1)- (4.3) yields

$$\frac{\partial^2 u'_k}{\partial s^2} - \frac{mJ_k^2\cos\theta}{H_x}\frac{\partial^2 u'_k}{\partial t^2} = -\frac{h_x q_y J_k^2 \sin\theta\cos\theta}{H_x^2}. \tag{4.4}$$

$$\frac{\partial^2 y'_{2k}}{\partial s^2} - \frac{mJ_k^2\cos\theta}{H_x}\frac{\partial^2 y'_{2k}}{\partial t^2} = \frac{h_x q_y J_k^2\cos^2\theta}{H_x^2}. \tag{4.5}$$

$$\frac{\partial^2 z_{2k}}{\partial s^2} - \frac{mJ_k^2\cos\theta}{H_x}\frac{\partial^2 z_{2k}}{\partial t^2} = \frac{h_x q_z J_k^2\cos\theta}{H_x^2}. \tag{4.6}$$

If the cable is flat enough, then we use a constant to approximate the whole cable's slope by 1, i.e. $J_k = 1$, and then Eq. (4.4)- (4.6) become the equations given in Section 2.2. Now, for large-sagged cables, J_k is not a constant throughout the whole cable, so we need to apply NTM method to solve the equations. This procedure is similar to that presented in Chapter 3 except that in this case there are no concentrated masses at the points marked by i, see Fig. 1.4. The points, marked by k in this chapter, are actually those at which the slope of the cable is approximated. Therefore, the continuity conditions which are about the slope of the cable now become a little easier than those in Chapter 3. They are

$$\frac{dU_{k+1}(s_{k+1})}{ds} = \frac{dU_k(s_{k+1})}{ds}. \tag{4.7}$$

$$\frac{dY_{2k+1}(s_{k+1})}{ds} = \frac{dY_{2k}(s_{k+1})}{ds}. \tag{4.8}$$

$$\frac{dZ_{2k+1}(s_{k+1})}{ds} = \frac{dZ_{2k}(s_{k+1})}{ds}. \tag{4.9}$$

which are simpler than those given in Chapter 3. The continuity conditions as well as the boundary conditions are the same as those given in Chapter 3. The procedure of solving Eq. (4.4)- (4.6) is also similar and thus the details are omitted here. The solutions are obtained as

$$\begin{aligned} U_k(s) &= C_{1k}\cos[\beta J_k(s-s_k)] + C_{2k}\sin[\beta J_k(s-s_k)] \\ &\quad - \frac{hq_y \sin\theta\cos\theta}{\beta^2 H_x^2}. \end{aligned} \tag{4.10}$$

$$\begin{aligned} Y_{2k}(s) &= C_{3k}\cos[\beta J_k(s-s_k)] + C_{4k}\sin[\beta J_k(s-s_k)] \\ &\quad + \frac{hq_y \cos^2\theta}{\beta^2 H_x^2}. \end{aligned} \tag{4.11}$$

$$\begin{aligned} Z_{2k}(s) &= C_{5k}\cos[\beta J_k(s-s_k)] + C_{6k}\sin[\beta J_k(s-s_k)] \\ &\quad + \frac{hq_z \cos\theta}{\beta^2 H_x^2}. \end{aligned} \tag{4.12}$$

where

$$\beta = \sqrt{\frac{m\cos\theta}{H_x}}\omega. \tag{4.13}$$

The integration constants C_{1k} to C_{6k} can be determined by Eq. (4.7)- (4.9) and the boundary conditions and continuity conditions. In the process of determining these constants, the following transfer matrices are obtained:

$$\begin{pmatrix} C_{1k} \\ C_{2k} \end{pmatrix} = [D_0^k] \begin{pmatrix} C_{10} \\ C_{20} \end{pmatrix}. \tag{4.14}$$

$$\begin{pmatrix} C_{3k} \\ C_{4k} \end{pmatrix} = [D_0^k] \begin{pmatrix} C_{30} \\ C_{40} \end{pmatrix}. \tag{4.15}$$

$$\begin{pmatrix} C_{5k} \\ C_{6k} \end{pmatrix} = [D_0^k] \begin{pmatrix} C_{50} \\ C_{60} \end{pmatrix}, \tag{4.16}$$

where $[D_0^k] = [D_{k-1}^k][D_0^{k-1}]$ with $[D_0^0] = I$(I is 2×2 identity matrix). The matrix $[D_{k-1}^k]$ is given by:

$$[D_{k-1}^k] = \begin{bmatrix} D_{k-1}^k(1,1) & D_{k-1}^k(1,2) \\ D_{k-1}^k(2,1) & D_{k-1}^k(2,2) \end{bmatrix},$$

and

$$
\begin{aligned}
D^k_{k-1}(1,1) &= \cos[\beta J_{k-1}(s_k - s_{k-1})], \\
D^k_{k-1}(1,2) &= \sin[\beta J_{k-1}(s_k - s_{k-1})], \\
D^k_{k-1}(2,1) &= -\frac{J_{k-1}}{J_k}\sin[\beta J_{k-1}(s_k - s_{k-1})], \\
D^k_{k-1}(2,2) &= \frac{J_{k-1}}{J_k}\cos[\beta J_{k-1}(s_k - s_{k-1})].
\end{aligned}
$$

The initial values for the recursive Eq. (4.14) to Eq. (4.16) are given by

$$C_{10} = \frac{hq_y \sin\theta\cos\theta}{\beta^2 H_x^2}. \tag{4.17}$$

$$C_{30} = -\frac{hq_y \cos^2\theta}{\beta^2 H_x^2}. \tag{4.18}$$

$$C_{50} = -\frac{hq_z \cos\theta}{\beta^2 H_x^2}. \tag{4.19}$$

$$QDC_{20} = (\frac{hq_y \sin\theta\cos\theta}{\beta^2 H_x^2})QN. \tag{4.20}$$

$$QDC_{40} = (-\frac{hq_y \cos^2\theta}{\beta^2 H_x^2})QN. \tag{4.21}$$

$$QDC_{60} = (-\frac{hq_z \cos\theta}{\beta^2 H_x^2})QN. \tag{4.22}$$

where

$$QD = D_0^N(1,2)\cos[\beta J_N(L_s - s_n)] + D_0^N(2,2)\sin[\beta J_N(L_s - s_n)]. \tag{4.23}$$

$$\begin{aligned}
QN &= 1 - D_0^N(1,1)\cos[\beta J_N(L_s - s_n)] \\
&\quad - D_0^N(2,1)\sin[\beta J_N(L_s - s_n)].
\end{aligned} \tag{4.24}$$

Note that in both the recursive formulas given by Eq. (4.14)- (4.16) and Eq. (4.17)- (4.22), the non-homogeneous terms which appeared in Eq. (3.67)- (3.69) become zero since the point masses are all zeros here. This makes the dynamic analysis in this chapter relatively easier than that in Chapter 3.

The frequency equation can still be derived using the Hooke's Law and the similar procedures described before as

$$[\frac{\beta^3 L_s^3}{\lambda^2} - \beta L_s \cos\theta]h$$

$$+\frac{\beta^2 H_x^2}{q^2}\sum_{k=0}^{n}\{\frac{1}{J_k}(\sin[\beta J_k(s_{k+1}-s_k)],1-\cos[\beta J_k(s_{k+1}-s_k)])[D_0^k]\cdot$$
$$\left(q_y\sin\theta\begin{pmatrix}C_{10}\\C_{20}\end{pmatrix}-q_y\cos\theta\begin{pmatrix}C_{30}\\C_{40}\end{pmatrix}-q_z\begin{pmatrix}C_{50}\\C_{60}\end{pmatrix}\right)\}$$
$$=\ 0. \tag{4.25}$$

where L_e and the static profile s are the same as that defined in Chapter 2, and $\lambda^2=(\frac{AE}{L_e})(\frac{L_s}{H_x})^3q^2$ which is also the same as that given in Chapter 2.

Now, we can discuss the mode shape functions given by Eq. (4.10)- (4.12) and Eq. (4.17)- (4.22) with the help of the recursive formulas Eq. (4.14)- (4.16). The procedure is similar to that described in Chapter 3 except that the constants here are different. Thus, similarly, we need to consider two cases: $h=0$ and $h\neq 0$.

1. When $h=0$, the first frequency is determined by the equation $QD=0$, where QD is given by Eq. (4.23). Furthermore, substituting $h=0$ into Eq. (4.25) results in

$$Aq_yC_{20}+Bq_yC_{40}+Cq_zC_{60}\ =\ 0 \tag{4.26}$$

where the constants A, B and C are given in Appendix A. Another equation needed for the discussion of the mode shapes can be obtained following the same procedure described in Chapter 2, is given by

$$C_{20}\ =\ DC_{40}+EC_{60} \tag{4.27}$$

where the constants D and E are also given in Appendix A. Next eliminate C_{20} from Eq. (4.26) and Eq. (4.27) to obtain an equation

$$\tilde{F}C_{40}+\tilde{G}C_{60}\ =\ 0 \tag{4.28}$$

where $\tilde{F}$ and $\tilde{G}$ are given in Appendix A.

Therefore, by a similar discussion based on Eq. (4.28), we have the following results.

(a) If $\tilde{F} = \tilde{G} = 0$, then C_{20} can be obtained from Eq. (4.27) where both C_{40} and C_{60} can be chosen arbitrarily. The mode shapes are given by

$$\begin{aligned} U_k(s) &= \left(\cos[\beta J_k(s - s_k)] \quad \sin[\beta J_k(s - s_k)] \right) \\ &\qquad \begin{pmatrix} D_0^k(1,2) \\ D_0^k(2,2) \end{pmatrix} C_{20}, \\ Y_{2k}(s) &= \left(\cos[\beta J_k(s - s_k)] \quad \sin[\beta J_k(s - s_k)] \right) \\ &\qquad \begin{pmatrix} D_0^k(1,2) \\ D_0^k(2,2) \end{pmatrix} C_{40}, \\ Z_{2k}(s) &= \left(\cos[\beta J_k(s - s_k)] \quad \sin[\beta J_k(s - s_k)] \right) \\ &\qquad \begin{pmatrix} D_0^k(1,2) \\ D_0^k(2,2) \end{pmatrix} C_{60}. \end{aligned}$$

(b) If $\tilde{F} = 0$, $\tilde{G} \neq 0$, then Eq. (4.27) gives $C_{20} = DC_{40}$ where C_{40} is arbitrary and Eq. (4.28) results in $C_{60} = 0$. The mode shapes are

$$\begin{aligned} U_k(s) &= \left(\cos[\beta J_k(s - s_k)] \quad \sin[\beta J_k(s - s_k)] \right) \\ &\qquad \begin{pmatrix} D_0^k(1,2) \\ D_0^k(2,2) \end{pmatrix} C_{20}, \\ Y_{2k}(s) &= \left(\cos[\beta J_k(s - s_k)] \quad \sin[\beta J_k(s - s_k)] \right) \\ &\qquad \begin{pmatrix} D_0^k(1,2) \\ D_0^k(2,2) \end{pmatrix} C_{40}, \\ Z_{2k}(s) &= 0. \end{aligned}$$

(c) If $\tilde{F} \neq 0$, $\tilde{G} = 0$, then similarly, Eq. (4.27) produces $C_{20} = EC_{60}$ where C_{60} is arbitrary while $C_{40} = 0$ determined from Eq. (4.28). The mode shapes are

$$\begin{aligned} U_k(s) &= \left(\cos[\beta J_k(s - s_k)] \quad \sin[\beta J_k(s - s_k)] \right) \\ &\qquad \begin{pmatrix} D_0^k(1,2) \\ D_0^k(2,2) \end{pmatrix} C_{20}. \\ Y_{2k}(s) &= 0, \\ Z_{2k}(s) &= \left(\cos[\beta J_k(s - s_k)] \quad \sin[\beta J_k(s - s_k)] \right) \end{aligned}$$

$$\begin{pmatrix} D_0^k(1,2) \\ D_0^k(2,2) \end{pmatrix} C_{60}.$$

(d) If $\tilde{F} \neq 0$, $\tilde{G} \neq 0$, then Eq. (4.28) gives $C_{60} = \frac{\tilde{F}}{\tilde{G}} C_{40}$ and it follows from Eq. (4.27) that $C_{20} = (D + E\frac{\tilde{F}}{\tilde{G}})C_{40}$ where C_{40} is arbitrary. The mode shapes in this subcase are in the same expressions as given in case (a) but they are actually different due to the different values of the constants.

Similar to discussions given in Chapter 2 and 3, the first subcase has two independent mode shapes associated with one single *repeated frequency*, while the remaining three subcases only give one independent mode shape function. The second mode shape as well as the associated frequency can be obtained from the case $h \neq 0$.

2. If $h \neq 0$, then the frequency is determined by Eq. (4.25). Solving C_{20}, C_{40} and C_{60} from Eq. (4.20)- (4.22) and substituting them into Eq. (4.25) results in

$$[\frac{(\beta L_s)^3}{\lambda^2} - \beta L_s \cos\theta] + \cos\theta \sum_{k=0}^{n} \{\frac{1}{J_k} \begin{pmatrix} V_1 & V_2 \end{pmatrix} [D_0^k] \begin{pmatrix} 1 \\ \frac{QN}{QD} \end{pmatrix}\} = 0$$

where

$$\begin{aligned} V_1 &= \sin[\beta J_k(s_{k+1} - s_k)], \\ V_2 &= 1 - \cos[\beta J_k(s_{k+1} - s_k)]. \end{aligned}$$

By solving this frequency equation with a simple iterative numerical method, we can find the second frequency for the three cases (b), (c) and (d).

The mode shapes in y' and z' directions are given by Eq. (4.11) and Eq. (4.12) which can be written as

$$Y_{2k}(s) = C_{3k}\cos[\beta J_k(s - s_k)] + C_{4k}\sin[\beta J_k(s - s_k)] - C_{30}, \quad (4.29)$$

$$Z_{2k}(s) = C_{5k}\cos[\beta J_k(s - s_k)] + C_{6k}\sin[\beta J_k(s - s_k)] - C_{50}. \quad (4.30)$$

where C_{30} and C_{50} are given by Eq. (4.18) and Eq. (4.19), respectively. Similarly, the mode shape in x' direction can be obtained by using the above two equations,

the static profile given in Chapter 2, the equation obtained from the Hooke's Law and the recursive formulas Eq. (4.14)- (4.16). The resulting differential equation for $U_k(s)$ is given by

$$\frac{dU_k(s)}{ds} = LS_3/LS_2 - LS_1(-C_{3k}LS_{bs} + C_{4k}LS_{bc})/LS_2 \quad (4.31)$$

$$- \frac{q_z}{q_y \cos\theta} LS_1(-C_{5k}LS_{bs} + C_{6k}LS_{bc})/LS_2 \quad (4.32)$$

where the constants LS_i $(i = 1 \ldots 4)$ is given in Appendix A. Similarly, we can solve this differential equation by a simple numerical approach.

4.2 Results and discussion

The results given in this chapter are obtained again using the cable considered in previous two chapters (the parameter values are given in Appendix B). However, here we use discrete approximation for the slopes of the cable. Similarly, the solid and dash curves denote the mode shapes associated with $h \neq 0$ and $h = 0$, respectively; and the Lagrangian coordinate is used as an independent variable and three different inclinations are investigated: 0^o, 30^o and 60^o. Similarly, ω_1 and ω_2 are frequencies in the figures respectively correspond to the solid and dash mode shapes.

It is observed from the presented figures that the effect of the large sag on the mode shapes of the cable is more clearly revealed on the y and z mode shapes. (see parts (b) and (c) in each figure). Whether a mode shape is associated with $h = 0$ or $h \neq 0$, it is far different from sine waves. Contractions can be seen at the center parts of the mode shapes.

For the same order frequencies, similar to that discussed in Chapter 2, the two sets of mode shapes in u' direction are completely different while they are similar in y' and z directions. By comparing the two sets of mode shapes in y' and z directions, we can conclude that these two sets of mode shapes behave quite differently. For example, in Fig. 4.1 (b), the two y' modes are almost in the opposite phase at the left-end part but at last almost in the same phase at the right-end part. But the two modes in part (c) of the same figure begin with almost the same phase at the left-end

part but ends with almost opposite phase at the right-end part. This is also true for other figures no matter the cable is inclined or not.

For the different order frequencies, there are symmetric and asymmetric mode shapes for both the two sets of mode shapes in y' and z directions when the cable is horizontal. When the cable is inclined, this type of regularity becomes quasi-symmetric and quasi-asymmetric. However, although the same type of regularity exists for the dash curves ($h \neq 0$) in u mode shapes, the solid curves ($h = 0$) of the u mode shapes remain symmetric.

When the cable is inclined, y and z mode shapes (both solid and dash curves) are more influenced than u mode shapes. This trend is clear by observing in Fig. 4.5 (b) (c) and Fig. 4.6 (b), (c).

Similarly, there is the decreasing trend on the frequency. Moreover, the decrease of the frequency considered in this chapter is much larger than those presented in previous chapters. This may be due to the large sag of the cable.

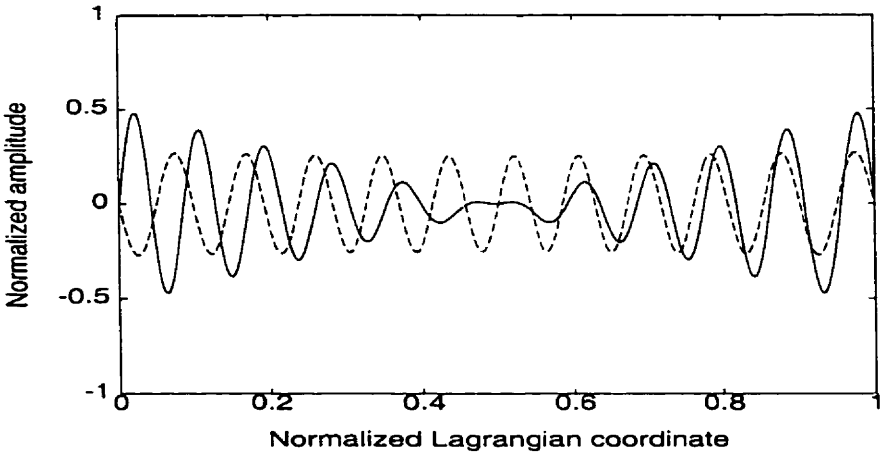

(a)

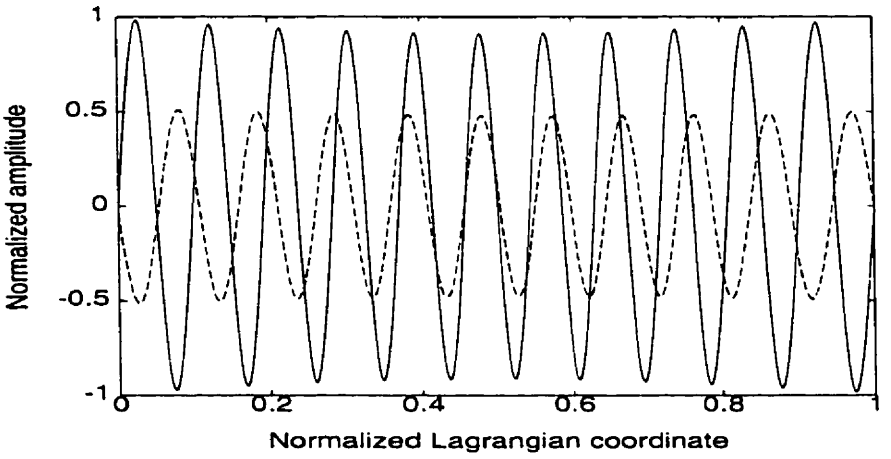

(b)

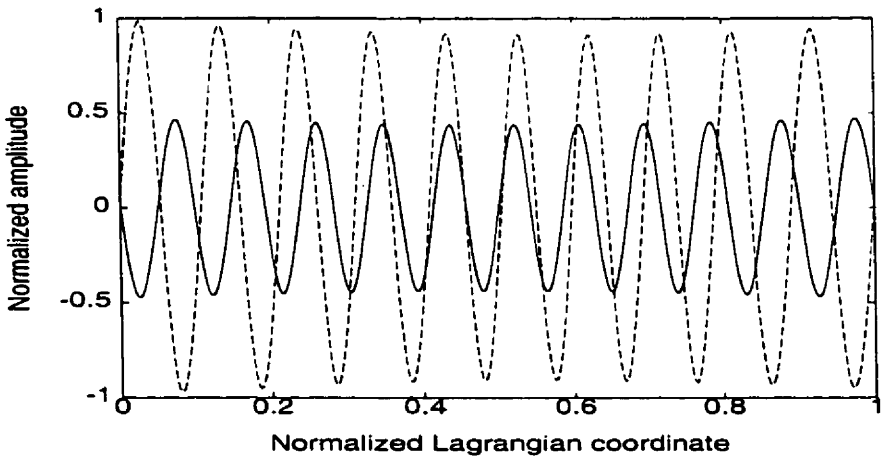

(c)

Figure 4.1: Asymmetric mode shapes associated with frequencies $\omega_1 = 6.52Hz$, $\omega_2 = 6.8Hz$ for the horizontal support without concentrated loads for large sagged cable

(a) u'-mode; (b) y'-mode; and (c) z-mode

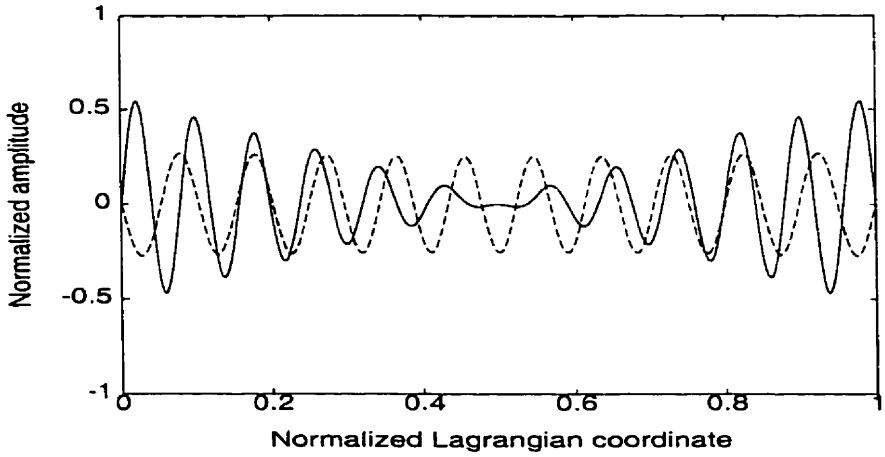

(a)

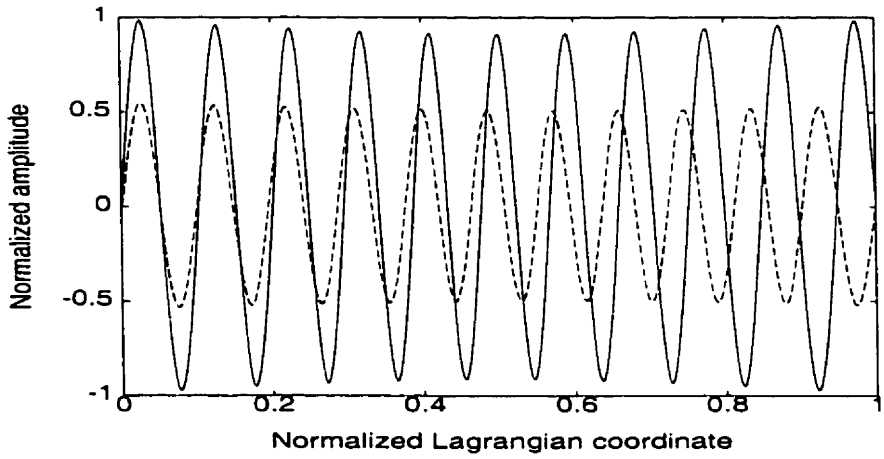

(b)

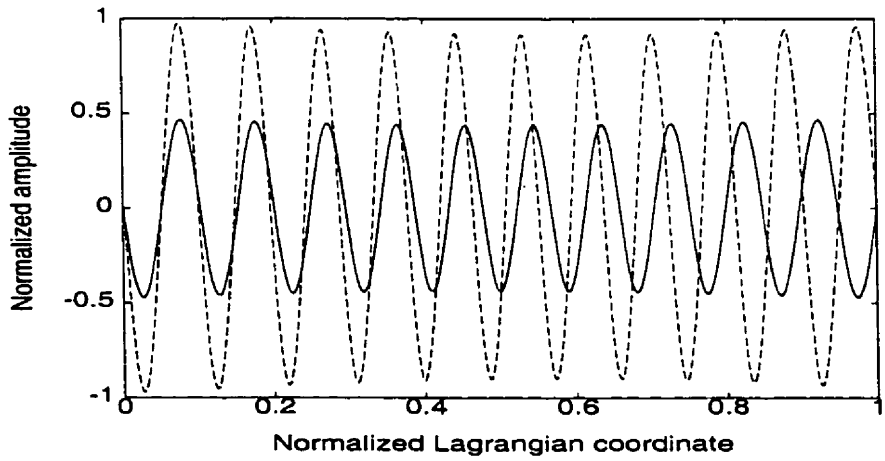

(c)

Figure 4.2: Symmetric mode shapes associated with frequencies $\omega_1 = 6.25Hz$, $\omega_2 = 7.45Hz$ for the horizontal support without concentrated loads for large sagged cable

(a) u'-mode; (b) y'-mode; and (c) z-mode

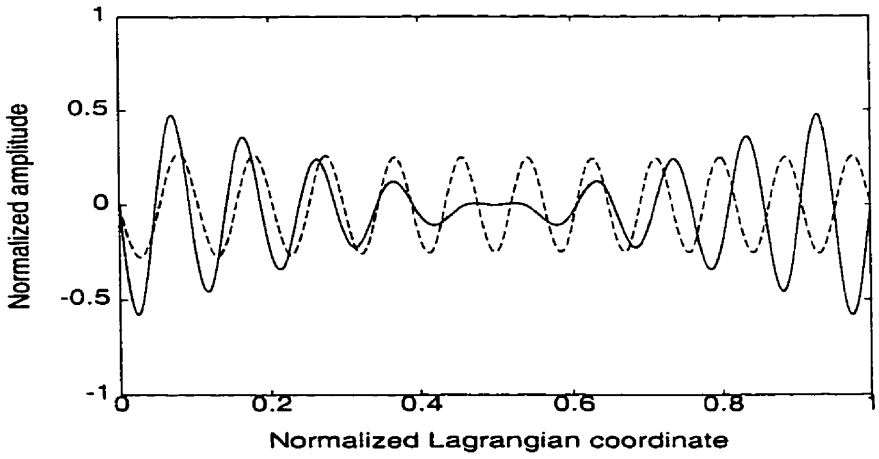

(a)

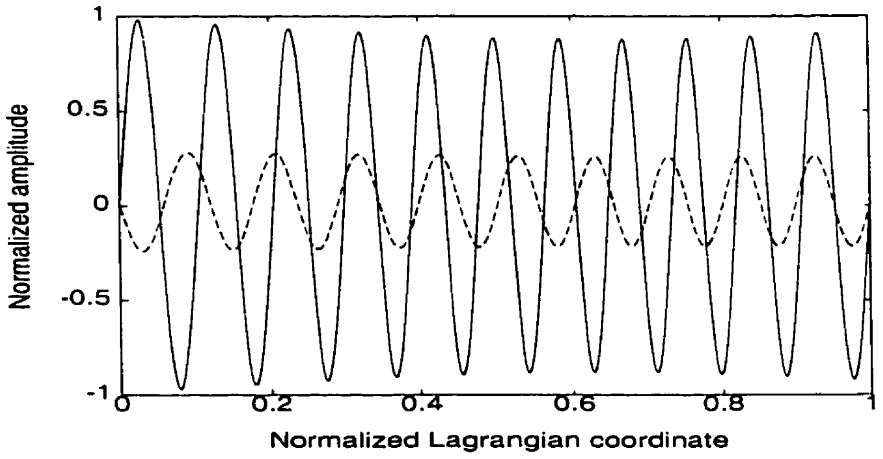

(b)

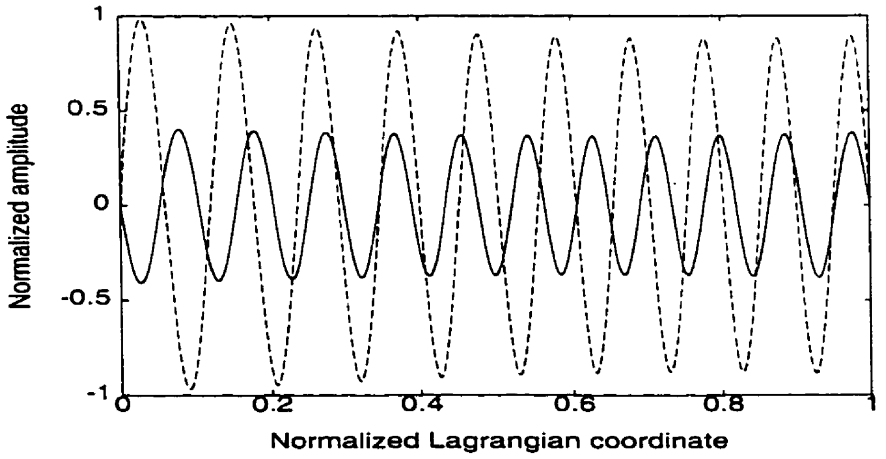

(c)

Figure 4.3: Asymmetric mode shapes associated with $\omega_1 = 5.67Hz$, $\omega_2 = 5.9Hz$ for the inclined support without concentrated loads for the large sagged cable with 30^o

(a) u'-mode; (b) y'-mode; and (c) z-mode

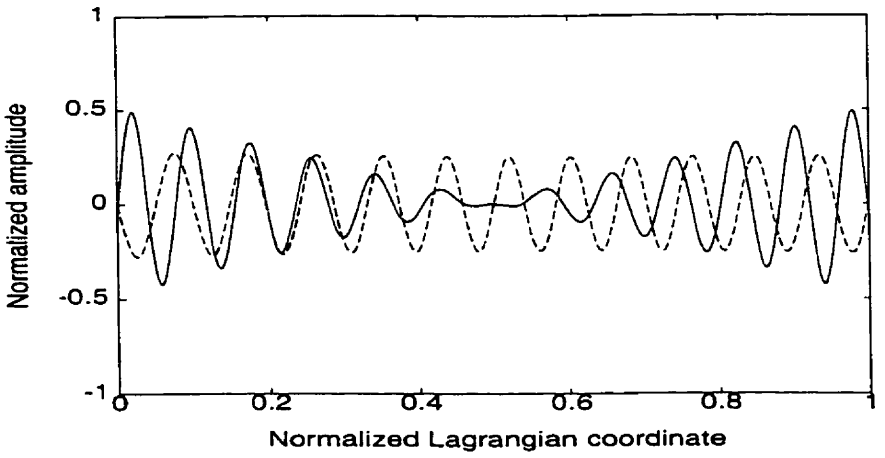

(a)

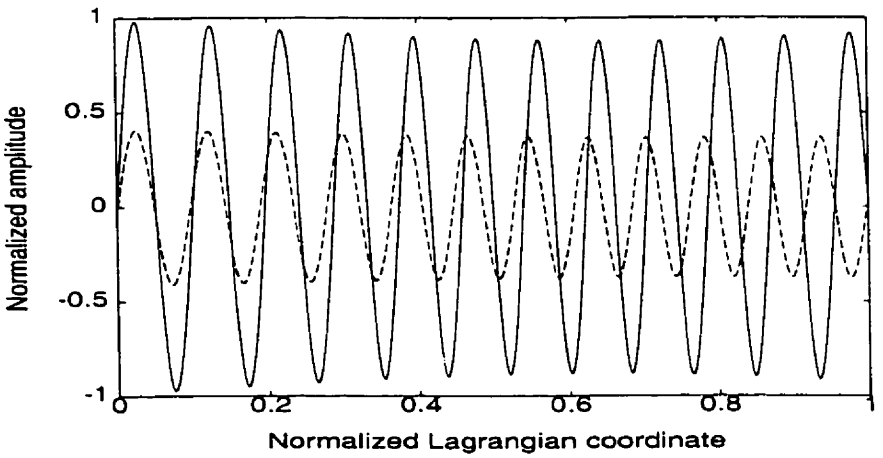

(b)

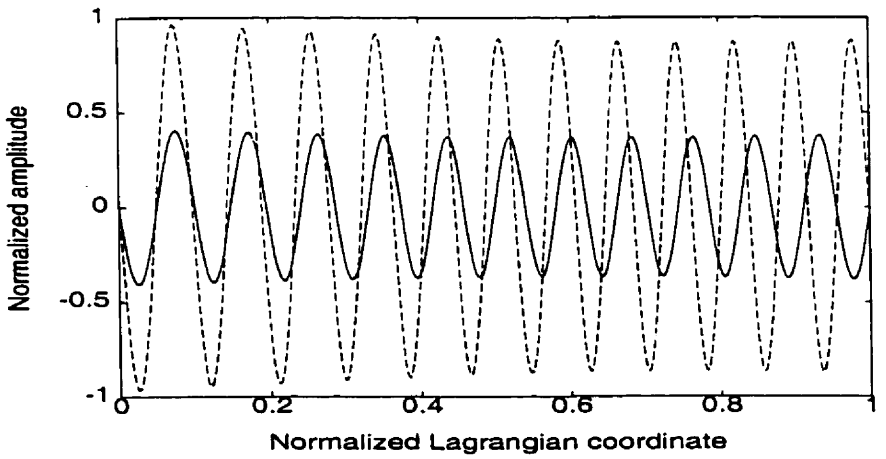

(c)

Figure 4.4: Symmetric mode shapes associated with frequencies $\omega_1 = 5.93Hz$, $\omega_2 = 7.5Hz$ for the inclined support without concentrated loads for the large sagged cable with 30^o

(a) u'-mode: (b) y'-mode; and (c) z-mode

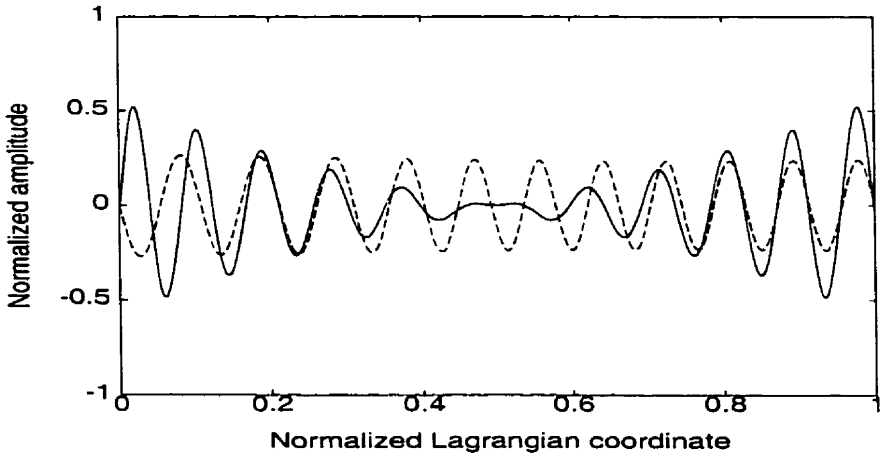

(a)

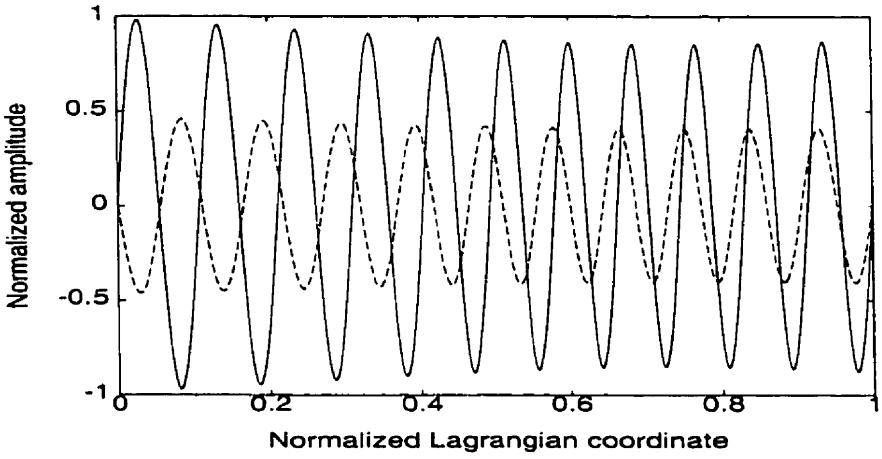

(b)

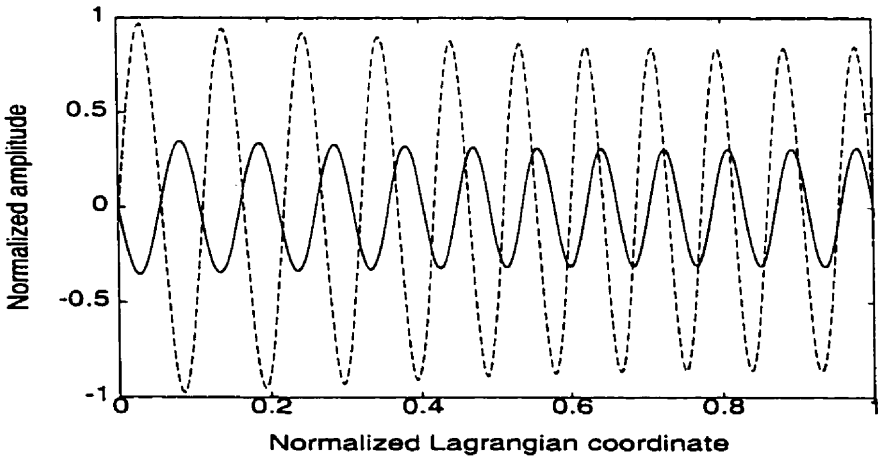

(c)

Figure 4.5: Asymmetric mode shapes associated with $\omega_1 = 3.29Hz$, $\omega_2 = 3.44Hz$ for the inclined support without concentrated loads for the large sagged cable with 60^o

(a) u'-mode; (b) y'-mode; and (c) z-mode

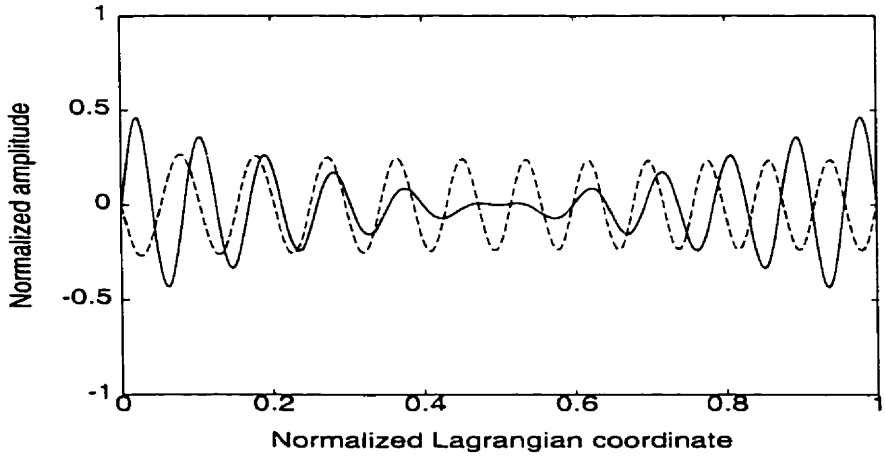

(a)

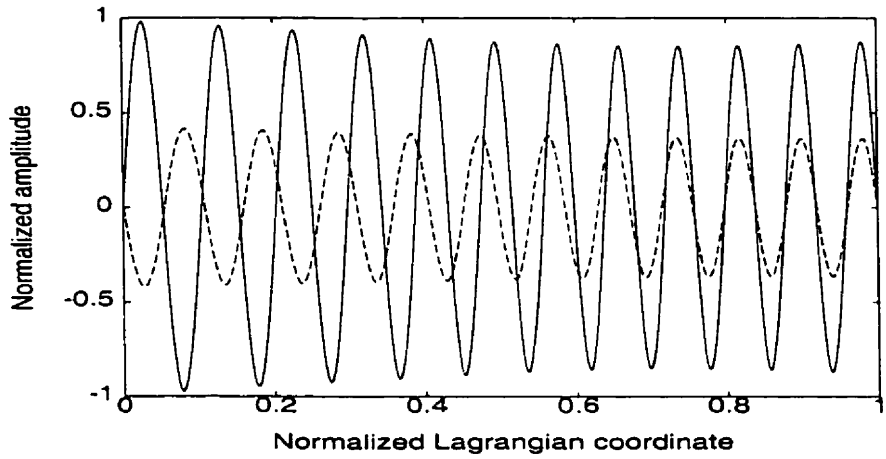

(b)

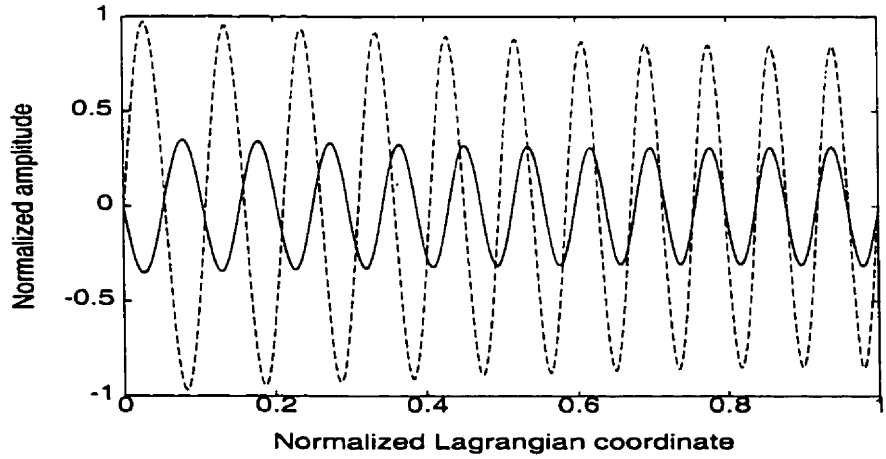

(c)

Figure 4.6: Symmetric mode shapes associated with $\omega_1 = 3.44Hz$, $\omega_2 = 4.04Hz$ for the inclined support without concentrated loads for the large sagged cable with 60°

(a) u'-mode; (b) y'-mode; and (c) z-mode

Chapter 5

Large sagged cables with concentrated loads

In this chapter, the last model of the large-sagged cable with concentrated loads will be discussed. The method used in this chapter is a combination of all the methods used in the previous chapters.

For notations, we use two sets of subscripts to describe our model: one is i which has the same meaning as before, i.e. the i-th point at which a concentrated load is imposed, the other set is k, which is introduced for approximating the cable slope, which is similar to that of Chapter 3. The points marked by k are obtained by dividing each i-th segment of the cable into M subsegments, which are not necessarily equal. Thus the i-th point at which a concentrated load is located must satisfy $k = i \cdot M$, which can be used to control and identify the two sets of points. To express the two sets of points in a single formula, we introduce the generalized *Kronecker delta* symbol [33,34].

The approach of analyzing the dynamic response of the cable is similar to that described in the previous chapters. Therefore, only brief descriptions are given here for simplicity. The static analysis for the flat cable with concentrated loads considered in Chapter 3 is still valid for this chapter and thus omitted.

5.1 Dynamic analysis

First, similarly to Chapter 4, we will make some modifications on the assumptions which are only applicable to flat cables and then extend the analysis given in Chapter 3 to consider the last model.

By using the procedure of obtaining Eq. (1.27)- (1.29), one can obtain the differential equations describing the dynamic response of the cable formulated in rotated coordinate system as follows:

$$\frac{\partial}{\partial s}[(H_x + h_x)\frac{\partial u'}{\partial x} + h_x\frac{dx'}{dx}] = m\frac{\partial^2 u'}{\partial t^2} + m_i\delta(s - s_i)\frac{\partial^2 u'}{\partial t^2}, \quad (5.1)$$

$$\frac{\partial}{\partial s}[(H_x + h_x)\frac{\partial y_2'}{\partial x} + h_x\frac{dy_1'}{dx}] = m\frac{\partial^2 y_2'}{\partial t^2} + m_i\delta(s - s_i)\frac{\partial^2 y_2'}{\partial t^2}. \quad (5.2)$$

$$\frac{\partial}{\partial s}[(H_x + h_x)\frac{\partial z_2}{\partial x} + h_x\frac{dz_1}{dx}] = m\frac{\partial^2 z_2}{\partial t^2} + m_i\delta(s - s_i)\frac{\partial^2 z_2}{\partial t^2}. \quad (5.3)$$

where the assumptions $T = H_x\frac{ds}{dx}$ and $\tau(t) = h_x\frac{ds}{dx}$, and the static profile obtained in Chapter 3 have been used.

The assumption $H_x >> h_x$ is still valid but another assumption $dx = ds\cos\theta$ needs to be modified as $dx = J_k^2\, ds\cos\theta$. Furthermore, we can express the two sets of points mentioned above in a single set of equations Eq. (5.1)- (5.3) by using the generalized Kronecker symbol defined later.

With the process described in Appendix C.4, we can obtain the piece wisely smooth differential equations and the discontinuity conditions on the slope of the cable by using Eq. (5.1)- (5.3). The differential equations are

$$\frac{\partial^2 u_k'}{\partial s^2} - \frac{m\cos\theta}{H_x}J_k^2\frac{\partial^2 u_k'}{\partial t^2} = -\frac{h_x q_y \sin\theta\cos\theta}{H_x^2}J_k^2. \quad (5.4)$$

$$\frac{\partial^2 y_{2k}'}{\partial s^2} - \frac{m\cos\theta}{H_x}J_k^2\frac{\partial^2 y_{2k}'}{\partial t^2} = \frac{h_x q_y \cos^2\theta}{H_x^2}J_k^2. \quad (5.5)$$

$$\frac{\partial^2 z_{2k}}{\partial s^2} - \frac{m\cos\theta}{H_x}J_k^2\frac{\partial^2 z_{2k}}{\partial t^2} = \frac{h_x q_z \cos\theta}{H_x^2}J_k^2. \quad (5.6)$$

and the discontinuity conditions are

$$\frac{\partial u_{k+1}'(s_{k+1})}{\partial x} - \frac{\partial u_k'(s_{k+1})}{\partial x} = \frac{m_{i+1}}{H_x}\frac{\partial^2 u_i}{\partial t^2}\delta_{ki} + \frac{h_x P_{i+1}\sin\theta}{H_x^2}\delta_{ki}. \quad (5.7)$$

$$\frac{\partial y_{2k+1}'(s_{k+1})}{\partial x} - \frac{\partial y_{2k}'(s_{k+1})}{\partial x} = \frac{m_{i+1}}{H_x}\frac{\partial^2 y_i}{\partial t^2}\delta_{ki} - \frac{h_x P_{i+1}\cos\theta}{H_x^2}\delta_{ki}, \quad (5.8)$$

$$\frac{\partial z_{2k+1}(s_{k+1})}{\partial x} - \frac{\partial z_{2k}(s_{k+1})}{\partial x} = \frac{m_{i+1}}{H_x}\frac{\partial^2 z_i}{\partial t^2}\delta_{ki}, \quad (5.9)$$

where the Kronecker function is defined as

$$\delta_{ki} = \begin{cases} 0 & k = i\cdot M\ , \\ 1 & k \neq i\cdot M\ . \end{cases}$$

In order to find the frequency equation, we need to use the Hooke's Law. Note that although the static parts in this equation are the same as those given in Chapter 4, the dynamic parts are different.

Applying the method of separation of variables to Eq. (5.4)- (5.6) with the aid of a similar Hooke's Law yields

$$U_k = C_{1k}\cos[\beta J_k(s-s_k)] + C_{2k}\sin[\beta J_k(s-s_k)] - \frac{hq_y \sin\theta\cos\theta}{\beta^2 H_x^2}. \quad (5.10)$$

$$Y_{2k} = C_{3k}\cos[\beta J_k(s-s_k)] + C_{4k}\sin[\beta J_k(s-s_k)] + \frac{hq_y \cos^2\theta}{\beta^2 H_x^2}. \quad (5.11)$$

$$Z_{2k} = C_{5k}\cos[\beta J_k(s-s_k)] + C_{6k}\sin[\beta J_k(s-s_k)] + \frac{hq_z \cos\theta}{\beta^2 H_x^2}. \quad (5.12)$$

The integration constants can be determined from Eq. (5.7)- (5.9) and the continuity conditions and boundary conditions. However, they need to be adjusted according to the method of separation of variables, and the modification results in

$$\frac{dU_{k+1}(s_{k+1})}{ds} - \frac{dU_k(s_{k+1})}{ds} = -\frac{m_{i+1}}{m}\beta^2 J_k^2 U_k(s_{k+1})\delta_{ki} + \frac{hP_{i+1}J_k^2 \sin\theta\cos\theta}{H_x^2}\delta_{ki}, \quad (5.13)$$

$$\frac{dY_{k+1}(s_{k+1})}{ds} - \frac{dY_k(s_{k+1})}{ds} = -\frac{m_{i+1}}{m}\beta^2 J_k^2 Y_k(s_{k+1})\delta_{ki} + \frac{hP_{i+1}J_k^2 \cos^2\theta}{H_x^2}\delta_{ki}, \quad (5.14)$$

$$\frac{dZ_{k+1}(s_{k+1})}{ds} - \frac{dZ_k(s_{k+1})}{ds} = -\frac{m_{i+1}}{m}\beta^2 J_k^2 Z_k(s_{k+1})\delta_{ki}, \quad (5.15)$$

$$U_{k+1}(s_{k+1}) = U_k(s_{k+1}), \quad (5.16)$$

$$Y_{k+1}(s_{k+1}) = Y_k(s_{k+1}), \quad (5.17)$$

$$Z_{k+1}(s_{k+1}) = Z_k(s_{k+1}), \quad (5.18)$$

$$U_0(0) = 0 \qquad U_{\tilde{N}}(L_s) = 0, \quad (5.19)$$

$$Y_0(0) = 0 \qquad Y_{\tilde{N}}(L_s) = 0, \quad (5.20)$$

$$Z_0(0) = 0 \qquad Z_{\tilde{N}}(L_s) = 0, \quad (5.21)$$

where

$$\begin{aligned} \beta &= \sqrt{\frac{m\cos\theta}{H_x}}\omega. \\ \tilde{N} &= (N+1)M-1. \end{aligned}$$

The constants can be found recursively with the help of transfer matrix:

$$\begin{pmatrix} C_{1k} \\ C_{2k} \end{pmatrix} = [D_0^k]\begin{pmatrix} C_{10} \\ C_{20} \end{pmatrix} + \vec{\tau}_k\left(\frac{h\sin\theta\cos\theta}{\beta^2 H_x^2}\right). \tag{5.22}$$

$$\begin{pmatrix} C_{3k} \\ C_{4k} \end{pmatrix} = [D_0^k]\begin{pmatrix} C_{30} \\ C_{40} \end{pmatrix} + \vec{\tau}_k\left(-\frac{h\cos^2\theta}{\beta^2 H_x^2}\right), \tag{5.23}$$

$$\begin{pmatrix} C_{5k} \\ C_{6k} \end{pmatrix} = [D_0^k]\begin{pmatrix} C_{50} \\ C_{60} \end{pmatrix} + \vec{s}_k\left(-\frac{h\cos\theta}{\beta^2 H_x^2}\right), \tag{5.24}$$

where $[D_0^k]$ is the transfer matrix given by $[D_0^k] = [D_{k-1}^k][D_0^{k-1}]$ with $[D_0^0] = I$(I is a 2×2 identity matrix). The matrix $[D_{k-1}^k]$ is given by

$$[D_{k-1}^k] = \begin{bmatrix} D_{k-1}^k(1,1) & D_{k-1}^k(1,2) \\ D_{k-1}^k(2,1) & D_{k-1}^k(2,2) \end{bmatrix}$$

where

$$\begin{aligned} D_{k-1}^k(1,1) &= \cos[\beta J_{k-1}(s_k - s_{k-1})], \\ D_{k-1}^k(1,2) &= \sin[\beta J_{k-1}(s_k - s_{k-1})], \\ D_{k-1}^k(2,1) &= -\frac{J_{k-1}}{J_k}\sin[\beta J_{k-1}(s_k - s_{k-1})] \\ &\quad -\frac{m_i}{m}\frac{J_{k-1}^2}{J_k}\beta\cos[\beta J_{k-1}(s_k - s_{k-1})]\delta_{ki}, \\ D_{k-1}^k(2,2) &= \frac{J_{k-1}}{J_k}\cos[\beta J_{k-1}(s_k - s_{k-1})] \\ &\quad -\frac{m_i}{m}\frac{J_{k-1}^2}{J_k}\beta\cos[\beta J_{k-1}(s_k - s_{k-1})]\delta_{ki} \end{aligned}$$

The vectors $\vec{\tau}_k$ and $\vec{s}_k$ are

$$\begin{aligned} \vec{\tau}_k &= [D_{k-1}^k]\vec{\tau}_{k-1} + \begin{pmatrix} 0 \\ \beta[P_i + (\frac{m_i}{m})q_y]\frac{J_{k-1}^2}{J_k}\delta_{ki} \end{pmatrix}, \\ \vec{s}_k &= [D_{k-1}^k]\vec{s}_{k-1} + \begin{pmatrix} 0 \\ \beta(\frac{m_i}{m})q_z\frac{J_{k-1}^2}{J_k}\delta_{ki} \end{pmatrix}. \end{aligned}$$

with $\vec{r}_0 = \vec{s}_0 = \vec{0}$.

The initial values for the above recursive formulas are

$$C_{10} = \frac{hq_y \sin\theta\cos\theta}{\mathcal{J}^2 H_x^2}. \tag{5.25}$$

$$C_{30} = -\frac{hq_y \cos^2\theta}{\mathcal{J}^2 H_x^2}. \tag{5.26}$$

$$C_{50} = -\frac{hq_z \cos\theta}{\mathcal{J}^2 H_x^2}. \tag{5.27}$$

$$QDC_{20} = Q.N_x(\frac{h \sin\theta\cos\theta}{\mathcal{J}^2 H_x^2}). \tag{5.28}$$

$$QDC_{40} = Q.N_y(-\frac{h\cos^2\theta}{\mathcal{J}^2 H_x^2}). \tag{5.29}$$

$$QDC_{60} = Q.N_z(-\frac{h\cos\theta}{\mathcal{J}^2 H_x^2}). \tag{5.30}$$

where QD, $Q.N_x$, $Q.N_y$ and $Q.N_z$ are given in Appendix A.

Then, with the process described in Appendix C.4, one can find the frequency equation as:

$$\begin{aligned}
\frac{h}{AE}L_e = {} & \frac{q_y q_z \sin\theta}{q_y^2+q_z^2}\sum_{k=0}^{n}\{(A_k,B_k)D_{1i}([D_0^k]\begin{pmatrix}C_{10}\\C_{20}\end{pmatrix}+\vec{r}_k(\frac{h\sin\theta\cos\theta}{\mathcal{J}^2H_x^2}))\} \\
& -\frac{q_y q_z\cos\theta}{q_y^2+q_z^2}\sum_{k=0}^{n}\{(A_k,B_k)D_{1i}([D_0^k]\begin{pmatrix}C_{30}\\C_{10}\end{pmatrix}+\vec{r}_k(-\frac{h\cos^2\theta}{\mathcal{J}^2H_x^2}))\} \\
& +\frac{q_y^2}{q_y^2+q_z^2}\sum_{k=0}^{n}\{(A_k,B_k)D_{1i}([D_0^k]\begin{pmatrix}C_{50}\\C_{60}\end{pmatrix}+\vec{s}_k(-\frac{h\cos\theta}{\mathcal{J}^2H_x^2}))\} \\
& +\frac{q_y\sin\theta}{H_x}\sum_{k=0}^{n}\{(D_k,E_k)D_{1i}([D_0^k]\begin{pmatrix}C_{10}\\C_{20}\end{pmatrix}+\vec{r}_k(\frac{h\sin\theta\cos\theta}{\mathcal{J}^2H_x^2}))\} \\
& -\frac{q_y\cos\theta}{H_x}\sum_{k=0}^{n}\{(D_k,E_k)D_{1i}([D_0^k]\begin{pmatrix}C_{30}\\C_{40}\end{pmatrix}+\vec{r}_k(-\frac{h\cos^2\theta}{\mathcal{J}^2H_x^2}))\} \\
& -\frac{q_z}{H_x}\sum_{k=0}^{n}\{(D_k,E_k)D_{1i}([D_0^k]\begin{pmatrix}C_{50}\\C_{60}\end{pmatrix}+\vec{s}_k(-\frac{h\cos\theta}{\mathcal{J}^2H_x^2}))\}
\end{aligned}$$

where the constants A_k, B_k, D_k and E_k can be found in the Appendix A.

As usual, there are two general cases we need to discuss for this model according to $h = 0$ and $h \neq 0$.

1. When $h = 0$, the frequency is determined from equation $QD = 0$. Substituting $h = 0$ into Eq. (5.31) yields

$$FC_{20} + GC_{40} + IC_{60} = 0 \tag{5.31}$$

where the constants F, G, and I are given in Appendix A.

Another equation needed to carry out the discussion for the dynamic response of the cable can be found by evaluating Hooke's Law at the right-end of the cable. With the aid of the static profile given in Eq. (3.38)- (3.41) and Appendix C.4, we obtain the equation

$$C_{20} = DC_{40} + EC_{60}. \tag{5.32}$$

Then eliminating C_{20} from Eq. (5.31) and Eq. (5.32) yields

$$\tilde{D}C_{40} + \tilde{E}C_{60} = 0 \tag{5.33}$$

where $\tilde{D}$ and $\tilde{E}$ can be found in Appendix A.

Therefore, we can discuss the dynamic response of the cable on the basis of Eq. (5.33). There are four subcases:

(a) If $\tilde{D} = \tilde{E} = 0$, then Eq. (5.33) indicates that C_{40} and C_{60} can be chosen arbitrarily, and then C_{20} is determined by Eq. (5.32). The mode shape functions are given by

$$U_k(s) = \begin{pmatrix} \cos[\beta J_k(s - s_k)] & \sin[\beta J_k(s - s_k)] \end{pmatrix} \begin{pmatrix} D_0^k(1,2) \\ D_0^k(2,2) \end{pmatrix} C_{20},$$

$$Y_{2k}(s) = \begin{pmatrix} \cos[\beta J_k(s - s_k)] & \sin[\beta J_k(s - s_k)] \end{pmatrix} \begin{pmatrix} D_0^k(1,2) \\ D_0^k(2,2) \end{pmatrix} C_{40},$$

$$Z_{2k}(s) = \begin{pmatrix} \cos[\beta J_k(s - s_k)] & \sin[\beta J_k(s - s_k)] \end{pmatrix} \begin{pmatrix} D_0^k(1,2) \\ D_0^k(2,2) \end{pmatrix} C_{60}.$$

(b) If $\tilde{D} = 0$ but $\tilde{E} \neq 0$. Eq. (5.33) gives $C_{60} = 0$ and then Eq. (5.32) determines $C_{20} = DC_{40}$ where C_{40} can be chosen arbitrarily. Therefore, the mode shape functions are

$$\begin{aligned} U_k(s) &= \left(\cos[\beta J_k(s - s_k)] \quad \sin[\beta J_k(s - s_k)] \right) \\ &\qquad \begin{pmatrix} D_0^k(1,2) \\ D_0^k(2,2) \end{pmatrix} C_{20}, \\ Y_{2k}(s) &= \left(\cos[\beta J_k(s - s_k)] \quad \sin[\beta J_k(s - s_k)] \right) \\ &\qquad \begin{pmatrix} D_0^k(1,2) \\ D_0^k(2,2) \end{pmatrix} C_{40}, \\ Z_{2k}(s) &= 0. \end{aligned}$$

(c) If $\tilde{D} \neq 0$ but $\tilde{E} = 0$, then $C_{40} = 0$, $C_{20} = EC_{60}$, where C_{60} can be chosen arbitrarily. The mode shape functions in this subcase are given by

$$\begin{aligned} U_k(s) &= \left(\cos[\beta J_k(s - s_k)] \quad \sin[\beta J_k(s - s_k)] \right) \\ &\qquad \begin{pmatrix} D_0^k(1,2) \\ D_0^k(2,2) \end{pmatrix} C_{20}, \\ Y_{2k}(s) &= 0, \\ Z_{2k}(s) &= \left(\cos[\beta J_k(s - s_k)] \quad \sin[\beta J_k(s - s_k)] \right) \\ &\qquad \begin{pmatrix} D_0^k(1,2) \\ D_0^k(2,2) \end{pmatrix} C_{60}. \end{aligned}$$

(d) If $\tilde{D} \neq 0$ and $\tilde{E} \neq 0$, then $C_{60} = -\frac{\tilde{D}}{\tilde{E}} C_{40}$, and C_{40} can be chosen arbitrarily. The mode shape functions in this subcase are expressed by the same formulas as those for case (a). But they are different due to the different values chosen for the constants.

Note that case (a) has two independent mode shapes with one single *repeated frequency*, determined by $QD = 0$. For the cases (b), (c) and (d), there is one mode shape associated with this frequency. The second mode shape and its frequency can be found from the case $h \neq 0$.

2. When $h \neq 0$, we can solve Eq. (5.28)- (5.30) for C_{20}, C_{40}, and C_{60}. Then substituting these expressions into

The mode shape functions in y' and z' directions are given by Eq. (5.11) and Eq. (5.12) which can be rewritten as

$$Y_{2k} = C_{3k}\cos[\beta J_k(s-s_k)] + C_{4k}\sin[\beta J_k(s-s_k)] - C_{30}, \quad (5.34)$$

$$Z_{2k} = C_{5k}\cos[\beta J_k(s-s_k)] + C_{6k}\sin[\beta J_k(s-s_k)] - C_{50}. \quad (5.35)$$

with the aid of the initial values in the recursive formulas given by Eq. (5.26) and Eq. (5.27).

The mode shape function in x' direction can be obtained from the Hooke's Law. A brief description of the process given in Appendix C.4 leads to

$$\frac{dU_k(s)}{ds} = \frac{OS_7}{OS_3} + \frac{OS_8}{OS_3}(-C_{3k}OS_{bs} + C_{4k}OS_{bc}) + \frac{OS_9}{OS_3}(-C_{5k}OS_{bs} + C_{6k}OS_{bc}), \quad (5.36)$$

where OS_i $(i = 1 \ldots 9)$. OS_{bs} and OS_{bc} can be found in Appendix A.

5.2 Results and discussion

The same cable considered in previous chapters are used here to discuss the models in the same three different situations. Two curves representing two different mode shapes are solid lines and dash lines, associated with $h = 0$ and $h \neq 0$, respectively. Again, we use Lagrangian coordinates to represent our results. ω_1 and ω_2 in the figures are frequencies respectively correspond to the solid and dash mode shapes.

The large sag of the cable has an obvious effect on the mode shapes of the cable. Comparing Fig. 5.1 with Fig. 3.1 indicates that the curves given in this chapter are more smooth than those given in Chapter 3.

For the same order frequencies, the solid curves ($h \neq 0$) have some similarity while for the dash curves ($h = 0$) the z mode shapes are different from the y' mode shapes. The mode shapes when $h = 0$ and $h \neq 0$ still behave in an opposite sense. For example, in Fig. 5.1 (b) and Figure 5.2 (b), the two sets of mode shapes are almost in the same phase but in part (c) of these figures, the mode shapes have almost a 180° phase difference. However, this behavior changes in Fig. 5.3, where in part (b), the

mode shapes begin with almost the same phase at the left-end part but ends with almost an opposite phase at the right-end part: while part (c) reverses the trend.

For the different order frequencies, the mode shapes have no obvious changes. There are three different types of mode shapes in each direction for different frequencies under the same supports in Chapter 3. However, these do not exist here. Therefore, for each different inclination of the support, only the results of one frequency are given.

Similar to Chapter 3, when the cable is inclined, the mode shapes almost do not change. This again shows that the cables with concentrated loads are not sensitive to the inclination of the cable support, no matter whether they are flat cables or large-sagged cables.

A similar decreasing trend is also found for the same order frequencies, which has been found in previous chapters.

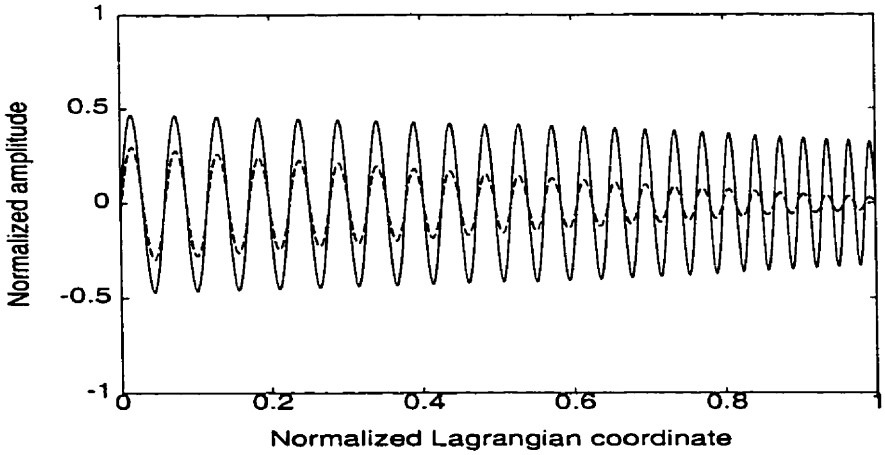

(a)

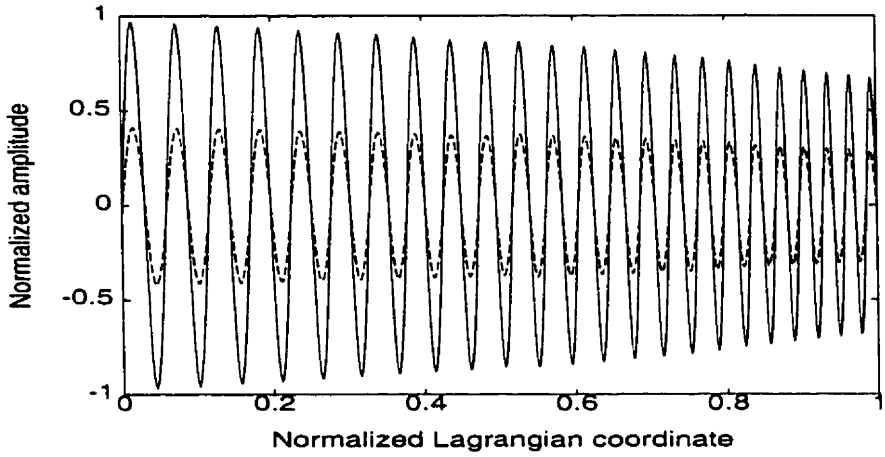

(b)

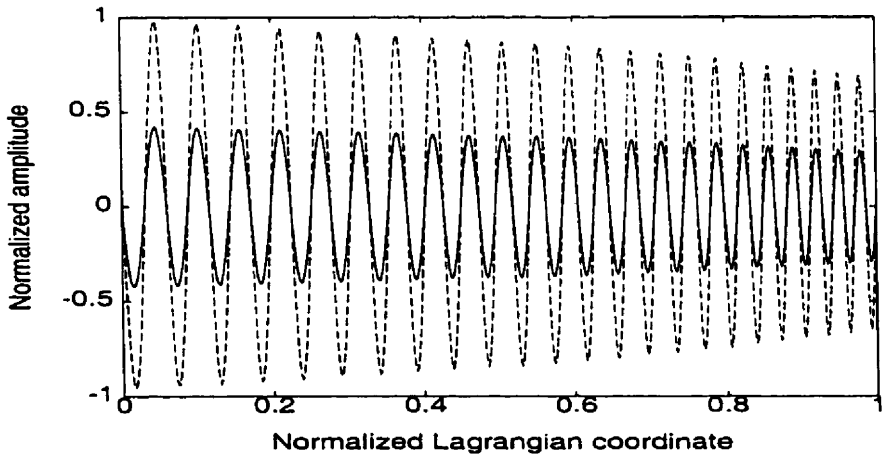

(c)

Figure 5.1: Mode shapes associated with frequencies $\omega_1 = 8.41Hz$, $\omega_2 = 8.5Hz$ for the horizontal support of large-sagged cable with concentrated loads. Two concentrated loads are at $0.517618L_s$ and $0.817734L_s$.

(a) u'-mode; (b) y'-mode; and (c) z-mode

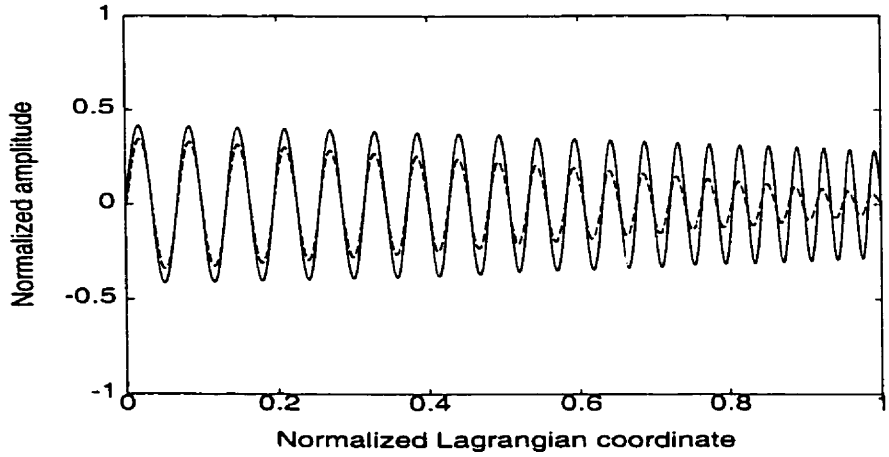

(a)

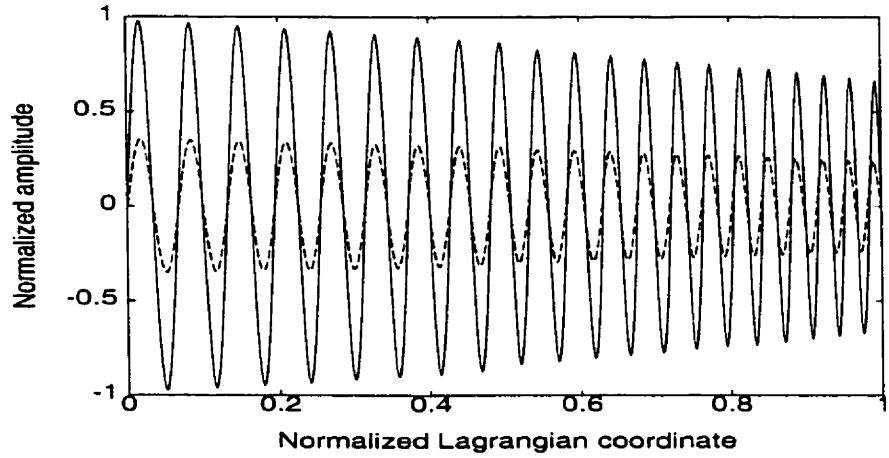

(b)

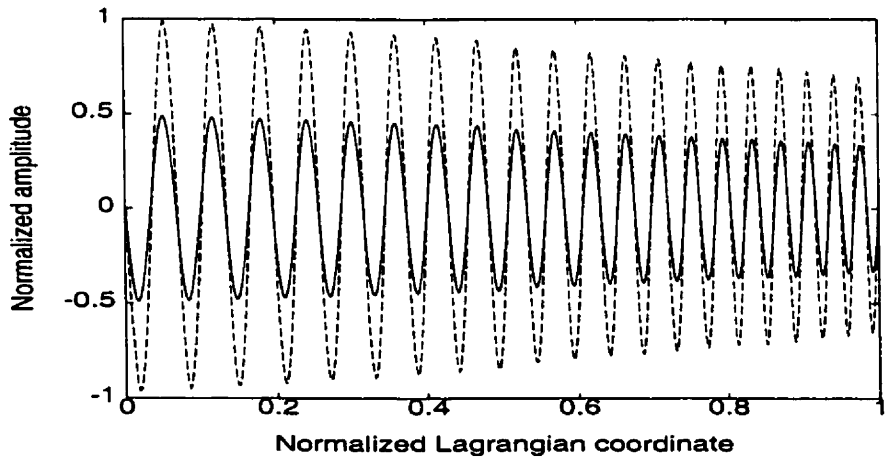

(c)

Figure 5.2: Mode shapes associated with $\omega_1 = 6.973Hz$, $\omega_2 = 7.0Hz$ for the inclined support of large-sagged cable with concentrated loads at 30^o. Two concentrated loads are at $0.518283L_s$ and $0.818236L_s$.

(a) u'-mode; (b) y'-mode; and (c) z-mode

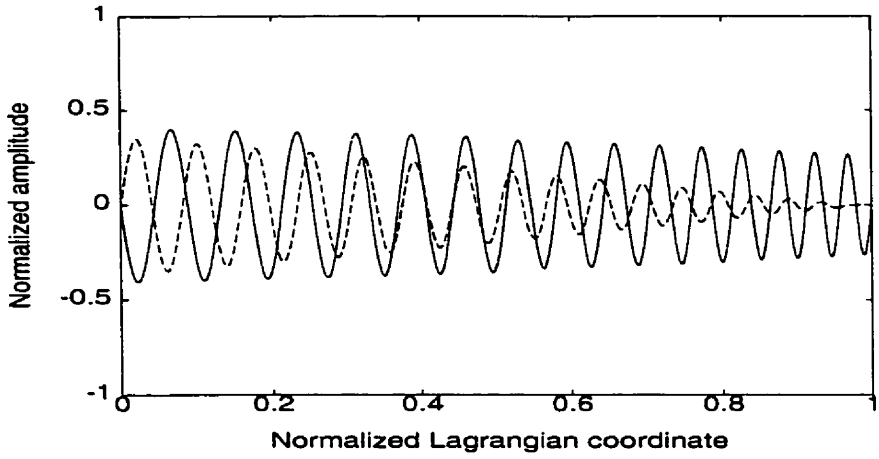

(a)

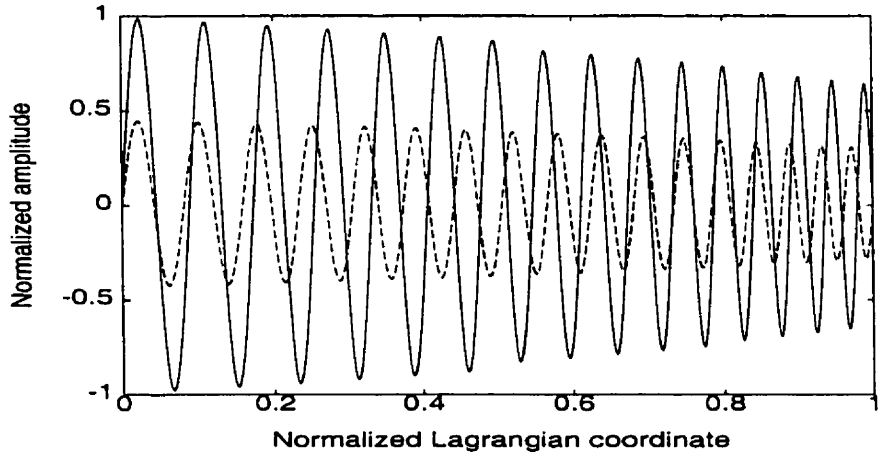

(b)

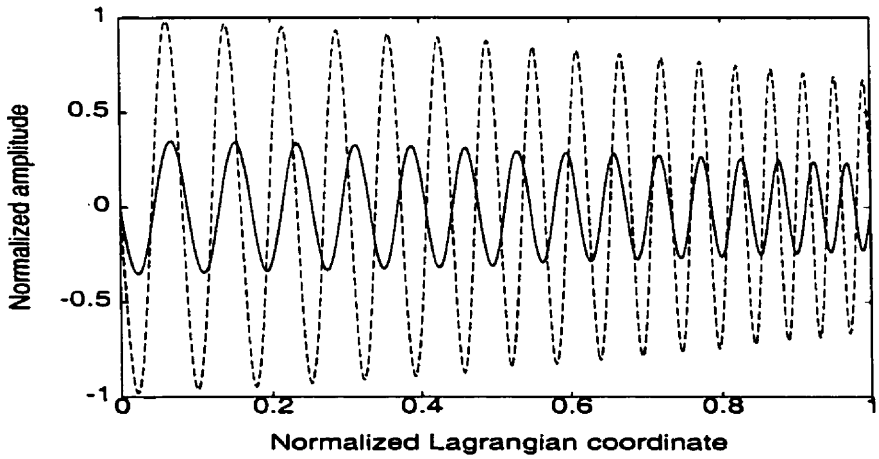

(c)

Figure 5.3: Mode shapes associated with $\omega_1 = 4.81Hz$, $\omega_2 = 5.11Hz$ for the inclined support of large-sagged cable with concentrated loads at 60^o. Two concentrated loads are at $0.519104L_s$ and $0.819078L_s$.

(a) u'-mode; (b) y'-mode; and (c) z-mode

Chapter 6

Conclusions and future work

6.1 Summary of the thesis

In this thesis, we have studied several cable models with fixed boundary conditions by using the method of coordinate transformation and the Non-homogeneous Transfer Matrix (NTM) approach.

There are two general models: one is for flat cables and the other for large-sagged cables. Each of the two cases is divided into two subcases: one is for bare cables and the other for the cables with concentrated loads. All the cases include both horizontal support and inclined support. The analysis for flat cables is relatively easy because it is assumed that the slope of a whole cable is a constant. For large-sagged cables, however, a cable needs to be divided into different segments which uses different approximation for the slope of the cable.

For the dynamic analysis, the differential equation in the x' direction can not be decoupled because of the rotation of the coordinates.

The inclusion of the differential equation in x' direction results in a difficulty that we can not discuss the dynamic response based on frequency equation only. Another supplementary equation is needed, which can be obtained from the evaluation of the Hooke's Law at the right-end support. Then the dynamic response can be thoroughly discussed on the basis of this supplementary equation together with the frequency equation.

The results presented in this thesis include the special cases with horizontal supports, i.e. $\theta = 0$, which has been studied in [11,12].

6.2 Conclusions and discussions

Although we are considering three dimensional cable models, there exist only two independent mode shapes which are mainly in in-plane and out-of-plane directions because of the constraint due to the Hook's Law. The two mode shapes are associated with either one repeated frequency or two independent frequencies. The mode shape in the x' direction always depends on one or both of the two independent mode shapes. This is similar to the case with horizontal support [12].

As to the effect of inclination, flat bare cables are more sensitive to its changes than the flat cables with concentrated loads or large-sagged cables.

For the effect of concentrated loads, compared to large sagged cables, flat cables are easier to diminish the reliance on the inclination and can dramatically decrease the amplitudes of vibration. However, the mode shapes for the cables with concentrated loads are sensitive to the load parameters such as the weight and the locations. Therefore, it is not easy to achieve an optimum design for controlling vibrations and a parametric study is needed [5].

As to the sag of the cables, the figures presented in this thesis show that the effect of concentrated loads on reducing vibration amplitude is impaired by large sags. Also, it has been seen that with large-sagged assumptions, the cable given in this thesis is insensitive to cable inclination.

Finally, it has been observed that the frequency decreases when the angle of inclination increases. This is true for all four models studied in this thesis.

6.3 Future work

We use the NTM approach combined with the coordinate rotation to obtain closed-form solutions. Basically, we use the method of separation of variables to convert original partial different equations to ordinary differential equations. Numerical approaches, such as FEM and FED can be applied directly to the partial differential equations. One task of future work is to develop a numerical simulation package comparisons between the analytical predictions and numerical results.

In this thesis, we only implemented program packages to compute the frequencies from the frequency equations to obtain the frequencies. Therefore, a complete user-friendly software packages needs to be developed. Moreover, for calculating high-order frequencies, better numerical methods should be adopted to achieve better convergence. A 3-DOF model model for transmission lines with concentrated loads and a complete software package have been developed by Yu [5] to carry out galloping analysis. However, this model is only applicable for horizontal supports. A similar 3-DOF model describing inclined cables and software package should be developed.

For the practical design to control cable vibration, a parametric study is needed [5] because of the sensitivity of cables on concentrated loads. A software package written in FORTRAN 77 for the parametric study of the 3-DOF model mentioned above has been developed [5]. It can be used to investigate the influence of detuning pendulums and to analyze the effects of structural parameters in reducing the possibility of the indication of galloping. A similar parametric study needs to be performed for inclined cables by using the results obtained in this thesis.

Appendix A

Constants used in this thesis

A.1 Constants used in Chapter 2

For Section 2.1.1

$$
\begin{aligned}
P_1 &= \frac{1}{mg}\cosh\left(\frac{mgL_x}{H_x}+2C_3\right)\sinh\left(\frac{mgL_x}{H_x}\right)-\frac{L_x}{H_x}\\
P_2 &= \sinh^2\left(\frac{mgL_x}{2H_x}+C_3\right)\sinh^2\left(\frac{mgL_x}{2H_x}\right)\\
P_3 &= \frac{AE}{L_e}\\
P_4 &= \frac{AEH_x}{L_eL_x}\\
Q_2 &= q_y^2+q_z^2\\
L_e &= \frac{H_x}{mg}\left[\sinh\left(\frac{mgL_x}{H_x}+C_3\right)+\frac{1}{3}\sinh^3\left(\frac{mgL_x}{H_x}+C_3\right)\right.\\
&\quad \left.-\sinh\left(C_3\right)-\frac{1}{3}\sinh^3\left(C_3\right)\right]
\end{aligned}
$$

For Section 2.1.2

$$
P_{31} = \frac{\sqrt{q_y^2+q_z^2}}{2H_x}L_x - CONST_1
$$

For Section 2.2

$$
L_e = \int_0^{L_x}\left(\frac{ds}{dx}\right)^2 dx
$$

$$= \frac{(\cos^2\theta q_y^2 + q_z^2)H_x}{2\cos^2\theta(q_y^2+q_z^2)^{\frac{3}{2}}}\cosh(2CONST_1)\sinh\left(\frac{\sqrt{q_y^2+q_z^2}}{H_x}L_x\right) + \frac{(\cos^2\theta q_y^2 + q_z^2)L_x}{2\cos^2\theta(q_y^2+q_z^2)}$$

$$\lambda^2 = \left(\frac{AE}{L_e}\right)\left(\frac{L_s}{H_x}\right)^3(q_y^2+q_z^2)\cos\theta$$

$$CONST_1 = \sinh^{-1}\left[\frac{\sin\theta L_x}{2H_x\sqrt{\frac{\cos^2\theta q_y^2+q_z^2}{q_y^2+q_z^2}}\sinh\left(\frac{\sqrt{q_y^2+q_z^2}}{2H_x}L_x\right)}\right]$$

$$CONST_2 = \sin\theta\frac{q_y^2}{q_y^2+q_z^2} + \frac{q_y}{q_y^2+q_z^2}\sqrt{\cos^2 q_y^2+q_z^2}\cdot \sinh\left(\frac{\sqrt{q_y^2+q_z^2}}{2H_x}L_x - CONST_1\right)$$

$$A = \frac{C}{C\tan\theta - \sec\theta}$$

$$B = \frac{C\frac{q_z}{q_y\cos\theta}}{C\tan\theta - \sec\theta}$$

$$C = CONST_2 - \frac{q_y\cos\theta}{h_x}L_s$$

$$\tilde{C} = (-q_y\sin\theta A + q_y\cos\theta)[1-\cos(\beta L_s)]$$

$$\tilde{D} = (-q_y\sin\theta B + q_z)[1-\cos(\beta L_s)]$$

$$TCS_1 = CONST_2 - \frac{q_y\cos\theta}{H_x}s$$

$$TCS_2 = -\tan(\theta)TCS_1 + \frac{1}{\cos\theta}$$

$$TCC = \frac{1-\cos(\beta L_s)}{\sin(\beta L_s)}\beta\cos(\beta s) - \beta\sin(\beta s)$$

A.2 Constants used in Chapter 3

For Section 3.1

$$a = 2 + \frac{1}{2}TC_1TC_3$$

$$b = 1 + TC_1TC_3 - TC_2\sum_{k=0}^{N}[\tilde{C}_i(x_{i+1}-x_i)]$$

$$c = -\frac{1}{2H_x^2}TC_1\sum_{k=0}^{N}\{[\tilde{C}_i^{\,2}+\tilde{E}_i^{\,2}](x_{i+1}+x_i)\}$$

$$
\begin{aligned}
& - \frac{TC_1}{H_x} \sum_{k=0}^{N} \{[\tilde{E}_i - \tilde{C}_i \tan\theta][y'(x_{i+1}) - y'(x_i)]\} \\
& - TC_2 \sum_{k=0}^{N} [\tilde{C}_i (x_{i+1} - x_i)]
\end{aligned}
$$

$$C_i = \sum_{k=1}^{n} P_k \sin\theta (1 - \frac{x_k}{L_x}) - \sum_{k=1}^{i} P_k \sin\theta + h_x \frac{L}{L_x}$$

$$D_i = \sum_{k=1}^{i} \frac{P_k \sin\theta}{H_x + h_x} x_k$$

$$E_i = \sum_{k=0}^{n} P_k \cos\theta (\frac{x_k}{L_x} - 1) + \sum_{k=1}^{i} P_k \cos\theta$$

$$F_i = - \sum_{k=0}^{i} \frac{P_k \cos\theta x_k}{H_x + h_x}$$

$$TC_1 = \frac{AE}{2H_x L_e}$$

$$TC_2 = \frac{AE}{H_x^2 L_e \cos\theta}$$

$$TC_3 = \int_0^{L_x} (\frac{dy_1'}{dx})^2 dx (\frac{q_y^2 + q_z^2}{q_y^2 \cos^2\theta})$$

$$TC_4 = \sinh[\frac{\sqrt{q_y^2 + q_z^2}}{H_x} \frac{L_x}{2} + CONST_1]$$

$$TC_5 = \sinh[\frac{\sqrt{q_y^2 + q_z^2}}{H_x} (-\frac{L_x}{2}) + CONST_1]$$

$$L_e = (\frac{\cos^2\theta q_y^2 + q_z^2}{\cos^2\theta (q_y^2 + q_z^2)})^{\frac{3}{2}} \frac{H_x}{\sqrt{q_y^2 + q_z^2}} (TC_4 - TC_5 + \frac{1}{3} TC_4^3 - \frac{1}{3} TC_5^3)$$

$$\tilde{C}_i = \sum_{k=1}^{n} P_k \sin\theta (1 - \frac{x_k}{L_x}) - \sum_{k=1}^{i} P_k \sin\theta$$

$$TI_0 = \sqrt{1 + \frac{q_y^2 D_{10}^2}{q_y^2 + q_z^2} + \frac{2q_y q_z \sin\theta\cos\theta D_{10} - q_y^2 \sin^2\theta}{(q_y^2 + q_z^2)\cos^2\theta}}$$

$$TI_1 = \sqrt{1 + \frac{q_y^2 D_{1i}^2}{q_y^2 + q_z^2} + \frac{2q_y q_z \sin\theta\cos\theta D_{1i} - q_y^2 \sin^2\theta}{(q_y^2 + q_z^2)\cos^2\theta}}$$

$$TI_{11} = \sqrt{1 + \frac{q_y^2 D_{1(i+1)}^2}{q_y^2 + q_z^2} + \frac{2q_y q_z \sin\theta\cos\theta D_{1(i+1)} - q_y^2 \sin^2\theta}{(q_y^2 + q_z^2)\cos^2\theta}}$$

$$TI_N = \sqrt{1 + \frac{q_y^2 D_{1N}^2}{q_y^2 + q_z^2} + \frac{2q_y q_z \sin\theta\cos\theta D_{1N} - q_y^2 \sin^2\theta}{(q_y^2 + q_z^2)\cos^2\theta}}$$

$$
\begin{aligned}
TI_2 &= (\frac{\sqrt{q_y^2+q_z^2}}{H_x})x - E_{1i} \\
TI_3 &= \frac{\sqrt{q_y^2+q_z^2}}{H_x}x_{i+1} - E_{1i} \\
TI_{31} &= \frac{\sqrt{q_y^2+q_z^2}}{H_x}x_{i+1} - E_{1(i+1)} \\
TI_{3N} &= \frac{\sqrt{q_y^2+q_z^2}}{H_r}L_x - E_{1n} \\
TI_4 &= \frac{q_y q_z \cos\theta}{q_y^2+q_z^2}(D_{1(i+1)} - D_{1i}) \\
D_{1i} &= \sum_{k=1}^{n}\frac{q_z P_k}{q_y H_x}(1-\frac{x_k}{L_x}) - \sum_{k=1}^{i}\frac{q_z P_k}{q_y H_x} \\
D_{2i} &= \sum_{k=1}^{i}\frac{q_z P_k x_k}{q_y H_x} \\
G_0 &= \frac{H_x}{\sqrt{q_y^2+q_z^2}}TI_0 \sinh(E_{10}) \\
G_{i+1} &= G_i + \frac{H_x}{\sqrt{q_y^2+q_z^2}}TI_1 \sinh(TI_3) - \frac{H_x}{\sqrt{q_y^2+q_z^2}}TI_{11}\sinh(TI_{31})
\end{aligned}
$$

For Section 3.2

$$
\begin{aligned}
q^2 &= q_y^2+q_z^2 \\
\lambda^2 &= (\frac{AE}{L_e})(\frac{L_s}{H_x})^3 q^2 \\
L_e &= L_s + \sum_{k=o}^{n}\{[\frac{q_y^2 D_{1i}^2}{q_y^2+q_z^2} + \frac{2q_y q_z \sin\theta\cos\theta D_{1i} - q_y^2\sin^2\theta}{(q_y^2+q_z^2)\cos^2\theta}](s_{i+1}-s_i)\} \\
&\quad + \frac{q_y^2+q_z^2}{H_x^2}\frac{1}{3}\sum_{k=0}^{n}[(s_{i+1}-G_i)^3 - (s_i-G_i)^3] \\
A &= \sum_{k=0}^{n}\{[\sin\beta(s_{i+1}-s_i)\sin\theta - \beta\sin\theta\frac{P_i}{q_y}]D_0^i(1,2) \\
&\quad + [1-\cos\beta(s_{i+1}-s_i)]\sin\beta D_0^i(2,2)\} \\
B &= \sum_{k=0}^{n}\{[-\sin\beta(s_{i+1}-s_i)\cos\theta + \beta\cos\theta\frac{P_i}{q_y}]D_0^i(1,2) \\
&\quad - [1-\cos\beta(s_{i+1}-s_i)]\cos\theta D_0^i(2,2)\} \\
C &= \sum_{k=0}^{n}\{\sin\beta(s_{i+1}-s_i)D_0^i(1,2) \\
&\quad + [1-\cos\beta(s_{i+1}-s_i)]\cos\theta D_0^i(2,2)\}
\end{aligned}
$$

$$
\begin{aligned}
D &= (SC_1 + SC_2)/SC_3 \\
E &= (SC_4 + SC_5)/SC_3 \\
\tilde{D} &= Aq_yD + Bq_y \\
\tilde{E} &= Aq_yE - Cq_z \\
SC_1 &= \frac{(q_z \cos\theta D_{1N} - q_y \sin\theta)q_y}{q_y^2 + q_z^2} \\
SC_2 &= \frac{q_y \cos\theta}{H_x}(s^*_{N+1} - G_N) \\
SC_3 &= \tan\theta SC_1 + \tan\theta SC_2 + \frac{1}{\cos\theta} \\
SC_4 &= \frac{q_z SC_1}{q_y \cos\theta} \\
SC_5 &= \frac{q_z SC_2}{q_y \cos\theta} \\
SU_1 &= \frac{(q_z \cos\theta D_{1i} - q_y \sin\theta)q_y}{q_y^2 + q_z^2} \\
SU_2 &= \frac{q_y \cos\theta}{H_x}(s_i - G_i) \\
SU_3 &= \tan\theta SU_1 + \tan\theta SU_2 + \frac{1}{\cos\theta} \\
SU_4 &= \frac{q_z}{q_y \cos\theta} SU_1 \\
SU_5 &= \frac{q_z}{q_y \cos\theta} SU_2 \\
SU_7 &= \frac{h}{AE}\{[1 + \frac{q_y^2 D_{1i}^2}{q_y^2 + q_z^2} + \frac{(2q_yq_z \sin\theta\cos\theta D_{1i} - q_y^2 \sin^2\theta)}{(q_y^2 + q_z^2)\cos^2\theta}] \\
&\quad + \frac{q_y^2 + q_z^2}{H_x^2}(s_i - G_i)^2\} \\
SU_8 &= SU_1 + SU_2 \\
SU_9 &= SU_4 + SU_5 \\
SU_{bc} &= \beta \cos[\beta(s - s_i)] \\
SU_{bs} &= \beta \sin[\beta(s - s_i)]
\end{aligned}
$$

A.3 Constants used in Chapter 4

For Section 4.1

$$
\begin{aligned}
A &= \sum_{k=0}^{n}\{\frac{1}{J_k}\{\sin[\beta J_k(s_{k+1}-s_k)]D_0^k(1,2)\sin\theta \\
&\quad + D_0^k(2,2)\{1-\cos[\beta J_k(s_{k+1}-s_k)]\}\sin\theta\}\} \\
B &= \sum_{k=0}^{n}\{\frac{1}{J_k}\{-\sin[\beta J_k(s_{k+1}-s_k)]D_0^k(1,2)\cos\theta \\
&\quad - D_0^k(2,2)\{1-\cos[\beta J_k(s_{k+1}-s_k)]\}\cos\theta\}\} \\
C &= \sum_{k=0}^{n}\{\frac{1}{J_k}\{-\sin[\beta J_k(s_{k+1}-s_k)]D_0^k(1,2) \\
&\quad - D_0^k(2,2)\{1-\cos[\beta J_k(s_{k+1}-s_k)]\}\}\} \\
D &= -\frac{LC_1}{LC_2} \\
E &= -\frac{\frac{q_z}{q_y\cos\theta}LC_1}{LC_2} \\
\tilde{F} &= Aq_yD + Bq_y \\
\tilde{G} &= Aq_yE + cq_z \\
LC_1 &= CONST_2 - \frac{q_y\cos\theta}{H_x}s_{N+1} \\
LC_2 &= -\tan\theta LC_1 + \frac{1}{\cos\theta} \\
LS_1 &= CONST_2 - \frac{q_y\cos\theta}{H_x}s \\
LS_2 &= -\tan\theta LS_1 + \frac{1}{\cos\theta} \\
LS_3 &= \frac{h}{AE}[\frac{q_y^2+q_z^2}{q_y^2\cos^2\theta}LS_1^2 - \frac{2\sin\theta}{\cos^2\theta}LS_1 + \frac{1}{\cos^2\theta}] \\
LS_4 &= \beta J_k(s-s_k) \\
LS_{bs} &= \beta J_k\sin(LS_4) \\
LS_{bc} &= \beta J_k\cos(LS_4)
\end{aligned}
$$

A.4 Constants used in Chapter 5

For Section 5.1

$$
\begin{aligned}
A_k &= \cos[\beta J_k(s_{k+1}-s_k)]-1 \\
B_k &= \sin[\beta J_k(s_{k+1}-s_k)] \\
D_k &= [s_i(s_{k+1})-G_i]\cos[\beta J_k(s_{k+1}-s_k)]-s_i(s_k)+G_i \\
&\quad -\frac{1}{\beta J_k}\sin[\beta J_k(s_{k+1}-s_k)] \\
E_k &= [s_i(s_{k+1})-G_i]\sin[\beta J_k(s_{k+1}-s_k)]+\frac{1}{\beta J_k}\cos[\beta J_k(s_{k+1}-s_k)] \\
&\quad -\frac{1}{\beta J_k} \\
F &= \sum_{k=0}^{n}\{D^k_{k-1}(1,2)[A_k D_{1i}\frac{q_y q_z\sin\theta}{q_y^2+q_z^2}+D_k\frac{q_y\sin\theta}{H_x}] \\
&\quad + D^k_{k-1}(2,2)(B_k D_{1i}\frac{q_y q_z\sin\theta}{q_y^2+q_z^2}+E_k\frac{q_y\sin\theta}{H_x})\} \\
G &= -\sum_{k=0}^{n}\{D^k_{k-1}(1,2)[A_k D_{1i}\frac{q_y q_z\cos\theta}{q_y^2+q_z^2}+D_k\frac{q_y\cos\theta}{H_x}] \\
&\quad + D^k_{k-1}(2,2)(B_k D_{1i}\frac{q_y q_z\cos\theta}{q_y^2+q_z^2}+E_k\frac{q_y\cos\theta}{H_x})\} \\
I &= \sum_{k=0}^{n}\{D^k_{k-1}(1,2)[A_k D_{1i}\frac{q_y^2}{q_y^2+q_z^2}-D_k\frac{q_z}{H_x}] \\
&\quad + D^k_{k-1}(2,2)(B_k D_{1i}\frac{q_y^2}{q_y^2+q_z^2}-E_k\frac{q_z}{H_x})\} \\
D &= (QC_1+QC_3)/QC_5 \\
E &= (QC_2+QC_4-D_{1\tilde{N}})/QC_5 \\
\tilde{N} &= (N+1)M-1 \\
\tilde{D} &= F\cdot D+G \\
\tilde{E} &= F\cdot E+I \\
QD &= D_0^N(1,2)\cos[\beta J_N(L_s-s_n)]+D_0^N(2,2)\sin[\beta J_N(L_s-s_n)] \\
QN_x &= q_y-[r_{N1}+D_0^N(1,1)q_y]\cos[\beta J_N(L_s-s_n)] \\
&\quad -[r_{N2}+D_0^N(2,1)q_y]\sin[\beta J_N(L_s-s_n)]
\end{aligned}
$$

$$
\begin{aligned}
QN_y &= q_y - [r_{N1} + D_0^N(1,1)q_y]\cos[\beta J_N(L_s - s_n)] \\
&\quad - [r_{N2} + D_0^N(2,1)q_y]\sin[\beta J_N(L_s - s_n)] \\
QN_z &= q_z - [s_{N1} + D_0^N(1,1)q_z]\cos[\beta J_N(L_s - s_n)] \\
&\quad - [s_{N2} + D_0^N(2,1)q_z]\sin[\beta J_N(L_s - s_n)] \\
QC_1 &= \frac{(q_z\cos\theta D_{1\tilde{N}} - q_y\sin\theta)q_y}{q_y^2 + q_z^2} \\
QC_2 &= \frac{q_z}{q_y\cos\theta}QC_1 \\
QC_3 &= \frac{q_y\cos\theta}{H_x}(s_{\tilde{N}+1} - G_{\tilde{N}}) \\
QC_4 &= \frac{q_z}{q_y\cos\theta}QC_3 \\
QC_5 &= \tan\theta QC_2 + \tan\theta QC_1 + \frac{1}{\cos\theta} \\
QS_1 &= \frac{(q_z\cos\theta D_{1i} - q_y\sin\theta)q_y}{q_y^2 + q_z^2} \\
QS_2 &= \frac{q_y\cos\theta}{H_x}(s_i - G_i) \\
QS_3 &= \tan\theta QS_1 + \tan\theta QS_2 + \frac{1}{\cos\theta} \\
QS_4 &= \frac{q_z}{q_y\cos\theta}QS_1 \\
QS_5 &= \frac{q_z}{q_y\cos\theta}QS_2 \\
QS_7 &= \frac{h}{AE}\{[1 + \frac{q_y^2 D_{1i}^2}{q_y^2 + q_z^2} + \frac{2q_yq_z\sin\theta\cos\theta D_{1i} - q_y^2\sin^2\theta}{(q_y^2 + q_z^2)\cos^2\theta}] \\
&\quad + \frac{q_y^2 + q_z^2}{H_x^2}(s_i - G_i)^2\} \\
OS_8 &= OS_1 + OS_2 \\
OS_9 &= OS_4 + OS_5 - D_{1\tilde{N}} - D_{1\tilde{N}} \\
OS_{bs} &= \beta J_k\sin[\beta J_k(s - s_k)] \\
OS_{bc} &= \beta J_k\cos[\beta J_k(s - s_k)]
\end{aligned}
$$

Appendix B

Parameter values for the numerical simulation

Parameter	Notation	Value
Cross-Section Area	A	402.9 mm^2
Modulus Of Elasticity	E	63.358 kN/mm^2
Span Length	L_x	125 m
Tension (Horizontal)	H_x	15 kN
Bare cable self-weight	m	1.663 Kg

Table B.1: Parameter values for the numerical simulation

Appendix C

Outline of some derivations

C.1 Brief derivations for Chapter 2

The process of solving the static profile of simple model

For the differential equations

$$H_x \frac{d^2x'}{dx^2} = q_y \sin\theta \frac{ds}{dx}. \tag{C.1}$$

$$H_x \frac{d^2y'}{dx^2} = -q_y \cos\theta \frac{ds}{dx}. \tag{C.2}$$

if the cable is not entirely vertical, let

$$p = \frac{dx'}{dx}. \tag{C.3}$$

$$q = \frac{dy'}{dx}. \tag{C.4}$$

and then Eq. (C.1)÷Eq. (C.2) results in

$$p = -\tan\theta q + C_1. \tag{C.5}$$

Thus,

$$x' = \tan\theta y' + C_1 x + C_2. \tag{C.6}$$

Applying the boundary conditions $x'(0) = y'(0) = 0$, $x'(L_x) = \sqrt{L_x^2 + h}$ and $y'(L_x) = 0$ yields

$$C_1 = \frac{1}{\cos\theta}, \tag{C.7}$$

$$C_2 = 0. \tag{C.8}$$

Because

$$\frac{ds}{dx} = \sqrt{p^2+q^2}, \tag{C.9}$$

So substitute Eq. (C.3), Eq. (C.7) and Eq. (C.8) into Eq. (C.2) gives

$$H_x\frac{dq}{dx} = -q_y\cos\theta\sqrt{1+\frac{1}{\cos^2\theta}(q-\sin\theta)^2}. \tag{C.10}$$

Therefore,

$$q = \sin\theta - \cos\theta\sinh[(\frac{q_y}{H_x})x - C_3], \tag{C.11}$$

and thus,

$$y' = \sin\theta x - \cos\theta\frac{H_x}{q_y}\cosh[(\frac{q_y}{H_x})x - C_3] + C_4. \tag{C.12}$$

From the boundary conditions $y'(0)=0$ and $y'(L_x)=0$, we find C_3 and C_4 given by Eq. (2.5) and Eq. (2.6), respectively.

The differential equations for the static tenstion increase due to out-of-plane load

Transform Eq. (1.21)-Eq. (1.23) ($P_i = 0$ because there is no concentrated loads here)into the rotated coordinate system and use the differential equations for static profile to simplify the resulting equation to obtain

$$\frac{d}{ds}[(T+\tau)\frac{du'}{ds}+\tau\frac{dx'}{ds}] = (q_y+mg)\sin\theta, \tag{C.13}$$

$$\frac{d}{ds}[(T+\tau)\frac{dy_2'}{ds}+\tau\frac{dy_1'}{ds}] = -(q_y+mg)\cos\theta, \tag{C.14}$$

$$\frac{d}{ds}[(T+\tau)\frac{dz_2}{ds}+\tau\frac{dz_1}{ds}] = -q_z. \tag{C.15}$$

With the aid of $T = H_x\frac{ds}{dx}$ and $\tau = h_x\frac{ds}{dx}$, Eq. (C.13)-Eq. (C.15) can be further simplified to

$$\frac{d^2u'}{dx^2} = \frac{(q_y+mg)\sin\theta}{H_x+h_x}\frac{ds}{dx} - \frac{h_x}{H_x+h_x}\frac{d^2x'}{dx^2},$$

$$\frac{d^2y_2'}{dx^2} = \frac{-(q_y+mg)\cos\theta}{H_x+h_x}\frac{ds}{dx} - \frac{h_x}{H_x+h_x}\frac{d^2y_1'}{dx^2},$$

$$\frac{d^2z_2}{dx^2} = \frac{-q_z}{H_x+h_x}\frac{ds}{dx}.$$

which are Eq. (2.13)-Eq. (2.15).

The 3rd-degree polynomial for the static tension increase

By using the following two equations:

$$\begin{aligned}(ds')^2 &= (dx'+du')^2+(dy_1'+dy_2')^2+(dz_2)^2,\\ (ds)^2 &= (dx')^2+(dy_1')^2.\end{aligned}$$

we can transform Eq. (2.16) into:

$$\frac{h_x}{AE}(\frac{ds}{dx})^3 = \frac{dx'}{dx}\frac{du'}{dx}+\frac{1}{2}(\frac{du'}{dx})^2+\frac{dy_1'}{dx}\frac{dy_2'}{dx}+\frac{1}{2}(\frac{dy_2'}{dx})^2+\frac{1}{2}(\frac{dz_2}{dx})^2. \quad \text{(C.16)}$$

In order to integrate this equation to obtain a 3rd-degree polynomial, we must first solve Eq. (2.13) and Eq. (2.15) to find the expression for the displacement increase due to q_z. It is not difficult to solve these equations with the fixed boundary conditions and the static profile given in Eq. (2.3)-Eq. (2.9). The results are:

$$\begin{aligned}u' &= \frac{(q_y+mg)\sin\theta}{H_x+h_x}(\frac{H_x}{mg})^2\cosh(\frac{mgx}{H_x}+C_3)\\ &\quad+\frac{h_x\sin\theta}{H_x+h_x}\frac{H_x}{mg}\cosh(\frac{mgx}{H_x}+C_3)+D_1x+D_2, \quad \text{(C.17)}\\ y_2' &= -\frac{(q_y+mg)\cos\theta}{H_x+h_x}(\frac{H_x}{mg})^2\cosh(\frac{mgx}{H_x}+C_3)\\ &\quad-\frac{h_x\cos\theta}{H_x+h_x}\frac{H_x}{mg}\cosh(\frac{mgx}{H_x}+C_3)+D_3x+D_4, \quad \text{(C.18)}\\ z_2 &= -\frac{q_z}{H_x+h_x}(\frac{H_x}{mg})^2\cosh(\frac{mgx}{H_x}+C_3)+D_5x+D_6. \quad \text{(C.19)}\end{aligned}$$

where D_1 to D_6 are given by

$$\begin{aligned}D_1 &= \frac{\sin\theta}{(H_x+h_x)L_x}(\frac{H_x}{mg})[(\frac{q_y}{mg}+1)H_x+h_x][\cosh(C_3)-\cosh(\frac{mgL_x}{H_x}+C_3)],\\ D_2 &= -\frac{\sin\theta}{H_x+h_x}(\frac{H_x}{mg})\cosh(C_3)[(\frac{q_y}{mg}+1)H_x+h_x],\\ D_3 &= \frac{\cos\theta}{(H_x+h_x)L_x}(\frac{H_x}{mg})[(\frac{q_y}{mg}+1)H_x+h_x][\cosh(\frac{mgL_x}{H_x}+C_3)-\cosh(C_3)],\\ D_4 &= \frac{\cos\theta}{H_x+h_x}(\frac{H_x}{mg})\cosh(C_3)[(\frac{q_y}{mg}+1)H_x+h_x],\end{aligned}$$

$$D_5 = \frac{q_z}{(H_x+h_x)L_x}(\frac{H_x}{mg})^2[\cosh(\frac{mgL_x}{H_x}+C_3)-\cosh(C_3)],$$
$$D_6 = \frac{q_z}{H_x+h_x}(\frac{H_x}{mg})^2\cosh(C_3),$$

in which C_3 and C_4 have already been given by Eq. (2.5) and Eq. (2.7).

By using Eq. (2.3), Eq. (2.4), Eq. (2.9) and Eq. (C.17) to Eq. (C.19), we can obtain the 3rd-degree polynomial of $\frac{h_x}{H_x}$ by integrating Eq. (C.16). This equation has been obtained, see Eq. (2.17).

Frequency equation

In order to derive the frequency equation, we need to use Eq. (2.53). Substituting Eq. (2.22) to Eq. (2.25) into Eq. (2.53) yields

$$\begin{aligned}\frac{h_x}{AE}(\frac{ds}{dx})^2 &= -\tan\theta(CONST_2-\frac{q_y\cos\theta}{H_x}s)\frac{du'}{ds}+\frac{1}{\cos\theta}\frac{du'}{ds}\\ &\quad+(CONST_2-\frac{q_y\cos\theta}{H_x}s)\frac{dy_2'}{ds}\\ &\quad+\frac{q_z}{q_y\cos\theta}(CONST_2-\frac{q_y\cos\theta}{H_x}s)\frac{dz_2}{ds}.\end{aligned} \tag{C.20}$$

By using the method of separation of variables, Eq. (C.20) can be transformed into

$$\begin{aligned}\frac{h}{AE}(\frac{ds}{dx})^2 &= -\tan\theta(CONST_2-\frac{q_y\cos\theta}{H_x}s)\frac{dU}{ds}+\frac{1}{\cos\theta}\frac{dU}{ds}\\ &\quad+(CONST_2-\frac{q_y\cos\theta}{H_x}s)\frac{dY}{ds}\\ &\quad+\frac{q_z}{q_y\cos\theta}(CONST_2-\frac{q_y\cos\theta}{H_x}s)\frac{dZ}{ds},\end{aligned} \tag{C.21}$$

which can be further simplified into

$$\begin{aligned}\frac{h}{AE}L_e &= -\frac{q_y\sin\theta}{H_x}\int_0^{L_s}U(s)ds+\frac{q_y\cos\theta}{H_x}\int_0^{L_s}Y(s)ds\\ &\quad+\frac{q_z}{H_x}\int_0^{L_s}Z(s)ds.\end{aligned} \tag{C.22}$$

With the aid of Eq. (2.44) to Eq. (2.46), Eq. (C.22) can be transformed into the frequency equation Eq. (2.54).

Supplementary frequency equation

The supplementary frequency equation was obtained from Eq. (C.21) and Eq. (2.44) to Eq. (2.46) as:

$$\begin{aligned} & -\tan\theta(CONST_2 - \frac{q_y\cos\theta}{H_x}L_s)[-f_1\beta\sin(\beta L_s) + f_2\beta\cos(\beta L_s)] \\ & + \frac{1}{\cos\theta}[-f_1\beta\sin(\beta L_s) + f_2\beta\cos(\beta L_s)] \\ & + (CONST_2 - \frac{q_y\cos\theta}{H_x}L_s)[-f_3\beta\sin(\beta L_s) + f_4\beta\cos(\beta L_s)] \\ & + \frac{q_z}{q_y\cos\theta}(CONST_2 - \frac{q_y\cos\theta}{H_x}L_s)[-f_5\beta\sin(\beta L_s) + f_6\beta\cos(\beta L_s)] \\ = \; & 0 \end{aligned}$$

where the fact $h = 0$ is used. A simplification of this equation results in the supplementary frequency equation Eq. (2.56).

U-mode fuction

We need to use Eq. (C.20) to derive this U-mode function. From Eq. (2.22) to Eq. (2.25), we can find

$$\begin{aligned} (\frac{ds}{dx})^2 = \; & \frac{q_y^2 + q_z^2}{q_y^2\cos^2\theta}(CONST_2 - \frac{q_y\cos\theta}{H_x}s)^2 \\ & - \frac{2\sin\theta}{\cos^2\theta}(CONST_2 - \frac{q_y\cos\theta}{H_x}s) + \frac{1}{\cos^2\theta}. \end{aligned} \tag{C.23}$$

Then using Eq. (2.71) and Eq. (2.72) together with Eq. (C.23) yields the U-mode function given in Eq. (2.74).

C.2 Brief derivations for Chapter 3

3rd-degree polynomial for the static tension increase

In order to obtain this polynomial of $\frac{h_x}{H_x}$, substituting the static profile given by

Eq. (2.22) to Eq. (2.25) and the dynamic profile given by Eq. (3.18) to Eq. (3.20) into Eq. (3.21) and then integrating the result produces an equation:

$$\begin{aligned}
\frac{h_x}{AE} &= \frac{h_x^2}{2(H_x+h_x)^2}\int_0^{L_x}(\frac{dy_1'}{dx})^2 dx(\frac{q_y^2+q_z^2}{q_y^2\cos^2\theta}) \\
&+ \frac{h_x}{(H_x+h_x)^2}\sum_{k=0}^{N}\{[\tilde{C}_i\tan\theta - E_i][y_1'(x_{i+1})-y_1'(x_i)]\} \\
&+ \frac{1}{2(H_x+h_x)^2}\sum_{k=0}^{N}[(\tilde{C}_i^{\,2}+E_i^2)(x_{i+1}-x_i)] \\
&+ \frac{h_x L}{(H_x+h_x)^2 L_x}\sum_{k=0}^{N}[\tilde{C}_i(x_{i+1}-x_i)] \\
&+ \frac{h_x^2 L^2}{2(H_x+h_x)^2 L_x} + \frac{h_x^2}{L_x}2(H_x+h_x)^2\cos^2\theta \\
&- \frac{h_x}{(H_x^2+h_x^2)^2\cos\theta}\sum_{k=0}^{N}[\tilde{C}_i(x_{i+1}-x_i)] - \frac{h_x^2 L}{(H_x+h_x)^2\cos\theta} \\
&- \frac{h_x}{H_x+h_x}\sum_{k=0}^{L_x}(\frac{dy_1'}{dx})^2 dx(\frac{q_y^2+q_z^2}{q_y^2\cos^2\theta}) \\
&+ \frac{1}{(H_x+h_x}\sum_{k=0}^{N}\{(E_i-\tilde{C}_i\tan\theta)[y_1'(x_{i+1})-y_1'(x_i)]\} \\
&+ \frac{1}{(H_x+h_x)}\frac{1}{\cos\theta}\sum_{k=0}^{N}[\tilde{C}_i(x_{i+1}-x_i)] \\
&+ \frac{h_x L}{H_x+h_x}\frac{1}{\cos\theta} - \frac{h_x}{(H_x+h_x)\cos^2\theta}L_x. \qquad \text{(C.24)}
\end{aligned}$$

Then collect the equation according to $\frac{h_x}{H_x}$, we can obtain the polynomial given by Eq. (3.22).

Frequency equation

Substituting the static profile given by Eq. (3.38) to Eq. (3.41) into Eq. (3.54) gives

$$\begin{aligned}
\frac{h_x}{AE}(\frac{ds}{dx})^2 &= \tan\theta\frac{(q_z\cos\theta D_{1i}-q_y\sin\theta)q_y}{q_y^2+q_z^2}\frac{du_i'}{ds} + \tan\theta\frac{q_y\cos\theta}{H_x}(s_i-G_i)\frac{du_i'}{ds} \\
&+ \frac{1}{\cos\theta}\frac{du_i'}{ds} - \frac{(q_z\cos\theta D_{1i}-q_y\sin\theta)q_y}{q_y^2+q_z^2}\frac{dy_{2i}'}{ds} \\
&- \frac{q_y\cos\theta}{H_x}(s_i-G_i)\frac{dy_{2i}'}{ds} - \frac{(q_z\cos\theta D_{1i}-q_y\sin\theta)q_z}{(q_y^2+q_z^2)\cos\theta}\frac{dz_{2i}'}{ds}
\end{aligned}$$

$$- \frac{q_z}{H_x}(s_i - G_i)\frac{dz'_{2i}}{ds} + D_{1i}\frac{dz_{2i}}{ds}. \tag{C.25}$$

By using the method of separation of variables, we can transform Eq. (C.25) into

$$\begin{aligned}
\frac{h}{AE}(\frac{ds}{dx})^2 &= \tan\theta\frac{(q_z\cos\theta D_{1i} - q_y\sin\theta)q_y}{q_y^2+q_z^2}\frac{dU_i}{ds} + \tan\theta\frac{q_y\cos\theta}{H_x}(s_i - G_i)\frac{dU_i}{ds} \\
&+ \frac{1}{\cos\theta}\frac{dU_i}{ds} - \frac{(q_z\cos\theta D_{1i} - q_y\sin\theta)q_y}{q_y^2+q_z^2}\frac{dY_i}{ds} \\
&- \frac{q_y\cos\theta}{H_x}(s_i - G_i)\frac{dY_i}{ds} - \frac{(q_z\cos\theta D_{1i} - q_y\sin\theta)q_z}{(q_y^2+q_z^2)\cos\theta}\frac{dZ_i}{ds} \\
&- \frac{q_z}{H_x}(s_i - G_i)\frac{dZ_i}{ds} + D_{1i}\frac{dZ_i}{ds}.
\end{aligned} \tag{C.26}$$

With the results given by Eq. (3.55) to Eq. (3.57), Eq. (C.26) can be written as

$$\begin{aligned}
\frac{h}{AE}L_e &= \frac{q_yq_z\sin\theta}{q_y^2+q_z^2}\int_0^{L_s} D_{1i}dU_i(s) + \frac{q_y\sin\theta}{H_x}\int_0^{L_s}(s_i - G_i)dU_i(s) \\
&- \frac{q_yq_z\cos\theta}{q_y^2+q_z^2}\int_0^{L_s} D_{1i}dY_i(s) - \frac{q_y\cos\theta}{H_x}\int_0^{L_s}(s_i - G_i)dY_i(s) \\
&- \frac{q_z^2}{q_y^2+q_z^2}\int_0^{L_s} D_{1i}dZ_i(s) - \frac{q_z}{H_x}\int_0^{L_s}(s_i - G_i)dZ_i(s) \\
&+ \int_0^{L_s} D_{1i}dZ_i(s).
\end{aligned} \tag{C.27}$$

A further algebraic manipulation on Eq. (C.27) leads to the frequency equation given by Eq. (3.76).

Supplementary frequency equation

In order to obtain the supplementary frequency equation, we need to evaluate Eq. (C.26) at the right-end point of the cable. With the ai of Eq. (3.55) to Eq. (3.57), we have the final result as

$$\begin{aligned}
&[\tan\theta\frac{(q_z\cos\theta D_{1N} - q_y\sin\theta)q_y}{q_y^2+q_z^2} + \tan\theta\frac{q_y\cos\theta}{H_x}(L_s - G_N) + \frac{1}{\cos\theta}]C_{20} \\
= &[\frac{(q_z\cos\theta D_{1N} - q_y\sin\theta)q_y}{q_y^2+q_z^2} + \frac{q_y\cos\theta}{H_x}(L_s - G_N)]C_{40} \\
&+ [\frac{(q_z\cos\theta D_{1N} - q_y\sin\theta)q_z}{(q_y^2+q_z^2)\cos\theta} + \frac{q_z}{H_x}(L_s - G_N) - D_{1N}]C_{60}
\end{aligned} \tag{C.28}$$

which is equivalent to Eq. (3.78).

U-mode function

Eq. (C.25) is used to derive the U-mode function. From Eq. (3.38) to Eq. (3.41), we can find

$$(\frac{ds_i}{dx})^2 = [1 + \frac{q_y^2 D_{1i}^2}{q_y^2+q_z^2} + \frac{2q_y q_z \sin\theta\cos\theta D_{1i} - q_y^2\sin^2\theta}{(q_y^2+q_z^2)\cos^2\theta}] + \frac{q_y^2+q_z^2}{H_x^2}(s_i - G_i)^2. \qquad (C.29)$$

Then use the results given by Eq. (3.89) and Eq. (3.90) together with Eq. (C.29) to obtain the equation for U-mode function gien by Eq. (3.91).

C.3 Brief derivations for Chapter 4

Frequency equation

Because the static profile is the as that obtained in Chapter 2, we can directly use Eq. (C.22) here to derive the frequency equation.

With the help of the Eq. (4.10) to Eq. (4.12), we have

$$\begin{aligned}
\frac{h}{AE}L_e = & -\frac{q_y\sin\theta}{H_x\beta}\sum_{k=0}^{n}\{\frac{1}{J_k}\{C_{1k}\sin[\beta J_k(s_{k+1}-s_k)] \\
& - C_{2k}\cos[\beta J_k(s_{k+1}-s_k)] + C_{2k}\}\} \\
& + \frac{q_y\cos\theta}{H_x\beta}\sum_{k=0}^{n}\{\frac{1}{J_k}\{C_{3k}\sin[\beta J_k(s_{k+1}-s_k)] \\
& - C_{4k}\cos[\beta J_k(s_{k+1}-s_k)] + C_{4k}\}\} \\
& + \frac{q_z}{H_x\beta}\sum_{k=0}^{n}\{\frac{1}{J_k}\{C_{5k}\sin[\beta J_k(s_{k+1}-s_k)] \\
& - C_{6k}\cos[\beta J_k(s_{k+1}-s_k)] + C_{6k}\}\} \\
& + \frac{h(q_y^2+q_z^2)\cos\theta}{\beta^2 H_x^3}L_s,
\end{aligned}$$

which can be put inthe form Eq. (4.25).

Supplementary frequency equation

From the supplementary frequency equation, we can directly use Eq. (C.21) but with the aid of new results obtained from Eq. (4.10) to Eq. (4.12). Substituting Eq. (4.10) and Eq. (4.11) into Eq. (C.21) yields

$$
\begin{aligned}
&-\tan\theta(CONST_2 - \frac{q_y\cos\theta}{H_x}L_s)\{-D_0^N(1,2)C_{20}\beta J_N\sin[\beta J_N(L_s - s_N)] \\
&\quad + D_0^N(2,2)C_{20}\beta J_N\cos[\beta J_N(L_s - s_N)]\} \\
&+\frac{1}{\cos\theta}\{-D_0^N(1,2)C_{20}\beta J_N\sin[\beta J_N(L_s - s_N)] \\
&\quad + D_0^N(2,2)C_{20}\beta J_N\cos[\beta J_N(L_s - s_N)]\} \\
&+(CONST_2 - \frac{q_y\cos\theta}{H_x}L_s)\{-D_0^N(1,2)C_{40}\beta J_N\sin[\beta J_N(L_s - s_N)] \\
&\quad + D_0^N(2,2)C_{40}\beta J_N\cos[\beta J_N(L_s - s_N)]\} \\
&+\frac{q_z}{q_y\cos\theta}(CONST_2 - \frac{q_y\cos\theta}{H_x}L_s)\{-D_0^N(1,2)C_{60}\beta J_N\sin[\beta J_N(L_s - s_N)] \\
&\quad + D_0^N(2,2)C_{60}\beta J_N\cos[\beta J_N(L_s - s_N)]\} \\
=\ & 0. \qquad\qquad (C.30)
\end{aligned}
$$

Eq. (C.30) can be further simplified as

$$
\begin{aligned}
&[-\tan\theta(CONST_2 - \frac{q_y\cos\theta}{H_x}L_s) + \frac{1}{\cos\theta}]C_{20} + (CONST_2 - \frac{q_y\cos\theta}{H_x}L_s)C_{40} \\
&+\frac{q_z}{q_y\cos\theta}(CONST_2 - \frac{q_y\cos\theta}{H_x}L_s)C_{60} \\
=\ & 0,
\end{aligned}
$$

which is equivalent to Eq. (4.27).

U-mode functuion

Again, Eq. (C.20) can be used to derive this mode shape. Because the static profiles are the same with those given in Chapter 2, we will obtain the same result given by Eq. (C.23).

The only difference is that Eq. (4.29) and Eq. (4.30) are different from Eq. (2.71) and Eq. (2.72). With the aid of Eq. (4.29) and Eq. (4.30), one can finally obtain Eq. (4.32).

C.4 Brief derivations for Chapter 5

The differential equations and the continuity conditions

From Eq. (5.1)-Eq. (5.3), when $k \neq i \cdot m$, we have

$$\frac{\partial^2 u'_k}{\partial x \partial s} - \frac{m}{H_x + h_x}\frac{\partial^2 u'_k}{\partial t^2} = -\frac{h_x}{H_x + h_x}\frac{d^2 x'_k}{dx ds}. \tag{C.31}$$

$$\frac{\partial^2 y'_{2k}}{\partial x \partial s} - \frac{m}{H_x + h_x}\frac{\partial^2 y'_{2k}}{\partial t^2} = -\frac{h_x}{H_x + h_x}\frac{d^2 y'_{1k}}{dx ds}. \tag{C.32}$$

$$\frac{\partial^2 z'_{2k}}{\partial x \partial s} - \frac{m}{H_x + h_x}\frac{\partial^2 z'_{2k}}{\partial t^2} = -\frac{h_x}{H_x + h_x}\frac{d^2 z'_{1k}}{dx ds}. \tag{C.33}$$

By using the static profile given in Eq. (3.38)-Eq. (3.41), the right-hand sides of Eq. (C.31)-Eq. (C.33) can be simplified. With $H_x >> h_x$ and $ds = J_k^2\, ds\cos\theta$, the above equations can be transformed into Eq. (5.4)-Eq. (5.6).

If $k = i \cdot M$, then from static differential equations Eq. (3.23)-Eq. (3.25) we have

$$\frac{d^2 x'}{dx ds} = \frac{q_y \sin\theta}{H_x} - \frac{P_i \delta(s - s_i)}{H_x}\sin\theta, \tag{C.34}$$

$$\frac{d^2 y'_1}{dx ds} = -\frac{q_y \cos\theta}{H_x} + \frac{P_i \delta(s - s_i)}{H_x}\cos\theta, \tag{C.35}$$

$$\frac{d^2 z_1}{dx ds} = -\frac{q_z}{H_x}. \tag{C.36}$$

Then substituting Eq. (C.34)-Eq. (C.35) into Eq. (5.1)-Eq. (5.3) and then integrating the resulting equations yields Eq. (5.7)-Eq. (5.9).

Frequency equation

The procedure of deriving the frequency equation is similar to finding Eq. (C.26). With the aid of separation of variables, we can obtain

$$\frac{h}{AE}\left(\frac{ds}{dx}\right)^2 = \tan\theta\frac{(q_z\cos\theta D_{1i} - q_y\sin\theta)q_y}{q_y^2 + q_z^2}\frac{dU_k}{ds} + \tan\theta\frac{q_y\cos\theta}{H_x}(s_k - G_i)\frac{dU_k}{ds} + \frac{1}{\cos\theta}\frac{dU_k}{ds} - \frac{(q_z\cos\theta D_{1i} - q_y\sin\theta)q_y}{q_y^2 + q_z^2}\frac{dY_k}{ds}$$

$$- \frac{q_y \cos\theta}{H_x}(s_k - G_i)\frac{dY_k}{ds} - \frac{(q_z \cos\theta D_{1i} - q_y \sin\theta)q_z}{(q_y^2 + q_z^2)\cos\theta}\frac{dZ_k}{ds}$$
$$- \frac{q_z}{H_x}(s_k - G_i)\frac{dZ_k}{ds} + D_{1i}\frac{dZ_k}{ds}. \qquad \text{(C.37)}$$

Then a direct integration of the above equation yields

$$\begin{aligned}\frac{h}{AE}L_e &= \frac{q_y q_z \sin\theta}{q_y^2 + q_z^2}\int_0^{L_s} D_{1i}dU_k(s) + \frac{q_y \sin\theta}{H_x}\int_0^{L_s}(s_k - G_i)dU_k(s) \\ &\quad - \frac{q_y q_z \cos\theta}{q_y^2 + q_z^2}\int_0^{L_s} D_{1i}dY_k(s) - \frac{q_y \cos\theta}{H_x}\int_0^{L_s}(s_k - G_i)dY_k(s) \\ &\quad - \frac{q_z^2}{q_y^2 + q_z^2}\int_0^{L_s} D_{1i}dZ_k(s) - \frac{q_z}{H_x}\int_0^{L_s}(s_k - G_i)dZ_k(s) \\ &\quad + \int_0^{L_s} D_{1i}dZ_k(s). \qquad \text{(C.38)}\end{aligned}$$

Finally, a further algebraic manipulation leads to equation Eq. (5.31).

Supplementary frequency equation

The supplementary frequency equation can be obtained using Eq. (C.37) via Eq. (5.10) to Eq. (5.12). The equations cn be written as

$$\begin{aligned}&\{\tan\theta\frac{(q_z \cos\theta D_{1N} - q_y \sin\theta)q_y}{q_y^2 + q_z^2} + \tan\theta\frac{q_y \cos\theta}{H_x}(L_s - G_N) + \frac{1}{\cos\theta}\} \\ &\quad \{-C_{1\tilde{N}}\beta J_{\tilde{N}} \sin[\beta J_{\tilde{N}}(L_s - s_{\tilde{N}})] + C_{2\tilde{N}}\beta J_{\tilde{N}} \cos[\beta J_{\tilde{N}}(L_s - s_{\tilde{N}})]\} \\ &+ \{-\frac{(q_z \cos\theta D_{1N} - q_y \sin\theta)q_y}{q_y^2 + q_z^2} - \frac{q_y \cos\theta}{H_x}(L_s - G_N)\} \\ &\quad \{-C_{3\tilde{N}}\beta J_{\tilde{N}} \sin[\beta J_{\tilde{N}}(L_s - s_{\tilde{N}})] + C_{4\tilde{N}}\beta J_{\tilde{N}} \cos[\beta J_{\tilde{N}}(L_s - s_{\tilde{N}})]\} \\ &+ \{-\frac{(q_z \cos\theta D_{1N} - q_y \sin\theta)q_z}{(q_y^2 + q_z^2)\cos\theta} - \frac{q_z}{H_x}(L_s - G_N) + D_{1N}\} \\ &\quad \{-C_{5\tilde{N}}\beta J_{\tilde{N}} \sin[\beta J_{\tilde{N}}(L_s - s_{\tilde{N}})] + C_{6\tilde{N}}\beta J_{\tilde{N}} \cos[\beta J_{\tilde{N}}(L_s - s_{\tilde{N}})]\} \\ &= 0. \qquad \text{(C.39)}\end{aligned}$$

Theabove equations can be further simplified into

$$\begin{aligned}&[\tan\theta\frac{(q_z \cos\theta D_{1N} - q_y \sin\theta)q_y}{q_y^2 + q_z^2} + \tan\theta\frac{q_y \cos\theta}{H_x}(L_s - G_N) + \frac{1}{\cos\theta}]C_{20} \\ &= [\frac{(q_z \cos\theta D_{1N} - q_y \sin\theta)q_y}{q_y^2 + q_z^2} + \frac{q_y \cos\theta}{H_x}(L_s - G_N)]C_{40} \\ &\quad + [\frac{(q_z \cos\theta D_{1N} - q_y \sin\theta)q_z}{(q_y^2 + q_z^2)\cos\theta} + \frac{q_z}{H_x}(L_s - G_N) - D_{1N}]C_{60}\end{aligned}$$

which is equivalent to Eq. (5.32).

U-mode function

We can still use Eq. (C.37) to derive this mode shape function. Because the static profile is the same as that given in Chapter 3, a same equation as Eq. (C.28) can be found. However, the difference exists due to that Eq. (5.34) and Eq. (5.35) are different from Eq. (3.89) and Eq. (3.90). Simply using Eq. (5.34) and Eq. (5.35) yields Eq. (5.36).

REFERENCES

[1] Ahmed M. Abdel-G Haffar, Magdi A. Khalifa *1991 Importance of Cable Vibration on Dynamics of Cable-stayed Bridges* Journal of Engineering Mechanics 117:2571-2589

[2] Kamran A. Kashani *1988 Vibration of Hanging Cables* Computers and Structures 31:699–715

[3] A. Filiatrault; R. Tinawi; B. Massicotte *1993 Damage To Cable-stayed Bridge During 1988 Saguenay Earthquake* J. of Structural Engineering 119:1450–1463

[4] P. Yu, Y.M. Desai, N. Popplewell and A.H. Shah *1992 Modeling of Conductor Galloping Phase 1, Volumes I and II* Prepared for Canadian Electrical Association, Project No. 321T672, Montreal, Canada

[5] P. Yu and N. Popplewell *1994 Galloping Control of 477 KCMIL AL Subtransmission Lines* Prepared for Manitoba Hydro, Project No. T085e, Winnipeg, Canada

[6] H. P. Lin and N. C. Perkins *1995 Free Vibration of Complex Cable/Mass Systems: Theory and Experiment* J. of Sound and Vibration 179:131–149

[7] O. M. Griffin and F. Rosenthal *1985 Vortex-induced Vibrations of Marine Cables and Structures* U.S. Naval Research Laboratory Memorandum Report No. 5600

[8] H. M. Irvine and T. K. Caughey *1974 The Linear Theory of Free Vibrations of A Suspended Cable* Proc. Royal Soc. London A341 299-315

[9] S. P. Cheng and N. C. Perkins *1992 Closed-Form Vibration Analysis of Sagged Cable/Mass Suspensions* J. of Applied Mechanics 59:923–928

[10] S. P. Cheng and N. C. Perkins *1992 Free Vibrations of A Slack Cable Supporting A Discrete Mass* J. of The Acoustical Society of America 91:2654–2662

[11] P. Yu, P.S. Wong and F.Kaempffer *1995 Tension of Conductor Under Concentrated Loads* J. of Applied Mechanics 62:802–809

[12] P. Yu *1997 Explicit Vibration Solutions of a Cable Under Complicated Loads* J. of Applied Mechanics 64:957–964

[13] S. S. Sergev and W. D. Iwan *1981 The Natural Frequencies And Mode Shapes of Cables With Attached Mass* J. of Energy Resources Technology 103:237–242

[14] G. Rajagopal *1992 Mode Localization In Almost Periodic Structures: Theory and Experiments* Proceedings of The International Society of Polar and Offshore Engineering Conference II:426–433

[15] S. P. Cheng, N. C. Perkins *1992 Free Vibration of A Sagged Cable Supporting A Discrete Mass* The Journal of Acoustical Society of America 91:2654–2662

[16] S. P. Cheng, N. C. Perkins *1991 Approximate Linear Theories For The Dynamics of Slack Cables Supporting A Discrete Mass* Design Engineering Division, ASME 38:85–88

[17] William M. Henghold, John J. Russell, and Joseph D. Morgan *1977 Free Vibrations of Cable In Three Dimensions* J. of The Structural Division 103:1127–1136

[18] Armin B. Mehrabi, Habib Tabatabai *1998 Unified Finite Difference Formulation For Free Vibration of Cables* J. of Structural Engineering 124:1313–1322

[19] M. S. Triantafyllou *1991 Dynamics of Cables, Towing Cables and Mooring Systems* Shock and Vibration Digest 23, No. 7:3–8

[20] H. M. Irvine *1981 Cable Structures* MIT Press

[21] Yu Chen *1966 Vibrations: Theoretical Methods* Reading, Mass., Addison-Wesley Pub. Co.

[22] Austin Harris Church *1963 Mechanical Vibrations* New York, Wiley

[23] Benito M. Pacheco, Yozo Fujino *1993 Keeping Cables Calm* Civil Engineering 63:56–58

[24] Demeter G. Fertis *1995 Mechanical And Structural Vibrations* New York : Wiley

[25] Andrew D. Dimarogonas *1996 Vibration For Engineers* Upper Saddle River, N.J. : Prentice Hall

[26] H. McCallion *1973 Vibration of Linear Mechanical Systems* Longman

[27] William H. Press, Saul A. Teukolsky, William T. Vetterling and Brian P. Flannery *1992 Numerical Recipes in C* Cambridge University Press

[28] Anestis S. Veletsos and Georges R. Darbre *1983 Free Vibration of Parabolic Cables* J. of Structural Engineering 109:503–519

[29] H. M. Irvine *1978 Free Vibrations of Inclined Cables* J. of Structural Division 104:343–347

[30] John R. Rice *1983 Numerical Methods, Software, and Analysis* McGraw-Hill, Inc.

[31] Daniel J. Inman *1989 Vibration : with control, measurement, and stability* Englewood Cliffs, N.J. : Toronto : Prentice Hall

[32] Singiresu S. Rao *1995 Mechanical Vibrations* Reading, Mass. : Addison-Wesley

[33] Eutiquio C. Young *1978 Vector And Tensor Analysis* DEKKER

[34] Ray M. Bowen and C. C. Wang *1976 Introduction To Vectors and Tensors* Plenum Press

[35] Benson H. Tongue *1996 Principles of Vibration* New York : Oxford University Press

[36] William T.Thomson *1993 Theory of Vibration With Applications* Englewood Cliffs, N.J. : Prentice Hall

[37] Roger Alan Anderson *1967 Fundamentals of Vibrations* New York, Macmillan

[38] Matthew Hussey *1983 Fundamentals of Mechanical Vibrations* London : Macmillan

[39] P. Srinivasan *1990 Mechanical Vibration Analysis* New Delhi : Tata McGraw-Hill

[40] A.J. Pretlove *1985 BASIC Mechanical Vibrations* London ; Toronto : Butterworths

[41] D.E. Newland *1989 Mechanical Vibration Analysis And Computation* Harlow [England] : Longman Scientific and Technical : New York : Wiley

[42] M. S. Triantafyllou *1984 The Dynamics of Taut Inclined Cables* Quart. J. Mechanics and Applied Mathematics 37:421-440

[43] W. K. Chang, V. Pilipchuk, and R. A. Ibrahim *1997 Fluid Flow-induced Nonlinear Vibration of Suspended Cables* Nonlinear Dynamics 14:377-406

[44] O. M. Griffin, F. Rosenthal *1989 Dynamics of Slack Marine Cables* Journal of Offshore Mech-Arct Engineering 111:298-302

[45] P. Yu, Y.M. Desai, A.H. Shah and N. Popplewell *1993 Three Degrees-Of-Freedom Model For Galloping, Part I: Formulation* ASCE J. Engng. Mech., Vol. 119, No. 12:2404-2425

[46] P. Yu, Y.M. Desai, N. Popplewell and A.H. Shah *1993 Three Degrees-Of-Freedom Model For Galloping, Part II: Solutions* ASCE J. Engng. Mech., Vol. 119, No. 12:2426-2448

[47] P. Yu, N. Popplewell and A.H. Shah *1995 Instability Trends of Inertially Coupled Galloping, Part I: Initiation* J. Sound And Vib., Vol. 183, No. 4:663-678

[48] P. Yu, N. Popplewell and A.H. Shah *1995 Instability Trends of Inertially Coupled Galloping, Part II: Periodic Vibrations* J. Sound And Vib., Vol. 183, No. 4:679–691

[49] P. Yu, A.H. Shah and Popplewell *1992 Inertially Coupled Galloping of Iced Conductors* ASME J. Appl. Mech., Vol. 59:140–145

[50] P. Yu, N. Popplewell and A.H. Shah *1991 A Geometrical Approach Assessing Instability Trends For Galloping* ASME J. Appl. Mech., Vol. 58:784–791

[51] Y.M. Desai, P. Yu, N. Popplewell and A.H. Shah *1995 Finite Element Modeling of Overhead Transmission Line Galloping* J. Comput. Struct.,Vol. 57, No. 3:407–420

[52] P. Yu, N. Popplewell and A.H. Shah *1995 Free Vibration Analysis of Sagged Cables Under Distributed And Concentrated Loads* Proc. of 15th CANCAM, Vol. 1:374-375

[53] P. Yu *May 30 - June 1, 1997 Direct Perturbation Analysis On Cable Vibrations* 18th Annual Meeting of the Canadian Applied Mathematics Society, Toronto, Canada

[54] Alexander Tesar, Ludovit Fillo *1988 Transfer matrix method* D. Reidel Inc.